Naval Command,
Control and Ocean
Surveillance Center RDT&E Division San Diego, CA
92152-5001

Structural Performance of Cylindrical Pressure Housings of Different Ceramic Compositions Under External Pressure Loading

Part II, Zirconia Toughened Alumina Ceramic

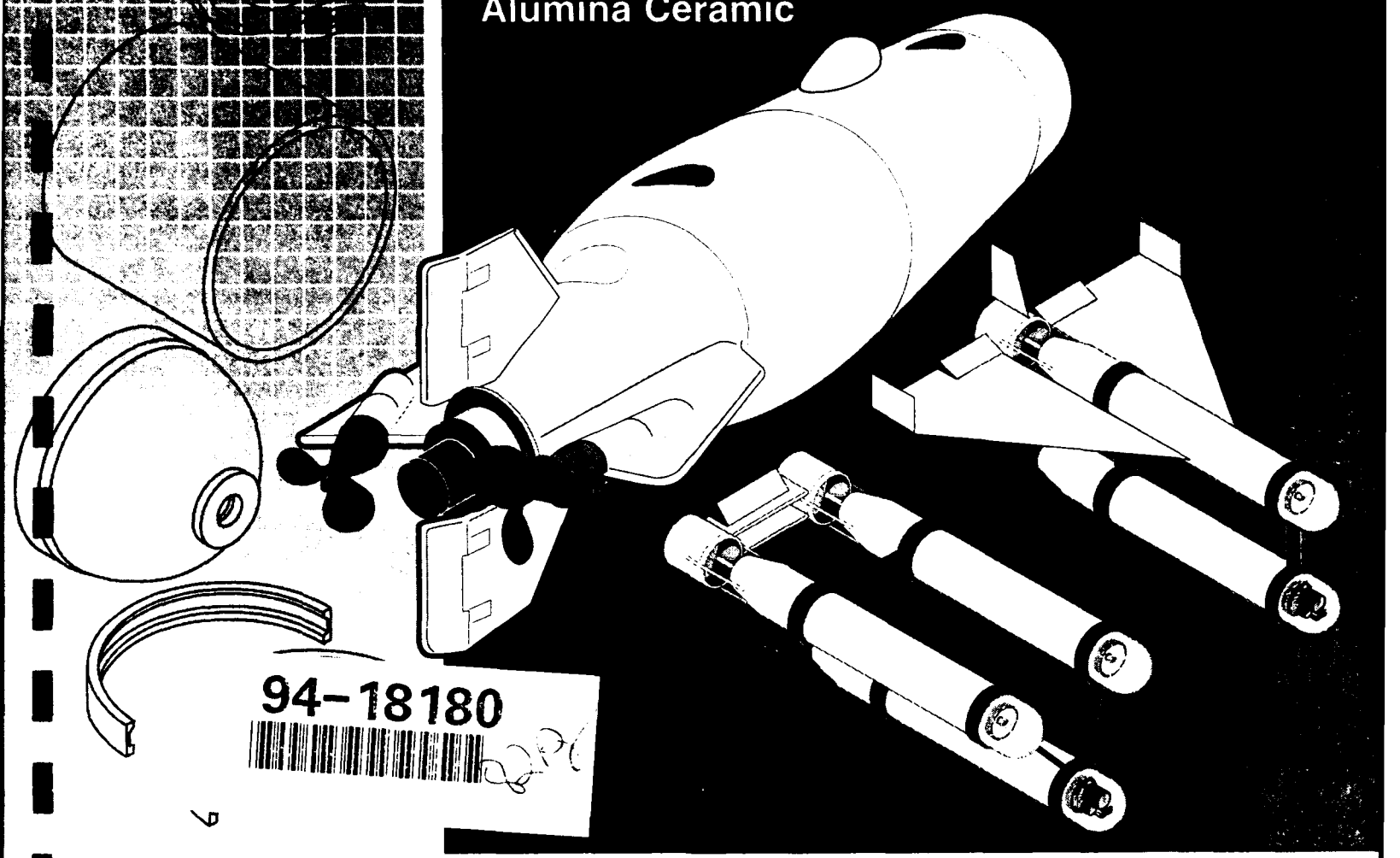

R. P. Johnson
R. R. Kurkchubasche
J. D. Stachiw
NRaD

P. C. Smith
WESGO, Inc.

Technical Report 1593
December 1993

Technical Report 1593
December 1993

Structural Performance of Cylindrical Pressure Housings of Different Ceramic Compositions Under External Pressure Loading

Part II, Zirconia Toughened Alumina Ceramic

R. P. Johnson
R. R. Kurkchubasche
J. D. Stachiw
NRaD

P. C. Smith
WESGO, Inc.

NAVAL COMMAND, CONTROL AND OCEAN SURVEILLANCE CENTER
RDT&E DIVISION
San Diego, California 92152–5001

K. E. EVANS, CAPT, USN
Commanding Officer

R. T. SHEARER
Executive Director

ADMINISTRATIVE INFORMATION

This work was performed by the Marine Materials Technical Staff, RDT&E Division of the Naval Command, Control and Ocean Surveillance Center, for the Naval Sea Systems Command, Washington, DC 20362.

Released by
J. D. Stachiw
Marine Materials
Technical Staff

Under authority of
N. B. Estabrook, Head
Ocean Engineering
Division

ES

SUMMARY

External pressure housings constructed with ceramic hull components offer clear advantages over equivalent metallic housings when minimum dry weight and maximum operation buoyancy are desired. Zirconia-toughened alumina (ZTA) ceramic was evaluated as a candidate housing material as part of a program to promote the application of ceramics to large external pressure housings for underwater vehicles (reference 7). Ten 12-inch-outside diameter (OD) by 18-inch-long by 0.412-inch-thick monocoque cylinders fabricated by WESGO, Inc. from ZTA ceramic were assembled into external pressure housings and experimentally evaluated under short-term, and cyclic-pressure loadings. The cylinders tested for this study represent the largest ZTA ceramic pressure housings that have been assembled and tested. Each external pressure housing consisted of a ZTA cylinder with adhesively bonded titanium end-cap joint rings for sealing and mating with end closures. Pressure test data was used to establish design criteria for external pressure housings constructed using ZTA ceramic as the principle hull material.

The addition of zirconia (zirconium dioxide) to an alumina matrix results in a ZTA ceramic composition with improved fracture toughness over commercially available alumina ceramics. The 20-percent zirconium dioxide by weight composition (density 4.07 g/cc) used in the test cylinders was found to have the following minimum mechanical and physical properties:

compressive strength: 392 kpsi
flexural strength: 41.6 kpsi
Weibull modulus: 25
fracture toughness (K_{IC}): 3.69 kpsi ($in^{1/2}$)
elastic modulus: 43 MPsi

Eight of the ZTA cylinders were external pressure cycled to peak pressure varying from 11,000 to 18,000 psi to determine their cyclic life as a function of the applied load during each cycle. The ZTA ceramic cylinders were found to have a cyclic fatigue life in excess of 1,000 dive cycles, at a peak external pressure of 13,000 psi generating nominal maximum membrane stresses of −190,000 psi in the hoop direction in the ceramic shell wall. The remaining two ZTA cylinders were subjected to short-term external pressure tests to determine the elastic stability of the monocoque cylindrical assembly. When capped with flat steel end closures, both ZTA cylinders survived proof tests to 20,000-psi external pressure. Repressurization of one of the short-term test cylinders resulted in failure by buckling at an external pressure of 20,600 psi.

Through its improved fracture toughness, ZTA monocoque cylinders demonstrated better fatigue life than isostatically pressed 96-percent alumina-ceramic cylinders tested to the same cyclic load levels (reference 6). ZTA's increased cyclic life must be traded off in the design of external pressure housings against its lower buckling resistance, increased weight, and higher fabrication costs when compared to alumina. When the amount of buoyancy generated by the ceramic pressure housing assembly is used as a means of comparison, ZTA housings outperform alumina housings for applications requiring more than 1,000 dive cycles. For pressure housings requiring lower numbers of dive cycles, ZTA and alumina housings have comparable weight-to-displacement (W/D) ratios in seawater and, consequently, an alumina pressure hull is a more attractive selection due to its lower fabrication costs.

CONTENTS

FIGURES

TABLES

INTRODUCTION

BACKGROUND

This report serves to evaluate zirconia-toughened alumina (ZTA) ceramic as a candidate material for the primary hull components used in external-pressure resistant housings for deep-submergence ocean engineering applications. The major portion of research by the Naval Command, Control and Ocean Surveillance Center (NCCOSC) RDT&E Division (NRaD) that has been performed to date on ceramic pressure housings has focused on the use of 94- or 96-percent alumina (aluminum oxide) as the principle housing structural material. The attraction of alumina over other ceramic compositions lies in its low material cost and mature manufacturing base that allows for fabrication of large (up to 32 inches in diameter) external pressure housing components. While alumina has been shown to be a viable material candidate for fabrication of external pressure housings, a number of structural ceramics exist which possess superior physical and mechanical properties. The use of these materials offers potential pressure housing designs with improved performance in terms of maximum buoyancy and increased cyclic fatigue life.

Three of the most attractive ceramic compositions, ZTA, silicon nitride (reference 8), and silicon carbide particulate-reinforced alumina (reference 9), were selected for evaluation as material candidates for future underwater pressure-resistant hull structures. This report serves to document testing performed to evaluate the structural performance of external pressure housing components fabricated from ZTA ceramic. This was accomplished by subjecting ten 12-inch-outer diameter (OD) by 18-inch-long by 0.412-inch-thick monocoque ZTA cylinders to various short-term and cyclic-loading pressure tests.

CYCLIC FATIGUE OF CERAMIC EXTERNAL PRESSURE HOUSINGS

Cyclic fatigue is one of the principle modes of failure that must be addressed when designing ceramic housings to withstand a number of dive cycles (reference 6). Fatigue of ceramic housings occurs because of tensile forces that occur at the ceramic hull bearing-surface/metallic joint-ring interface when subjected to depth loading. Over repeated dive cycles, tensile loading at the joint interface can initiate crack growth from preexisting flaws in the bearing surface regions of the ceramic hull components.

There are several approaches that designers can take to reduce the potential for crack propagation and thereby extend a housing's fatigue life:

- Limit the level of tensile forces that exist at joint interfaces through careful joint interface design and joint ring assembly techniques.
- Reduce the external pressures at which the housing operates.
- Control the presence of defects in the ceramic hull bearing surface regions through careful processing of the ceramic material during fabrication, especially during finish grinding.
- Monitor the level of defects that exist in the ceramic hull bearing surface region after manufacturing by using nondestructive inspection techniques.
- Employ ceramics that have higher fracture toughness and thereby reduce the material's susceptibility to crack growth from preexisting flaws.

The tensile forces that are calculated to exist at ceramic housing joint interfaces are radially oriented in the ceramic shell wall. This tensile loading leads to Mode I (opening mode) crack propagation from the ceramic end bearing surface. As the number of pressure cycles is increased, circumferencial cracks are observed to grow meridionally into the ceramic shell wall away from the plane axial bearing surfaces at the ceramic cylinder ends. The K_{IC} fracture toughness of isostatically pressed 96-percent alumina-ceramic cylinders tested in reference 6 ranged from 2.50 to 3.00 kpsi(in)$^{1/2}$. ZTA was selected as a candidate material for use in deep-submergence pressure housings because of its higher values of fracture toughness ranging from 3.70 up to 8.00 kpsi(in)$^{1/2}$. Pressure testing ten ZTA cylinders and comparing their performances to 96-percent alumina test data

(reference 6) provides a basis for evaluating the potential of ZTA ceramic components for pressure housings in which cyclic life is a primary concern.

By using the same cylinder geometry, assembly techniques, pressure test fixtures, and external test pressures as used for the 96-percent alumina cylinders (reference 6), any differences in test results could be attributed to the differences in material properties of these two ceramic compositions. It was anticipated that under identical test conditions, the ZTA ceramic would demonstrate increased cyclic life compared to alumina ceramic because of its improved toughness. Pressure test data generated for ZTA could then be used to develop structural design criteria that would dictate acceptable stress levels in ZTA pressure housing components as a function of the desired number of dive cycles to design depth. Once design criteria were established for ZTA, tradeoff studies between ZTA and 96-percent alumina and other ceramic compositions (references 8 and 9) could be undertaken to determine the optimum material selection for each external pressure housing application.

ZTA CERAMIC

In order to improve the mechanical properties of alumina ceramic, micron-sized particles of zirconium dioxide, or zirconia, are added to the 96-percent alumina composition powders at the ceramic batching stage. The small particles of zirconia toughen the alumina in two ways. First, since the zirconia and alumina have different mechanical properties, a crack running into a zirconia particle tends to be deflected around it. This deflection on a micro level requires the crack to generate more free surface area than it would have had to generate in a monolithic material, thus requiring more expended energy to do so. This effectively toughens the ceramic. The second mechanism relates to the phase stability of the zirconia particles. Zirconia has a crystalline phase instability that develops during the cooling portion of the ceramic article fabrication cycle. This tetragonal-to-monoclinic phase transformation results in a 6-percent volume expansion of the zirconia particles. The expansion can occur either spontaneously on cooling, or as a result of the perturbation created by the passage nearby of a crack front. These point-source expansion events can cause the crack to slow down because the crack, in order to continue, must first overcome the compressive stresses generated by the expanded particles. Advancing cracks also are often steered off course by local stress fields around the particles, or blunted by micro cracks generated by the expanded particles. Either one, or both, of these phenomena result in toughening.

FABRICATION

MANUFACTURING

The engineering drawing for the 12-inch-OD ZTA cylinders fabricated by WESGO, Inc. is shown in figure 1.[1] Target values for material properties such as modulus of elasticity, compressive strength, flexural strength (modulus of rupture, or MOR), fracture toughness, density, and Weibull Modulus are listed in note 2 of figure 1 along with appropriate military or industrial standards for measuring each of these properties. Note 3 of figure 1 provides visual inspection techniques for the finished ZTA parts.

ZTA was considered a worthy candidate for fabrication of ceramic hull components for underwater pressure housings because of its relatively high values of fracture toughness and comparable strength and modulus values with alumina. Because ZTA is essentially an alumina matrix, much of the mature fabrication technology that exists for alumina also can be applied to manufacturing large ZTA cylinders. The drawback of ZTA is that while the addition of zirconia (zirconium dioxide) crystals increases the toughness of the material, it also increases the density of the ceramic composition as compared to 96-percent alumina (4.07 g/cc for ZTA, versus 3.74 g/cc for 96-percent alumina). This tradeoff of increased fatigue life (through higher fracture toughness) for increased dry weight may not be attractive for ocean engineering applications where maximum housing buoyancy, not cyclic fatigue life, is the primary design consideration.

[1]Figures and tables are placed at the end of the text.

The ZTA cylinders evaluated in this report were fabricated by WESGO, Inc. (477 Harbor Boulevard, Belmont, CA 94002) using an AL-600 alumina matrix toughened with zirconium dioxide. AL-600 is a WESGO, Inc. trade name for their 96-percent aluminum oxide composition. The AL-600 ZTA cylinders discussed here consisted of 20-percent zirconia by weight. AL-600 ZTA cylinders are fabricated in a manner similar to those made from pure AL-600 alumina (reference 6). Carefully prepared powder raw materials are mixed in a ball mill with water, binders, and milling additives. The key ingredients are aluminum oxide, glass-forming oxides, and the zirconia-toughening particles. After milling, the mixture forms a thick slip which is atomized into a fine shower and dried into uniformly blended spherical agglomerates of the powder mixture. This process, called spray drying, produces a fine and free-flowing powder blend. The powder then is compacted into the desired cylindrical shape at pressures near 10,000 psi in an isostatic press. Powder particles are kept dry during this operation using steel and rubber tooling.

At this point, the powder reaches 50- to 60-percent density and physically resembles a piece of blackboard chalk in both its character and physical properties. Shaping is then accomplished using conventional single-point turning machine tools in a process called green machining. In the next process step, cylinders are loaded into a high-temperature furnace to allow the process of solid-state sintering to occur. During sintering, each powder particle diffuses into its neighboring particles. Solid-state chemical reactions occur that create a two-phase mixture of solid alumina and zirconia particles in a liquid glassy matrix. During cooling, the glassy matrix solidifies and bonds the alumina and zirconia particles together. At this point, the ceramic is fully dense and has developed its desired mechanical properties. Final shaping is done by diamond abrasive grinding.

Zirconia raw materials used in this project were special high-purity grades selected to minimize fabrication risks. This, together with the characteristically higher cost of zirconia, make the ZTA source powders about 10 times more expensive than their pure alumina counterparts. Raw material costs, however, only partly effect total fabrication costs. The fabrication process of ZTA differs from that of pure AL-600 alumina in the slightly more complicated milling, significantly more-complicated sintering temperature cycles during cooling, and considerably more-difficult diamond grinding as a result of the material toughening.

MATERIAL PROPERTY SPECIFICATIONS

In order to compare the material properties of ZTA to other ceramic compositions, a survey was conducted of military and industrial specifications that could be used as guidelines for determining the mechanical and physical properties of ceramic. To ensure the material property data is of use in evaluating the ceramic cylinders, several factors were considered. Test coupons used for material property data were to be either cut from a finished cylinder or co-processed with the cylinders using the identical powder lot, and fabricated using the same pressing, sintering and grinding techniques. This way, the size and distribution of any fabrication defects would be as similar as possible in the test specimen as in the finished cylinder. Since it is understood that the final steps of grinding do not necessarily remove surface damage introduced during earlier grinding steps, the entire sequence of grinding steps was to be the same for the test specimens as used for the cylinders. An appropriate sample size was to be used to determine the material properties of interest. "Fliers" generated during specimen tests were to be included in the data package, as long as all test procedures were followed correctly. Finally, experimental errors were to be minimized to ensure the validity of all data that was generated.

From the survey, the following specifications were selected for measuring material properties in the ZTA cylinders:

Flexural strength (modulus of rupture): MIL-STD-1942, Procedure B (reference 2), through fracturing 3 mm by 4 mm by 45 mm rectangular beam specimens by applying four-point bending.

Compressive strength: ASTM C773, procedure B (reference 13), using 0.250-inch-diameter by 0.500-inch-long cylindrical test specimens.

Density: ASTM C373 (reference 14).

Elastic modulus: ASTM C848 (reference 15) by recording resonance frequencies of test specimens in the flexural mode of vibration.

Fracture toughness: ASTM B771-87 (reference 10) by applying an opening load to a material specimen containing a chevron-shaped slot.

MATERIAL PROPERTY MEASUREMENTS

The ZTA cylinders tested for this report were manufactured in five separate lots. Lot 1 was cylinder 001, lot 2 included cylinders 002 through 004, lot 3 included cylinders 005 and 006, lot 4 included cylinders 008 through 010, and lot 5 included cylinders 011 and 012. Cylinder 005 was rejected after ultrasonic inspection and was never pressure tested, while cylinder 007 was never delivered. The following table presents the average strength values and density measured for each lot. Average flexural strenghts (MORs) are based on breaking 10 specimens for each lot. Weibull Modulus calculations were based on flexural strength data. Average compressive strengths are based on breaking three specimens for each lot.

Lot	Cylinder Part #	Flexural Strength (kpsi)	Weibull Modulus	Compressive Strength (kpsi)	Density (g/cc)
1	001	62.6	31	498.4	4.08
2	002-004	43.1	37	408.3	4.07
3	005, 006	43.4	62	420.1	4.07
4	008-010	41.6	34	392.5	4.06
5	011, 012	62.7	25	415.2	4.05

Three specimens were used from each lot to measure fracture toughness. All three fracture toughness measurements for each lot are presented below. The second toughness specimen from lot 3 failed before the test procedure could be completed.

Lot	Cylinder Part #	Fracture Toughness kpsi($in^{1/2}$)
1	001	5.18, 3.69, 3.86
2	002-004	7.64, 8.08, 7.39
3	005, 006	5,84, NA, 4.05
4	008-010	8.90, 7.51, 7.55
5	011, 012	5.32, 4.69, 5.55

The elastic modulus measured between 43 Mpsi to 43.5 Mpsi for all five cylinder lots. The considerable variability in material properties among the cylinders is attributed to differences in the cooling rates between cylinder lots after sintering. Below 1,200 degrees C, cooling rates are largely controlled by the thermal mass of the furnace and other ceramic bodies that are present inside the furnace. The tendency of the zirconia transformation toughening mechanism to occur near 1,250 degrees C makes resulting fracture toughness values particularly sensitive to lower temperature cooling rate changes.

The ranges of average material properties from the three lots used to fabricate the AL-600 96-percent alumina-ceramic cylinders tested in reference 6 are compared to the data above for ZTA:

	AL-600	ZTA
Flexural Strength (kpsi)	47.7-53.0	41.6-62.7
Weibull Modulus	23.2-38.5	24.8-61.5
Compressive Strength (kpsi)	358.4-432.1	392.5-498.4
Density (g/cc)	3.73-3.74	4.05-4.08
Elastic Modulus (Mpsi)	47.0	43.0-43.5

The material property data for the ZTA varies more widely than the data measured for the AL-600 96-percent alumina ceramic. The greatest variations in the ZTA data were found for fracture toughness and flexural strength. While the fracture toughness of ZTA is substantially higher than that of AL-600, the strength properties of the two compositions are comparable. On the down side, the elastic modulus of ZTA is 3.5 to 4.0 Mpsi (8 to 9 percent) less than that for AL-600, and the density of ZTA is 9 percent higher than that of AL-600.

INSPECTION

After fabrication of the ZTA cylinders, a thorough nondestructive evaluation (NDE) plan was devised to ensure the quality of each cylinder. Dimensional inspections were performed by WESGO, Inc. Dimensional range data forms for cylinders 001 and 010 are included in appendix A of this report. Dimensional data forms indicate that outstanding dimensional tolerances were achieved by diamond grinding the ZTA ceramic cylinders. OD, wall thickness and length were generally held to within 0.002 of an inch for each of the 12-inch-OD cylinders. Bearing surface flatness of less than 0.001 of an inch was achieved and bearing surface finishes ranging from 4 to 16 microinches at the ends of each cylinder were measured mechanically with a diamond stylus indicator.

In addition to a complete dimensional inspection against the engineering drawing, a visual inspection of each cylinder to detect the presence of any surface flaws was performed. Dye penetrant was applied to the cylinder surfaces to detect any cracks, blisters, holes, porous areas or inclusions that could effect the structural integrity of the finished part. Each part also was inspected to ensure that the surfaces were of uniform color and free of any adherent foreign material. The ZTA cylinders were noticeably heavier than the isostatically pressed alumina cylinders described in reference 6, but otherwise had the same general appearance with respect to surface texture and color as the 96-percent alumina cylinders.

A complete ultrasonic NDE evaluation was performed on each of the 10 ZTA cylinders using the same calibration standards (witness specimens) and fixtures used for the alumina cylinders as discussed in reference 6. Since the ZTA cylinders are primarily composed of an alumina matrix, the 96-percent alumina calibration standards were considered to be adequate for inspecting the ZTA cylinders as well. A sample of the ZTA composition

was compared ultrasonically to the alumina calibration standards to determine if any new ZTA calibration standards were needed. This comparison showed that the sound travel characteristics of the two material compositions were similar enough to not require additional witness specimens.

Calibration standard SK9402-093-C2 (reference 6) with preformed 0.030 pores was used to calibrate the ultrasonic equipment for a full-immersion pulse-echo inspection of the ZTA cylinders. A C-scan was generated for each cylinder using an index of 0.010 of an inch. Table 1 lists the number, size, and depth of the defects found in each cylinder. The size of defects is indicated by a percentage of the average amplitude of reflection from the 0.030 pores in standard SK9402-093-C2. The depth of each defect is measured from the OD of the cylinder via an A-scan recording of each indication.

Based on this inspection, all cylinders were accepted for the pressure testing with the exception of cylinder 005 which was found to have a 6.5-inch-long internal crack that was not detected by visual inspection. The crack started at approximately 4.5 inches from one end of the cylinder and ran in an axial direction toward the other end. The ultrasonic C-scan of the cracked region of cylinder 005 is shown in figure 2. Subsequent visual inspection of the cracked region using candling techniques verified the presence of the crack. All other cylinders, with the exception of cylinder 010, had zero defects, or only a small number of internal pores less than 0.030 of an inch in size, as summarized in table 1. Cylinder 010 had a single void that was of the same order of size as the 0.030 pores in calibration standard SK9402-093-C2. Cylinder 009 had no detectable internal inclusions, but the C-scan did detect variations in the cylinder shell wall thickness that appeared to have been introduced during finish diamond grinding.

TEST PLAN

TEST CONFIGURATIONS

Pressure testing of the 10 ZTA cylinders used the same fixtures that were designed to test the isostatically pressed alumina-ceramic cylinders (reference 6). Three fixture configurations were used to perform all pressure testing. Test assembly I used Mod 1, Type 2, end-cap joint rings epoxy

bonded to the ends of the ZTA cylinders with titanium hemispheres serving as end closures. Test assembly II used Mod 1, Type 2 end-cap joint rings epoxy bonded to the ends of the ZTA cylinder with flat steel-plate end closures. Test assembly III used Mod 1, Type 1 end-cap joint rings with flat steel end closures. The test assembly I configuration was used to perform all pressure tests that subjected the ZTA cylinders to external pressures up to and including 13,000 psi. ZTA cylinders tested with external pressures greater than 13,000 psi used the test assembly II configuration, unless the pressure testing time was of short duration, and then the test assembly III configuration was employed.

Each of the ZTA cylinders that was pressure tested used five water-proofed biaxial strain gage rosettes bonded to the interior surface of the cylinder shell wall at midbay. These gages were equally spaced around the circumference of the internal diameter (ID) and were oriented to read axial and hoop strains during pressure testing. Resistance strain gages (0.250 inch, 120 Ohm), part number CEA-06-250UT-120, manufactured by Micro-Measurements Division were used. Pressure testing was performed at Southwest Research Institute (SWRI) in San Antonio, TX using a 15-inch-ID pressure vessel rated for a maximum pressure of 30,000 psi.

Figure 3 shows the test assembly I configuration. The Mod 1, Type 2 titanium end-cap joint rings bonded to each end of the ZTA cylinder for this assembly is shown in figure 4. The manila spacer shown in figure 5 ensures a minimum 0.010 of an inch epoxy-filled axial clearance between the bearing surface of the ceramic cylinder and the seat of the metal joint during assembly. The weight of the 12-inch-OD ZTA cylinder with titanium Mod 1, Type 2 end-cap joint rings is 45.6 pounds, of which 5 pounds is contributed by the two end-cap joint rings. The cylindrical assembly has a W/D ratio of 0.60 when submerged in seawater. The important design features of the Mod 1, Type 2 joint ring are:

> The length of the encapsulating joint ring flanges should be a minimum of 2.5t, where t is the thickness of the ceramic shell wall at the bearing surface.
>
> The thickness of the encapsulating joint ring flanges should be a minimum that stress analysis allows, the epoxy adhesive-filled radial clearance between the flanges of the joint ring and the ceramic hull OD and ID should be 1/1,000th of the hull OD.

The titanium hemispherical end closures used for test assembly I are shown in figure 6. Sealing and closure of the hemisphere/joint-ring interface is maintained with an O-ring and clamp band (figures 7 and 8). The steel plug (figure 9) is assembled to each hemispherical end closure with the aid of a washer (figure 10). The steel plug is used to pass strain gage wires through one end of the test assembly and to capture a drain plug at the opposite end to check for leaks. The wood plug (figure 11) is placed in the interior of the test assembly to mitigate the effects of an implosion during pressure testing in case a cylinder should fail.

The test assembly II configuration shown in figure 12 is identical to the test assembly I configuration with the exception of the end closures. Flat steel bulkheads (figure 13) are substituted for the titanium hemispheres to allow the ZTA cylinders to be cycled to higher external pressures.

Figure 14 shows the test assembly III configuration used to perform short-term proof tests of the ZTA cylinders to 20,000-psi external pressure or for pressurizing the cylinders to failure by buckling. The test assembly III configuration used Mod 1, Type 1 titanium end-cap joint rings epoxy bonded to each end of the ceramic cylinder (figure 15). The looser radial clearances and simpler design to the Type 1 end-cap joint ring was considered acceptable for tests with short submersion times. The Type 2 end-cap joint rings used for the test assembly I and II configurations use tighter radial clearances and a flared external flange for capturing a bead of room-temperature vulcanizing (RTV) sealant. These features of the Type 2 end cap act to prevent water intrusion into the cylinder/joint-ring epoxy bond during extensive testing. Closure of the flat steel bulkheads is maintained with four external tie rods (figure 16). Strain gage wires are passed to the exterior of the test assembly through the flat end plates with the aid of the feedthrough

shown in figure 17. A wood plug (figure 18) is placed in the interior of the test assemblies to minimize damaging the test fixture hardware should pressure testing result in catastrophic failure of the ZTA cylinder.

TEST PROCEDURES

After delivery of the 10 ZTA cylinders to NRaD, two Mod 1 end-cap joint rings were assembled to each cylinder. An example of a ZTA cylinder with Mod 1, Type 1, end-cap joint rings epoxy-bonded in place is shown in figures 19 and 20. The cylinders were then shipped to SWRI where all external pressure testing took place. Table 2 outlines the pressure testing plan for the cylinders. Tests 01 through 08 used test assembly I and test assembly II configurations to determine fatigue behavior of the ZTA cylinders subjected to external pressure cycles. Fatigue performance was determined by cycling the cylinders to the pressures specified in the test pressure column of table 2 for either a fixed number of cycles or until the cylinders failed catastrophically. Cylinders that did not fail during cyclic testing were subsequently reinspected using full-immersion pulse-echo ultrasonic NDE to determine the extent of any subcritical crack growth that occurred during pressure testing. Tests 09 and 10 used test assembly III configurations to evaluate the general instability failure of monocoque ZTA cylinders subjected to uniform external pressure loading.

All pressure testing was performed in tap water at ambient room temperatures. Each pressure test was preceded with a proof test to 10,000 psi. A pressurization rate during the proof test of approximately 1,000 psi/minute was used, followed by a 60-minute hold at 10,000 psi. The depressurization rate to 0 psi was not to exceed 10,000 psi/minute. The test configuration column of table 2 defines the end-cap joint-ring/end closure test configuration used for each test. All cyclic testing was performed using external pressure cycles from 50 psi to the peak pressure listed in the test pressure column of table 2 and then back to 50 psi. The peak pressure was maintained during each cycle for a duration of 1 minute. Pressurization and depressurization rates were not to exceed 10,000 psi/minute during cyclic testing.

During the first cycle of test 01 through 08, strains were recorded from the five biaxial strain gages at 1,000-psi increments up to the peak pressure and then were recorded after depressurization to measure any residual strains. After a proof test to 10,000 psi, the cylinders used in tests 09 and 10 were pressurized to 20,000 psi recording the strains at 1,000-psi intervals. After a 60-minute hold at 20,000 psi, the strains were recorded and then recorded once more for residual strains after depressurization at a rate not exceeding 10,000 psi/minute. Test assembly 10 was subsequently pressurized to catastrophic failure by elastic instability, recording the strains at 1,000-psi increments up to 18,000 psi, and at 500-psi increments thereafter. Figures 21 and 22 show a test assembly I configuration being prepared for cyclic testing. Figure 23 shows a test assembly II configuration ready to be lowered into the pressure vessel for cyclic testing.

STRUCTURAL ANALYSIS

Finite element analysis (FEA) was performed to determine the stress levels that would exist in the ZTA cylinders during each of the tests described in table 2. Calculations of the stress state in the ceramic cylinders at the peak pressures listed for each of these tests was performed using the finite element models (FEM) generated previously for each of the three test configurations as described in reference 6. Since the geometry of the cylinders and the pressure-testing hardware (titanium end-cap joint rings and end closures) were identical to that used for the AL-600 cylinders, the same FEMs could be used after updating the cylinder solid model with the correct elastic constants for ZTA. The following linear elastic isotropic material properties were used for ZTA:

$E = 43$ Mpsi
$v = 0.23$

where E is the elastic modulus and v is the Poisson's ratio. As expected, the only significant differences in the stresses in the ZTA cylinders compared with those in the AL-600 cylinders were the local stresses in the ceramic cylinder bearing

surface regions adjacent to the titanium end-cap joint rings. Because the elastic modulus of ZTA is a slightly closer match to that of titanium, the Poisson's- effect induced radial expansion mismatch between ZTA and the metallic joint ring is less than occurs with the relatively stiffer AL-600 cylinders. Consequently, the radial tensile stresses induced in the bearing-surface region of the ZTA cylinder are slightly less than would occur in an AL-600 alumina cylinder tested to the same external pressure. Tables 3 and 4 list the radial, axial, and hoop stresses that are calculated to exist in the ZTA cylinders for the various peak test pressures and test configurations used for this study.

When the type of end closure used in testing is changed from titanium hemispheres to flat steel bulkheads, there is a slight drop in radial tensile stress in the bearing-surface region of the ceramic cylinder. The more-rigid end constraints provided by flat-steel bulkheads are required at higher test pressures in order to avoid collapse caused by general instability failure of the cylinder. The more-rigid end constraints also had the effect of reducing the membrane stresses that existed in the ceramic cylinder end where it was supported by the end closure. Reduced compressive membrane stresses lower the Poisson's-induced radial expansion of the ceramic shell wall. This effectively lowers the tensile stresses in the ceramic ends caused by maintaining radial strain compatibility between the ceramic and titanium bearing surfaces when subjected to external pressure loading.

Buckling analysis of all three test configurations subjected to uniform external pressure was performed in addition to the stress analysis described above using computer-aided analysis and hand-calculation techniques. Again, the computer models used to predict buckling of the AL-600 monocoque cylinders (reference 6) were updated with the elastic constants of ZTA and rerun to predict collapse pressures for each of the ZTA test configurations. Using the BOSOR4 computer program (reference 1), test assembly I configuration was predicted to fail from general instability, with three lobes forming at an external pressure of 13,898 psi. Also with BOSOR4, test assembly configurations II and III were predicted to fail at an external pressure of 23,339 psi, with three circumferential waves (N=3) forming. Hand-calculation techniques used for the AL-600 cylinders were used again to calculate the critical buckling pressures of the three test configurations of the ZTA cylinders. The test assembly I configuration was predicted to buckle at an external pressure of 14,213 psi (N=3), and test assembly configurations II and III were calculated to buckle at an external pressure of 18,036 psi (N=3). The following table summarizes these buckling calculations for the various ZTA test configurations and compares them with results calculated for the AL-600 cylinders (reference 6).

Cylinder Composition	Test Configuration	Pcrit (psi) BOSOR4	Pcrit (psi) Hand Calcs.
ZTA	I	13,898	14,213
AL-600	I	15,128	15,536
ZTA	II, III	23,339	18,036
AL-600	II, III	25,430	19,713

The increase in predicted collapse pressure of the AL-600 cylinders over the ZTA cylinders is directly proportional to the increase in elastic modulus of the AL-600 material over the ZTA material.

TEST RESULTS

CYCLIC FATIGUE TESTS

The results of the 10 pressure tests performed with the ZTA cylinders are listed in table 5. The first eight pressure tests, 01 through 08, were structured to provide cyclic fatigue data by pressure cycling eight different ZTA cylinders to peak external pressures ranging from 11,000 to 18,000 psi. Selection of the peak external pressures used for these eight tests was based on the prior performance of the AL-600 cylinders tested in reference 6. The strains recorded during the first cycle for each of the eight fatigue tests are shown in figures 24 through 31. The cylinder used in test 01 completed 1,039 cycles to a peak pressure of 11,000 psi during each cycle. Figure 24 shows a plot of the strains recorded during the first pressure cycle to 11,000 psi. As expected, the strains increase linearly in direct proportion to the applied

external pressure. No residual strains were detected in the test 01 cylinder after depressurization from the first pressure cycle.

Cylinder test 01 was intended to be stopped after completion of approximately 1,000 cycles. This was done to ensure that the test would be ended prior to catastrophic failure of the cylinder in order to allow the bearing-surface regions of the cylinder to be inspected using NDE techniques. Inspection of the ZTA cylinder using ultrasonic and die-penetrant methods would indicate the level of subcritical crack growth that existed in the ceramic as a result of cyclic external pressure loading.

Cylinder test 02 called for cycling to 11,000 psi until failure or 4,000 cycles, whichever occurred first. The ZTA cylinder used for test 02 survived 4,059 cycles before the test was stopped. The plot in figure 25 indicates that there were some variations in the strains measured during the first pressure cycle from the five separate gages that were used. This was attributed to the fact that since the gages were bonded in place by hand, slight differences in the gage orientations on the cylinder surface effected the magnitude of the measured strains. Because the test 02 cylinder survived pressure cycling, it was returned to NRaD to be inspected for subcritical crack growth.

The test 03 cylinder withstood 5,689 cycles to 12,000 psi without failure. A plot of the strains recorded in the test 04 cylinder during its first pressure cycle to a peak pressure of 13,000 psi is shown in figure 27. The deviation in recorded hoop strains indicates that there is some misalignment between the five gages bonded to the ID of the cylinder.

The ZTA cylinder used for test 04 failed catastrophically after 1,854 cycles to 13,000-psi external pressure. In addition to recording strains, acoustic emissions were monitored during the first three pressure cycles to 13,000-psi external pressure. During the first pressure cycle, the test 04 assembly was quiet until the external pressure reached 3,000 psi. Between 3,000 and 13,000 psi, steady acoustic emissions were recorded, with a total of 144 acoustic events occurring by the time the peak pressure was reached. No further acoustic emission was recorded during the subsequent depressurization during the first cycle, nor was any noise recorded during the second and third pressure cycles.

Figure 28 shows the strains recorded during the first pressure cycle to 14,000 psi for the ZTA cylinder used for test 05. This cylinder failed catastrophically after 605 cycles to 14,000 psi. The ZTA cylinder used for test 06 completed 361 cycles to 15,000 psi when the test was stopped because of apparent leakage of the test assembly.

The test 07 cylinder survived 1,608 cycles to 16,000 psi before the test was halted so that the cylinder could be returned to NRaD for further inspection. The final ZTA cylinder tested to investigate fatigue was cycled to an external pressure of 18,000 psi for 88 cycles before it failed catastrophically. Material property measurements that were presented earlier were correlated with the five material lots used to fabricate the ZTA cylinders. Because of the substantial variation in material properties of the various ZTA cylinder lots, differences in cyclic fatigue performance of the tested cylinders was to be expected.

SHORT-TERM TESTS

Figure 32 shows the strains recorded during the proof test to 20,000 psi for the ZTA cylinder used in test 09. Comparison of the pressure-strain curves generated for each of the pressure tests indicate substantial variations in the slopes that are plotted. For example, the strains measured at 10,000-psi external pressure range from −2,700 to −3,300 microinches/inch for all the strain plots that are presented in this study. This implies there are differences in the stiffness of the material for the 10 ZTA cylinders tested for this report. Specifically, the cylinders from lots 1 and 4 would appear to have lower modulus values based on the higher strain values measured during testing. As noted earlier, no discernable residual strains were detected after the first pressure cycle for any of the cylinders used in fatigue tests 01 through 08. In contrast, after being pressurized to 20,000 psi and held for one hour, the cylinder used in test 09 was found to have residual strains after

depressurization. Residual hoop strains exceeding -100 microinches/inch were recorded on four of the five biaxial strain gages. Four of the five axial gages measured residual strains between -19 and -30 microinches/inch. This would imply that the ZTA cylinder had undergone some permanent compression after the proof test to 20,000 psi.

In addition to recording strains during the proof test to 20,000 psi for test 09, acoustic emissions were also monitored during the original pressurization of the cylinder to 10,000 psi and then monitored again during the full proof test to 20,000 psi. During the original pressurization to 10,000 psi, a steady stream of acoustic emissions occurred between 2,000 and 10,000 psi resulting in a total of 163 events. Upon repressurization of the cylinder to 20,000 psi, no acoustic events were recorded until the cylinder reached 10,000 psi again, and then a total of 26 additional acoustic emission events were recorded as the external pressure was increased from 10,000 to 20,000 psi.

Further study of the strain plot for test 09 (figure 32) indicates that the values of the recorded hoop strains from the five gages are beginning to diverge from one another as the external test pressure approaches 20,000 psi. Figure 33 shows the strains that were measured during the pressurization of the test 10 cylinder. This test called for increasing the external pressure on the test assembly until the cylinder collapsed from elastic instability. As discussed previously, the test assembly III configuration used for cylinder tests 09 and 10 was predicted to buckle from general instability, with three circumferential waves forming. The appearance of circumferential waves prior to collapse of the cylinder is indicated by the diverging strains in the figure 33 pressure-strain plot.

Comparison of the pressure-strain plots generated for the cylinders used for tests 09 and 10 indicates that the onset of circumferential waves occurs at a lower external pressure for the test 10 cylinder. Comparison of pressure-strain slopes for these two separate tests indicates no differences prior to the formation of lobes. This implies that there is very little variation in the elastic constants for the ZTA ceramic in these two cylinders. Test 09 used ZTA cylinder 001, while test 10 used cylinder 010. Dimensional-range data forms for these parts (appendix A) indicate that the geometric differences between these two cylinders are slight to none. Thus, the apparent discrepancies between the stability behavior of these two cylinders is difficult to account for. The observed structural performance differences between these two seemingly identical cylinders reinforces the need for adequate safety factors in designing compressively loaded structures like external pressure housings against failure by buckling.

The collapse of the test 10 cylinder at an external pressure of 20,600 psi compared well with the predicted critical buckling pressure determined using both hand calculations and computer-aided analysis techniques described earlier. The prediction based on hand calculations (18,036 psi) was roughly 14 percent lower than the actual tested result. The calculated buckling pressure based on the BOSOR4 computer model (23,339 psi) was approximately 12 percent higher than the actual test result for the test 10 cylinder. The differences between the calculations and the actual test results were very similar to those found for general instability failure of the monocoque AL-600 alumina-ceramic cylinder that was pressurized to failure in reference 6. In that case, hand calculations also gave slightly conservative results, while the BOSOR4 model also over-predicted the critical pressure at which the housing would collapse.

FINDINGS

SUBCRITICAL CRACK GROWTH DUE TO CYCLIC FATIGUE LOADING

All ZTA cylinders that survived tests 01 through 08 without failure were inspected for subcritical crack growth that occurred as a result of cyclic pressure testing. NDE of the test 01 cylinder that completed 1,039 cycles to 11,000 psi was performed by first removing the epoxy-bonded titanium end-cap joint rings from one end of the cylinder with the aid of heat and the clamping fixture described in reference 4. After thorough cleaning of the

bearing-surface region, a full-immersion pulse-echo ultrasonic C-scan was generated which indicated relatively uniform crack growth around the circumference of the bearing-surface region as shown in figure 34.

The C-scan in figure 34 is a full-scale two-dimensional plan view of the ceramic volume adjacent to the bearing surface at the end of the cylinder. Because a relatively high (0.050 of an inch) scanning index was used, the subcritical cracks seen in figure 34 appear as a mesh of coarse white square pixels. The C-scan indicates that the cracks have propagated as far as half of an inch from the bearing surface after 1,039 pressure cycles. This level of crack growth poses no threat to the structural performance of this cylinder since all cracks are well within the length of the cylinder end that is encapsulated by the titanium end-cap joint ring. These cracks would have to extend beyond the bond length of the joint-ring flanges (1.31 inches) before structural problems would arise. If the cracks propagate beyond the joint-ring flanges, the delaminated surface of the shell could become unstable and result in spalling of ceramic flakes from the surface. If spalling continues, the cylinder assembly could begin to leak, or eventually collapse, if enough load-bearing material in the shell wall is lost.

NDE of the test 02 cylinder that completed 4,059 cycles to 11,000 psi was performed after removal of the end-cap joint ring from one end of the cylinder. Dye penetrant was applied to the plane-bearing surface to detect cracks that formed during pressure testing. Figure 35 shows the bearing-surface region, where numerous short circumferential cracks were discovered. Figure 36 is a pulse-echo C-scan recording of the same bearing-surface region for the test 02 cylinder. Even though the test 02 cylinder has been subjected to roughly 3,000 more pressure cycles to the same peak load level as the test 01 cylinder, the test 02 cylinder has less extensive cracking around the circumference of the bearing surface. Comparisons of the C-scans for test 01 and 02 cylinders indicate that the depth of cracks that have formed are roughly equivalent, even though each cylinder was subjected to a substantially different number of pressure cycles.

Figure 37 shows the results of the dye penetrant inspection of the test 03 cylinder bearing-surface area after completing 5,689 cycles to 12,000 psi. Extensive numbers of short circumferential cracks are distributed throughout the plane-bearing surface area. Figure 38 is a pulse-echo C-scan of the bearing-surface region which indicates that a similar level of internal crack formation has occurred in the test 03 cylinder as was detected in cylinder tests 01 and 02. As with these prior pressure tests, the greatest depth that any of the cracks have penetrated from the bearing-surface region is about a half inch.

The cracks that developed in cylinder tests 01, 02, and 03 showed distinct differences from those that were found in 94- and 96-percent alumina cylinders that have previously been pressure tested and inspected (references 4 and 6). Dye penetrant inspection of these alumina cylinders (also tested with epoxy-bonded Mod 1 joint rings with a thin layer of epoxy adjacent to the cylinder and bearing surface) typically showed a few very-well-defined circumferential cracks located at the midplane of the bearing surface. The more extensive the pressure testing, the greater the circumferential length and axial depth of these cracks. Inspection of the bearing surfaces at the ends of pressure-cycled ZTA cylinders revealed a different type of crack pattern. Instead of several well-defined, centrally-located cracks, numerous short parallel cracks dispersed throughout the bearing-surface thickness were found.

It is hypothesized that in the ZTA cylinders, once the cracks had propagated to a certain depth, there was not enough additional energy in subsequent pressure cycles to continue to propagate existing cracks. Consequently, energy was dissipated through formation of additional parallel cracks which also eventually stalled. It appears that the loading levels to which these first three ZTA test cylinders were subjected was not sufficient to drive the cracks further than one-half inch from the bearing surface. This behavior can be compared to the endurance limit that exists for some metal alloys which will not fatigue as long as

the magnitude of the cyclic loading is below some threshold value. The differences that were observed in the crack patterns of the alumina cylinders and the ZTA cylinders could be attributed to the difference of fracture toughness for these two ceramic compositions. In the lower-toughness alumina material, energy can be absorbed through propagation of a few relatively larger cracks (i.e., with greater free-service area). In the tougher ZTA ceramic, long cracks require more energy to propagate, such that energy can only be dissipated through the creation of numerous shorter cracks.

Prior to machining material property test specimens from the test 07 cylinder that survived 1,608 cycles to a peak external pressure of 16,000 psi, a pulse-echo C-scan was generated for each end of the cylinder, with the titanium end caps still bonded in place. The C-scan of the cylinder revealed that no internal fatigue cracks had extended beyond the joint-ring flanges from the bearing-surface region. This implies that this cylinder would have been capable of withstanding even more pressure cycles to 16,000 psi without failure.

SPALLING DUE TO CYCLIC FATIGUE LOADING

Figure 39 shows the remains of one of the titanium end-cap joint rings that was bonded to the test 04 cylinder after it failed catastrophically on cycle 1,854 to 13,000 psi. A substantial amount of ZTA is still embedded in the joint ring. The inner flange of the joint ring was pushed inward at one location during collapse of the cylinder. It can also be seen that the remaining ceramic is a fine grit in the region of the deformed joint-ring flange, while larger fragments of ceramic are left elsewhere.

It is postulated that the region of the test 04 cylinder located near the deformed end-cap flange is where crack growth from the bearing surface of the cylinder became extensive enough to become critical. Numerous internal cracks in this area would explain the fine grit of the remaining ceramic. As these cracks extended beyond the flanges of the joint ring, flakes of the ceramic spalled off from the inner and/or outer surfaces of the ceramic cylinder. Once enough material was lost through spalling, or weakened by multiple delaminations, the external pressure pushed through the cylinder wall and drove the internal flange of the joint ring inward at this single location with enough resulting shock to destroy the entire cylinder. The tensile forces that are calculated to exist in the ceramic body at the cylinder end-bearing surfaces increase as the external pressure loading is increased. As these tensile forces in the ceramic become high enough, more energy becomes available to initiate cracks at bearing-surface flaws and propagate these cracks axially into the ceramic shell wall. It is hypothesized that at the right combination of load levels, and load cycles, crack growth can extend far enough into the cylinder wall for spalling to occur.

Removal of the test 06 cylinder assembly from the pressure vessel after 361 cycles to 15,000 psi because of apparent leakage revealed that the ZTA cylinder was still intact, but that substantial spalling had occurred at two locations. Spalling was found on the inner and outer surfaces at the same end of the cylinder. Figure 40 shows the spalled region found at the interface with the titanium joint ring on the ID of the cylinder. Inspection of this fractured area indicates distinct crack-front boundaries between stages of crack growth. Figure 41 shows the spalled region that occurred at the joint-ring interface on the outer surface of the ceramic cylinder.

A pulse-echo C-scan of the ceramic cylinder taken with the metallic joint ring still bonded in place is presented in figure 42. The joint ring was not removed prior to inspection in order to keep the cylinder as intact as possible. The C-scan in figure 42 covers only approximately 90 degrees of the cylinder circumference because this was the only area where cracks were detected to have extended beyond the joint-ring flanges. Ultrasonic inspection of the opposite end of the cylinder did not reveal any internal discontinuities beyond the encapsulating joint-ring flanges. The external spall is depicted in the C-scan near the 45-degree circumferential location and the internal spall is centered at about the 90-degree circumferential reference position.

While the C-scans clearly show regions where internal discontinuities exist, by themselves they

do not provide information about the total number of flaws that occur through the wall thickness or the exact distance of each flaw from the inner or outer surface of the cylinder. Regardless, C-scans generated with pulse-echo or through-transmission transducers have been found to be a very reliable means of determining whether some type of discontinuity exists. This technique could obviously be extended as a means of intermittently inspecting operational ceramic pressure housing components. Once cracks have been extended beyond the U-shaped joint ring, the part should be removed from service. An even better option is to design ceramic pressure housings to operate at load levels at which the chance of crack growth sufficient to cause spalling will not occur.

Figures 43 and 44 show the remains of both end-cap joints that were bonded to the test 08 cylinder that failed after 88 cycles to a peak external pressure of 18,000 psi. The inner flange of each joint ring has been driven inwards in one locale, which, as described previously, is characteristic of the evidence associated with failure of the ceramic cylinder by cyclic fatigue. The substantial external pressure used for this test has not only pushed in the inner joint-ring flange, but also has caused the bearing-surface region on the titanium joint ring to split out (figure 44).

At 18,000-psi external pressure, the end-cap joint ring and its epoxy bond with the ceramic cylinder are being pushed to the limits of the joint interface design. At this external pressure load, the stresses in the titanium joint ring are approaching the yield strength of the material (120 kpsi) in the regions of contact with the flat-steel end closure and around the O-ring gland. Additionally, at these high external pressures, the forces acting on the epoxy bonds between the joint rings and the ceramic are more severe, and, consequently, breakdown of the epoxy bond has been observed (primarily through extrusion from the annular clearance between the joint-ring inner flange and the ID surface of the ceramic cylinder). For these reasons, the cyclic fatigue performance of ceramic housing assemblies at higher load levels becomes dependent on the joint-ring components and adhesives that are used in addition to the structural capabilities of the ceramic itself. As tougher ceramic materials become available, allowing engineers to design to even higher operational stress levels, development of joint-ring configurations that can withstand this severe loading environment must be developed. Full use of the outstanding strength properties of ceramic materials can only occur if interface designs for joint rings, end closures, and penetrations also exist.

STRESS CRITERIA FOR ZTA EXTERNAL PRESSURE HOUSINGS

Figure 45 summarizes the results of tests 01 through 08 for evaluating the cyclic fatigue life of the 12-inch-OD monocoque ZTA ceramic cylinders. A data point is shown for each test on a plot of the log of the number of cycles completed, versus the peak external test pressure used during each cycle. Data points are distinguished based on whether the test was terminated by failure of the cylinder or whether the maximum number of desired load cycles was reached prior to failure. While there is a substantial amount of scatter in this data, it establishes a general trend of reduced cyclic life as the magnitude of cyclic loading is increased.

Based on FEMs of the three test assemblies described previously, the cyclic fatigue life data also can be generated as a function of the stress state that is calculated to exist in the ZTA cylinders at the peak pressure used for each test. Figure 46 is a plot of the maximum radial tensile stress that is predicted to occur at the bearing surface at the ends of each of the eight ZTA cylinders as a function of the log of the number of total pressure cycles. In addition, another non-failure point has been added to this plot corresponding to the bearing-surface radial tensile stress that existed in the test 09 cylinder when proof tested to 20,000-psi external pressure.

Since the fatigue cracks that form in the ceramic cylinders are observed to initiate in the bearing-surface region, it seems plausible that the fatigue data should be presented as a function of the load levels that exist in the ceramic at this locale. Yet, calculations of tensile stresses that exist in the ZTA cylinders at their interface with the titanium end-cap joint rings is undoubtedly sensitive to the

modeling techniques and assumptions used to construct the FEMs. Specifically, the methods used for modeling the epoxy bond that exists between the end-cap joint ring and the ends of the ceramic cylinder can have a substantial impact on the level of stresses that are calculated to exist. The assumption that the epoxy behaves as a linear elastic material is questionable, especially at the high load levels seen by the joint interface under external hydrostatic pressure loading.

For this reason, the cyclic fatigue data for the ZTA test cylinders is also presented as the function of the more easily calculated compressive membrane stresses that exist in the ceramic cylinder away from the joint region. Figure 47 is a plot of the cyclic life data as a function of the maximum compressive hoop stress in the ZTA cylinder shell wall. Based on this presentation of the fatigue data, the design curve for ZTA ceramic pressure-housing components shown in figure 48 is proposed. This curve is based on the performance of the WESGO ZTA ceramic cylinders described previously, assembled with NOSC[2] Mod 1 titanium end-cap joint rings using NRaD bonding procedures (reference 5, appendix A). Obviously, if different types of interface joint rings or bonding techniques are used, the loading on the ceramic in the critical bearing-surface regions of the cylinder will differ, and the design curve presented in figure 48 may not apply.

The curve in figure 48 can be used to design pressure housings using ZTA cylinders once the desired number of operation dive cycles is known. If a maximum number of 1,000 dive cycles is required for a ZTA housing, the maximum compressive hoop stress in the cylinder should not exceed −190,000 psi in any one dive cycle. For lower numbers of dive cycles, the maximum compressive hoop stresses can be increased as shown.

In addition to WESGO, Inc., other commercial manufacturers are capable of fabricating pressure-housing components from their own ZTA ceramic compositions. Applying structural performance data generated in this report to other vendors' ZTA materials is not advisable, unless it has been shown through destructive testing of material specimens that other materials possess properties that are equivalent or superior to the ZTA presented here. Again, it is important to note that the test specimens used for determining material properties should be representative of the properties in the ceramic pressure-housing components.

The 12-inch-OD by 18-inch-long by 0.412-inch-thick wall cylinders tested for this report represent some of the largest structural ceramic components fabricated from ZTA to date. Because of the size of these parts, extensive development by the manufacturer was required to make these cylinders. The substantial variability in material properties found for the ZTA cylinders is a reflection of the youthful state of the manufacturing expertise needed to fabricate large ZTA ceramic parts. As a comparison, the AL-600 96-percent alumina-ceramic cylinders tested in reference 6 have more uniform material properties since this composition has benefited from past experience on the part of the manufacturer in fabricating large alumina-ceramic parts.

If, in the future, larger pressure-housing components are fabricated from ZTA, the curve shown in figure 48 may require the use of a "knockdown" factor to reduce the design stress levels below those that are suggested here. Manufacture of larger ceramic parts may require fabrication techniques that will affect the material properties of the finished ceramic body, even if an identical ZTA composition to that used in this report is selected. Differences in the manufacturing process can affect the structural performance of the resulting ceramic body if residual stresses are introduced or if the microstructure of the ZTA composition is changed. The grinding procedure for larger ZTA components may require the use of different equipment and holding fixtures which could result in differences in the size and distribution of flaws on the ground surfaces than exist in the 12-inch-OD cylinders tested in this report. For this reason, it is suggested that prior to placing in service monocoque cylindrical ZTA housings with outside diameters greater than 12 inches designed on the basis of data generated in this study, a prototype should be

[2]NOSC is now the NRaD division of NCCOSC.

subjected to a qualification test program based on the housing's operation requirements.

DESIGN CURVES FOR ZTA EXTERNAL PRESSURE HOUSINGS

Once stress criteria for designing ZTA pressure-housing components has been developed, design curves for sizing wall thickness and calculating weight-to-displacement (W/D) ratios for cylindrical housing assemblies in seawater can be generated. Figure 49 shows various curves that can be used to size the wall thickness of monocoque ZTA ceramic cylinders of various lengths when capped with hemispherical end closures intended for 1,000 cycles to design depth. Wall thickness is based on providing an adequate safety margin against buckling and ensuring that compressive hoop stresses do not exceed -190,000 psi under depth load. A factor of safety (SF) of 1.5 was used for the critical buckling pressure required to collapse the monocoque cylinders by general instability as predicted using hand calculation techniques (reference 5). Wall thickness (figure 49) is presented as the ratio of wall thickness (t) to the OD of the cylinder (t/OD). The t/OD ratio is plotted as a function of the external pressure load on the ZTA housing assembly for five different length-to-outer-diameter ratios (L/OD); L/OD equal to 0.5, 1.0, 1.5, 3.0, and 10.0.

As shown in figure 49, each of the five L/OD curves are converging or have converged on a straight line corresponding to the wall thickness for which the hoop stresses equal -190,000 psi. The design pressure varies as a linear function of t/OD for the stress criteria, but varies as a nonlinear (approximately cubic) function of t/OD for the buckling criteria. Before the various L/OD curves converge on this straight line, the required wall thickness is driven by meeting the buckling requirement. The point of convergence between the nonlinear and linear portions of the L/OD curve represents an optimized wall thickness for monocoque cylinders which identically satisfies the design criteria for both stress and buckling. For 9,000-psi external design pressure, an optimized monocoque ZTA cylindrical housing design would have an L/OD ratio of 0.5 or less. At external pressures less than 9,000 psi, the wall thickness of an L/OD 0.5 housing is dictated by meeting the buckling criteria, and, consequently, the cylinder shell wall is understressed (magnitude of nominal compressive hoop stresses is less than 190,000 psi). At external pressures greater than 9,000 psi, the wall thickness of an L/OD 0.5 housing is overdesigned with respect to the selected buckling criteria.

Once t/OD ratios have been determined, it is easy to calculate the W/D ratio in seawater of the ZTA cylinder used in the cylindrical housing assembly (figure 50). The W/D ratios presented in figure 50 are for the ceramic cylinder only and do not include the weight of joint rings or any other hardware used to construct the cylindrical portion of the housing. One of the outstanding benefits of ceramic pressure housings is their relatively low W/D ratios as compared with traditional pressure-housing materials. Pressure housings with a lower W/D ratio provide increased buoyancy when submerged, which is an obvious benefit for many ocean engineering applications. As part of a complex system such as unmanned underwater vehicle (UUV), the buoyancy obtained from the pressure housings can be used to offset the weight of other components for a net neutrally buoyant vehicle in service.

As discussed in reference 6, monocoque hulls do not necessarily offer an optimized pressure housing design for minimum W/D, especially as the L/OD of the cylindrical portion of the housing is increased. The wall thickness of longer monocoque cylinders tends to be driven solely by the buckling criteria, and, consequently, the housing wall tends to be understressed, which does not use the excellent compressive strength of the ceramic material. The wall thickness, in these cases, can be reduced to achieve the desired design membrane stresses as long as additional means of stiffening the cylindrical hull are employed. The use of metallic joint-ring stiffened ceramic cylindrical hulls has been shown to be a viable means of optimizing ceramic pressure housings for minimum W/D.

COMPARISON OF ZTA AND AL-600 96-PERCENT ALUMINA

In general, the ZTA cylinders demonstrated better cyclic fatigue life than the AL-600 96-percent alumina-ceramic cylinders subjected to a similar test program in reference 6. The following chart compares the results of cyclic pressure tests performed with both ZTA and AL-600 cylinders.

External Pressure (psi)	No. Pressure Cycles ZTA	No. Pressure Cycles AL-600
9,000	NA	3,000 (nf)
11,000	4,059 (nf)	2,969
12,000	5,689 (nf)	1,065
13,000	1,854	762
14,000	605	214
15,000	361	707
16,000	1,608 (nf)	NA
18,000	88	NA

Cylinders that survived the listed number of cycles without failing are designated (nf) for no failure. Through the lower range of peak pressures used for these tests (up to 13,000 psi), the ZTA cylinders show better cyclic fatigue life than the AL-600 cylinders. Over the range of higher test pressures used (above 13,000 psi), the cyclic pressure data is inconclusive as to which of these two materials offers the best fatigue performance.

Figure 51 compares the W/D ratios for monocoque ZTA and 96-percent alumina-ceramic cylinders based on the design criteria discussed above and in reference 6 for 1,000 cycles to design depth. W/D curves are presented for L/OD ratios of 1.0 and 3.0 for both AL-600 and ZTA. For monocoque cylindrical housing designs where wall thickness is driven by stability, AL-600 cylinders have a lower W/D ratio since AL-600 has a higher specific modulus (elastic modulus/density ratio) than ZTA. On the other hand, ZTA has a higher specific design stress (maximum operational compressive hoop-stress/density ratio) for 1,000 cycles than AL-600 alumina. Consequently, if the hull wall thickness is driven by design stress criteria, the ZTA housing can be designed to have a lower W/D ratio than AL-600.

The two dashed curves in figure 51 are extensions of the W/D curves for ZTA and AL-600 monocoque cylindrical hulls where wall thickness is driven by the stress criteria. These dashed curves represent the lower limit of achievable W/D for ZTA and AL-600 over the range or design pressures shown. By using alternative stiffening methods such as intermittent metallic joint rings, the W/D ratio of a ceramic cylindrical assembly can be pushed toward these lower limits. For low L/OD ratio cylinders at high design pressures, the W/D curve has converged with the dashed line, and no further weight reduction is achievable. Since the lower W/D limit curve for ZTA is located slightly to the left of the limit curve for AL-600, lower W/D cylindrical housings should be achievable with ZTA, especially at the higher design pressures. For less than 1,000 dive cycles, the design stresses recommended for ZTA and AL-600 become closer in magnitude, and, consequently, the specific design stresses for each material are roughly equivalent. For housings designed for no more than 100 cycles to design depth, ZTA and AL-600 provide similar W/D ratios, making AL-600 alumina the more attractive material selection because of its lower cost.

The W/D curves for ZTA and AL-600 (figure 51) are intended to provide a relative comparison of the performance of these two compositions for exernal pressure housing applications. The curves are based on the W/D of the monocoque ceramic cylinder only and do not include other components required for an operational cylindrical housing assembly such as end-cap joint rings, clamp bands, and internal payload rails.

CONCLUSIONS

1. The 20-percent zirconia by weight ZTA composition supplied by WESGO, Inc. has been found to be an acceptable material candidate for fabricating external pressure housings used in ocean engineering applications.
2. Although the average flexural strength and compressive strength of WESGO's ZTA and 96-percent alumina AL-600 (reference 6) are comparable, there are substantial differences in the material properties of these two ceramic

compositions. The elastic modulus of ZTA (43 Mpsi) is 9 percent less than that for AL-600. The density of ZTA (4.06 g/cc) is 9 percent higher than that of AL-600. The fracture toughness of ZTA ranges as high as three times the values found in material specimens of AL-600.

3. Monocoque cylindrical hull components fabricated from WESGO ZTA have a demonstrated cyclic fatigue life in excess of 1,000 pressurizations to design depth, provided:

   —Cylinder end bearing-surface finish, titaniun end-cap joint ring design (Mod 1, Type 2), and joint-ring epoxy bonding procedures recommended in reference 6 are used.

   —The maximum nominal compressive membrane hoop stresses in the shell wall do not exceed 190,000 psi in any dive cycle.

4. Inspection of the first two test cylinders cycled to maximum nominal compressive membrane hoop stresses of approximately 160,000 psi revealed similar levels of subcritical crack growth in the bearing-surface regions at the cylinder ends. The extent of crack growth was equivalent in these cylinders, even though they were subjected to 1,000 and 4,000 pressure cycles, respectively. This indicates that at this loading, crack growth rate has slowed down or even stalled and the cyclic fatigue life of ZTA cylinders may exceed 5,000 pressure cycles. By comparison, at this same stress level, it is recommended that cylinders fabricated from AL-600 alumina (reference 6) not be subjected to more than 1,000 dive cycles.

5. The improvement in cyclic fatigue life of a ZTA pressure housing over an equivalent AL-600 housing must be traded off in design against reduced buckling resistance, increased weight, and higher fabrication costs. For housing applications requiring 100 dive cycles or less, the W/D ratios of ZTA and AL-600 are equivalent, and, thus, AL-600 alumina is a more economical material selection. ZTA pressure housings only offer a W/D advantage over AL-600 alumina in cases where the design requirements call for cyclic fatigue life in excess of 1,000 dive cycles. For a high number of dive cycles, ZTA housing components can be designed to operate at higher stress levels through reduced wall thickness than is recommended for AL-600, and, therefore, can provide increased buoyancy in service.

7. The state of manufacturing technology for ZTA ceramic is less mature than for 94- and 96-percent alumina compositions. The 12-inch-OD by 18-inch-long by 0.412-inch-thick monocoque cylinders fabricated for this study are the largest cylinders fabricated from WESGO ZTA composition to date. The 12-inch-OD cylinders tested in this report cost three times as much as the AL-600 cylinders that were evaluated in reference 6. This cost difference is attributable to higher material and fabrication costs associated with ZTA, and to the fact that the fabrication of large ZTA ceramic parts is currently in a developmental stage.

8. Ultimately, the attractiveness of ZTA over alumina compositions for future external pressure hull applications will depend on the reliability of structural properties that can be obtained for large ZTA ceramic parts. The design criteria presented for ZTA in this study had to be conservative to account for the variability in measured material properties as well as cylinder test results. Consequently, ZTA does not as yet offer a clear improvement in performance over alumina for all pressure housing applications.

REFERENCES

1. Bushnell, D. "BOSOR4 User's Manual," Lockheed Missiles and Space Co., Inc.

2. Department of Defense. 1990. "Flexural Strength of High Performance Ceramics at Ambient Temperatures," MIL-STD-1942A, Washington, DC. (Nov).

3. Jayatilaka, A. 1979. "Fracture of Engineering Brittle Materials," Applied Science Publishers LTD, London.

4. Johnson, R. P., R. R. Kurkchubasche, and J. D. Stachiw. 1993. "Effect of Different Axial Bearing Supports on the Cyclic Fatigue Life of Ceramic Pressure Housings," NCCOSC RDT&E Division TR 1607, San Diego, CA (Oct).

5. Johnson, R. P., R. R. Kurkchubasche, and J. D. Stachiw. 1993. "Exploratory Study of Joint Rings for Ceramic Underwater Pressure Housings," NCCOSC RDT&E Division TR 1586, San Diego, CA (May).

6. Johnson, R. P., R. R. Kurkchubasche, and J. D. Stachiw. 1993. "Structural Performance of Cylindrical Pressure Housings of Different Ceramic Compositions Under External Pressure Loading Part I, Isostatically Pressed Alumina Ceramic," NCCOSC RDT&E Division TR 1590, San Diego, CA (Aug).

7. Kurkchubasche, R. R., Johnson, R. P., and J. D. Stachiw. 1993. "Application of Ceramics to Large Housings for Underwater Vehicles: Program Outline," NCCOSC RDT&E Division TR 2585, San Diego, CA (Oct).

8. Kurkchubasche, R. R., Johnson, R. P., and J. D. Stachiw. 1994. "Part III, Sintered Reaction Bonded Silicon Nitride Ceramic," NCCOSC RDT&E Division TR 1592, San Diego, CA (Mar).

9. Kurkchubasche, R. R., Johnson, R. P., and J. D. Stachiw. 1993. "Part IV SiC Particulate Reinforced Alumina Ceramic," NCCOSC RDT&E Division TR 1594, San Diego, CA (Dec).

10. American Society for Testing Materials. 1987. "Short Rod Fracture Toughness of Cemented Carbides," B771-87, Philadelphia, PA.

11. Smith, P. C. 1992. "Ceramic Hull Reliability Considerations Twenty Weibulls Under the Sea," The Intervention/ROV 92 Committee of The Marine Technology Society, San Diego, CA.

12. Smith, P. C. 1987. "Making Ceramics Tougher," Materials Engineering, Penton Publishing, Inc., Cleveland, OH (Jan).

13. American Society for Testing Materials. 1988. "Standard Test Method for Compressive (Crushing) Strength of Fired Whiteware Materials," C773-88, Philadelphia, PA.

14. American Society for Testing Materials. 1988. "Standard Test Method for Water Absorption, Bulk Density, Apparent Porosity, and Apparent Specific Gravity of Fired Whiteware Products," C373-88, Philadelphia, PA.

15. American Society for Testing Materials. 1988. "Standard Test Method for Young's Modulus, Shear Modulus, and Poisson's Ration for Ceramic Whitewares by Resonance," C848-88, Philadelphia, PA.

16. Swanson Analysis Systems, Inc. 1991. "ANSYS-PC Reference Manual for Revision 4.4A," Houston, PA (May).

GLOSSARY

AL-600	WESGO, Inc. 96-percent aluminum oxide composition
alumina	aluminum oxide
ASTM	American Society for Testing of Materials
AUV	autonomous underwater vehicle
FEA	finite element analysis
FEM	finite element models
flexural strength	modulus of rupture
GFRP	graphite fiber-reinforced plastic
ID	inside diameter
L	Length
L/OD	length-to-outer-diameter ratio
MOR	modulus of rupture
NDE	Nondestructive Evaluation
NOSC	Naval Ocean Systems Center
OD	outside diameter
ROV	remotely operated vehicle
RTV	room-temperature vulcanizing sealant
SF	safety factor (factor of safety)
specific strength	strength-to-density ratio
SWRI	Southwest Research Institute
t	thickness
t/OD	thickness-to-outer-diameter ratio
UUV	unmanned underwater vehicle
W/D	weight-to-displacement ratio
zirconia	zirconium dioxide
ZTA	zirconia-toughened alumina

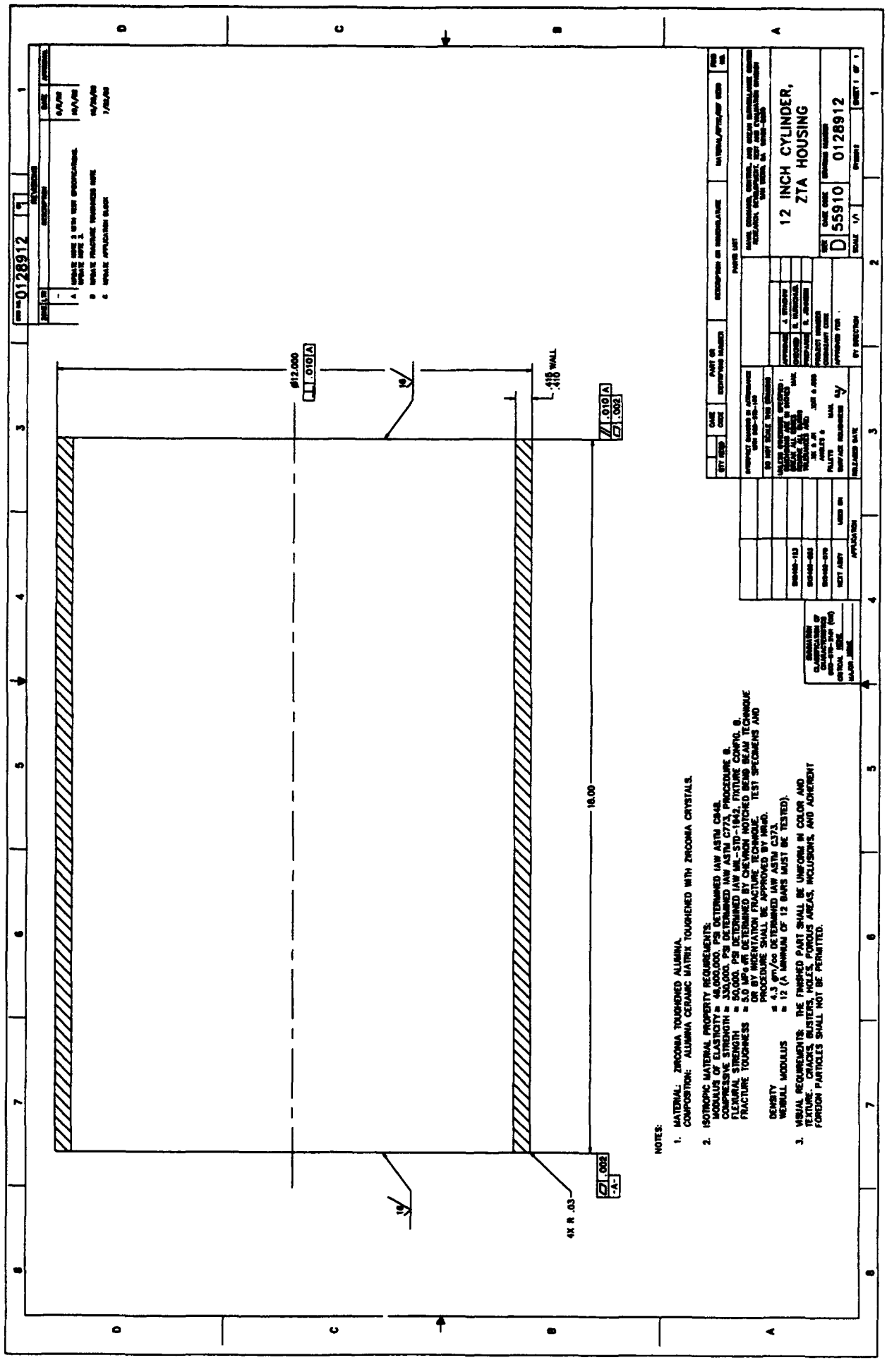

Figure 1. ZTA ceramic 12-inch-OD cylinder.

Figure 2. Pulse-echo C-scan recording of a 6.5-inch-long axial crack detected in cylinder part 005.

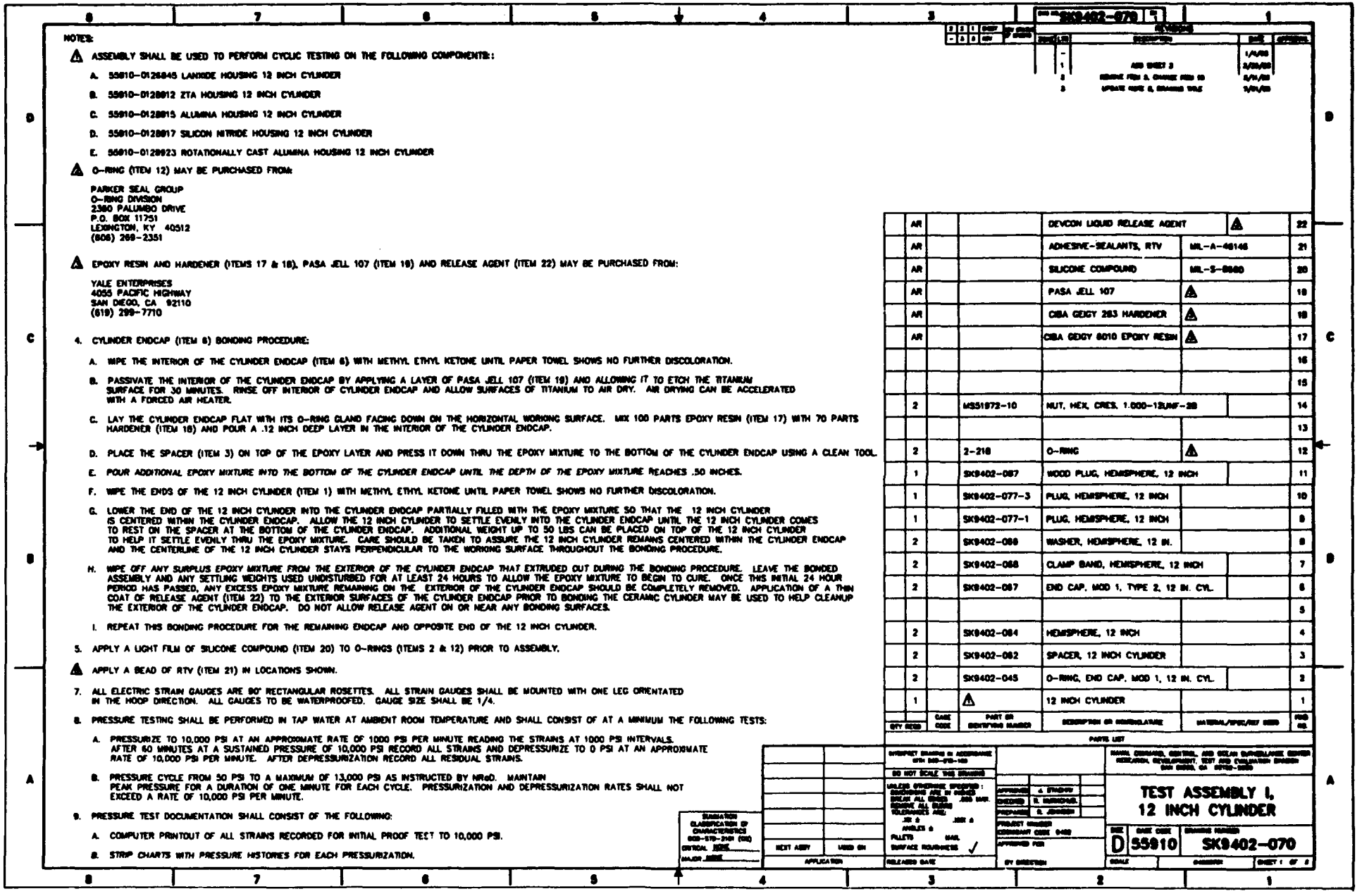

NOTES:

⚠ ASSEMBLY SHALL BE USED TO PERFORM CYCLIC TESTING ON THE FOLLOWING COMPONENTS:

A. 55810-0126845 LANXIDE HOUSING 12 INCH CYLINDER

B. 55810-0128912 ZTA HOUSING 12 INCH CYLINDER

C. 55810-0128915 ALUMINA HOUSING 12 INCH CYLINDER

D. 55810-0128917 SILICON NITRIDE HOUSING 12 INCH CYLINDER

E. 55810-0128923 ROTATIONALLY CAST ALUMINA HOUSING 12 INCH CYLINDER

⚠ O-RING (ITEM 12) MAY BE PURCHASED FROM:

PARKER SEAL GROUP
O-RING DIVISION
2360 PALUMBO DRIVE
P.O. BOX 11751
LEXINGTON, KY 40512
(606) 269-2351

⚠ EPOXY RESIN AND HARDENER (ITEMS 17 & 18), PASA JELL 107 (ITEM 19) AND RELEASE AGENT (ITEM 22) MAY BE PURCHASED FROM:

YALE ENTERPRISES
4055 PACIFIC HIGHWAY
SAN DIEGO, CA 92110
(619) 299-7710

4. CYLINDER ENDCAP (ITEM 6) BONDING PROCEDURE:

A. WIPE THE INTERIOR OF THE CYLINDER ENDCAP (ITEM 6) WITH METHYL ETHYL KETONE UNTIL PAPER TOWEL SHOWS NO FURTHER DISCOLORATION.

B. PASSIVATE THE INTERIOR OF THE CYLINDER ENDCAP BY APPLYING A LAYER OF PASA JELL 107 (ITEM 19) AND ALLOWING IT TO ETCH THE TITANIUM SURFACE FOR 30 MINUTES. RINSE OFF INTERIOR OF CYLINDER ENDCAP AND ALLOW SURFACES OF TITANIUM TO AIR DRY. AIR DRYING CAN BE ACCELERATED WITH A FORCED AIR HEATER.

C. LAY THE CYLINDER ENDCAP FLAT WITH ITS O-RING GLAND FACING DOWN ON THE HORIZONTAL WORKING SURFACE. MIX 100 PARTS EPOXY RESIN (ITEM 17) WITH 70 PARTS HARDENER (ITEM 18) AND POUR A .12 INCH DEEP LAYER IN THE INTERIOR OF THE CYLINDER ENDCAP.

D. PLACE THE SPACER (ITEM 3) ON TOP OF THE EPOXY LAYER AND PRESS IT DOWN THRU THE EPOXY MIXTURE TO THE BOTTOM OF THE CYLINDER ENDCAP USING A CLEAN TOOL.

E. POUR ADDITIONAL EPOXY MIXTURE INTO THE BOTTOM OF THE CYLINDER ENDCAP UNTIL THE DEPTH OF THE EPOXY MIXTURE REACHES .50 INCHES.

F. WIPE THE ENDS OF THE 12 INCH CYLINDER (ITEM 1) WITH METHYL ETHYL KETONE UNTIL PAPER TOWEL SHOWS NO FURTHER DISCOLORATION.

G. LOWER THE END OF THE 12 INCH CYLINDER INTO THE CYLINDER ENDCAP PARTIALLY FILLED WITH THE EPOXY MIXTURE SO THAT THE 12 INCH CYLINDER IS CENTERED WITHIN THE CYLINDER ENDCAP. ALLOW THE 12 INCH CYLINDER TO SETTLE EVENLY INTO THE CYLINDER ENDCAP UNTIL THE 12 INCH CYLINDER COMES TO REST ON THE SPACER AT THE BOTTOM OF THE CYLINDER ENDCAP. ADDITIONAL WEIGHT UP TO 50 LBS CAN BE PLACED ON TOP OF THE 12 INCH CYLINDER TO HELP IT SETTLE EVENLY THRU THE EPOXY MIXTURE. CARE SHOULD BE TAKEN TO ASSURE THE 12 INCH CYLINDER REMAINS CENTERED WITHIN THE CYLINDER ENDCAP AND THE CENTERLINE OF THE 12 INCH CYLINDER STAYS PERPENDICULAR TO THE WORKING SURFACE THROUGHOUT THE BONDING PROCEDURE.

H. WIPE OFF ANY SURPLUS EPOXY MIXTURE FROM THE EXTERIOR OF THE CYLINDER ENDCAP THAT EXTRUDED OUT DURING THE BONDING PROCEDURE. LEAVE THE BONDED ASSEMBLY AND ANY SETTLING WEIGHTS USED UNDISTURBED FOR AT LEAST 24 HOURS TO ALLOW THE EPOXY MIXTURE TO BEGIN TO CURE. ONCE THIS INITIAL 24 HOUR PERIOD HAS PASSED, ANY EXCESS EPOXY MIXTURE REMAINING ON THE EXTERIOR OF THE CYLINDER ENDCAP SHOULD BE COMPLETELY REMOVED. APPLICATION OF A THIN COAT OF RELEASE AGENT (ITEM 22) TO THE EXTERIOR SURFACES OF THE CYLINDER ENDCAP PRIOR TO BONDING THE CERAMIC CYLINDER MAY BE USED TO HELP CLEANUP THE EXTERIOR OF THE CYLINDER ENDCAP. DO NOT ALLOW RELEASE AGENT ON OR NEAR ANY BONDING SURFACES.

I. REPEAT THIS BONDING PROCEDURE FOR THE REMAINING ENDCAP AND OPPOSITE END OF THE 12 INCH CYLINDER.

5. APPLY A LIGHT FILM OF SILICONE COMPOUND (ITEM 20) TO O-RINGS (ITEMS 2 & 12) PRIOR TO ASSEMBLY.

⚠ APPLY A BEAD OF RTV (ITEM 21) IN LOCATIONS SHOWN.

7. ALL ELECTRIC STRAIN GAUGES ARE 90° RECTANGULAR ROSETTES. ALL STRAIN GAUGES SHALL BE MOUNTED WITH ONE LEG ORIENTATED IN THE HOOP DIRECTION. ALL GAUGES TO BE WATERPROOFED. GAUGE SIZE SHALL BE 1/4.

8. PRESSURE TESTING SHALL BE PERFORMED IN TAP WATER AT AMBIENT ROOM TEMPERATURE AND SHALL CONSIST OF AT A MINIMUM THE FOLLOWING TESTS:

A. PRESSURIZE TO 10,000 PSI AT AN APPROXIMATE RATE OF 1000 PSI PER MINUTE READING THE STRAINS AT 1000 PSI INTERVALS. AFTER 60 MINUTES AT A SUSTAINED PRESSURE OF 10,000 PSI RECORD ALL STRAINS AND DEPRESSURIZE TO 0 PSI AT AN APPROXIMATE RATE OF 10,000 PSI PER MINUTE. AFTER DEPRESSURIZATION RECORD ALL RESIDUAL STRAINS.

B. PRESSURE CYCLE FROM 50 PSI TO A MAXIMUM OF 13,000 PSI AS INSTRUCTED BY NRaD. MAINTAIN PEAK PRESSURE FOR A DURATION OF ONE MINUTE FOR EACH CYCLE. PRESSURIZATION AND DEPRESSURIZATION RATES SHALL NOT EXCEED A RATE OF 10,000 PSI PER MINUTE.

9. PRESSURE TEST DOCUMENTATION SHALL CONSIST OF THE FOLLOWING:

A. COMPUTER PRINTOUT OF ALL STRAINS RECORDED FOR INITIAL PROOF TEST TO 10,000 PSI.

B. STRIP CHARTS WITH PRESSURE HISTORIES FOR EACH PRESSURIZATION.

QTY REQD	CAGE CODE	PART OR IDENTIFYING NUMBER	DESCRIPTION OR NOMENCLATURE	MATERIAL/SPEC/GRADE	FIND NO.
AR			DEVCON LIQUID RELEASE AGENT ⚠		22
AR			ADHESIVE-SEALANTS, RTV	MIL-A-46146	21
AR			SILICONE COMPOUND	MIL-S-8660	20
AR			PASA JELL 107 ⚠		19
AR			CIBA GEIGY 283 HARDENER ⚠		18
AR			CIBA GEIGY 8010 EPOXY RESIN ⚠		17
					16
					15
2		MS51972-10	NUT, HEX, CRES, 1.000-12UNF-2B		14
					13
2		2-218	O-RING ⚠		12
1		SK9402-087	WOOD PLUG, HEMISPHERE, 12 INCH		11
1		SK9402-077-3	PLUG, HEMISPHERE, 12 INCH		10
1		SK9402-077-1	PLUG, HEMISPHERE, 12 INCH		9
2		SK9402-088	WASHER, HEMISPHERE, 12 IN.		8
2		SK9402-068	CLAMP BAND, HEMISPHERE, 12 INCH		7
2		SK9402-067	END CAP, MOD 1, TYPE 2, 12 IN. CYL.		6
					5
2		SK9402-064	HEMISPHERE, 12 INCH		4
2		SK9402-062	SPACER, 12 INCH CYLINDER		3
2		SK9402-045	O-RING, END CAP, MOD 1, 12 IN. CYL.		2
1		⚠	12 INCH CYLINDER		1

PARTS LIST

REV LTR	DESCRIPTION	DATE	APPROVED
-		1/4/93	
1	ADD SHEET 3	2/23/93	
2	REVISE ITEM 3, CHANGE REQ TO	5/11/93	
3	UPDATE NOTE 6, DRAWING TREE	7/21/93	

DWG NO. SK9402-070 REV 3

DO NOT SCALE THIS DRAWING

UNLESS OTHERWISE SPECIFIED: DIMENSIONS ARE IN INCHES. BREAK ALL EDGES .005 MAX. REMOVE ALL BURRS AND SHARP EDGES. TOLERANCES ARE: .XX ± .01 .XXX ± ANGLES ± FILLETS MAX. SURFACE ROUGHNESS ✓

NEXT ASSY | USED ON | APPLICATION | RELEASED DATE

SUMMATION CLASSIFICATION OF CHARACTERISTICS DOD-STD-2101 (NAVY) CRITICAL NONE MAJOR NONE

APPROVED A. STACHOW
CHECKED R. HARRIGAN
PREPARED R. JOHNSON
PROJECT ENGINEER
CONTRACT CODE 0402
APPROVED FOR
BY DIRECTION

NAVAL COMMAND, CONTROL AND OCEAN SURVEILLANCE CENTER RESEARCH, DEVELOPMENT, TEST AND EVALUATION DIVISION SAN DIEGO, CA 92152-5000

TEST ASSEMBLY I, 12 INCH CYLINDER

SIZE D | CAGE CODE 55910 | DRAWING NUMBER SK9402-070
SCALE | DRAWN | SHEET 1 OF 3

Figure 3. 12-inch cylinder test assembly I configuration, Sheet 1.

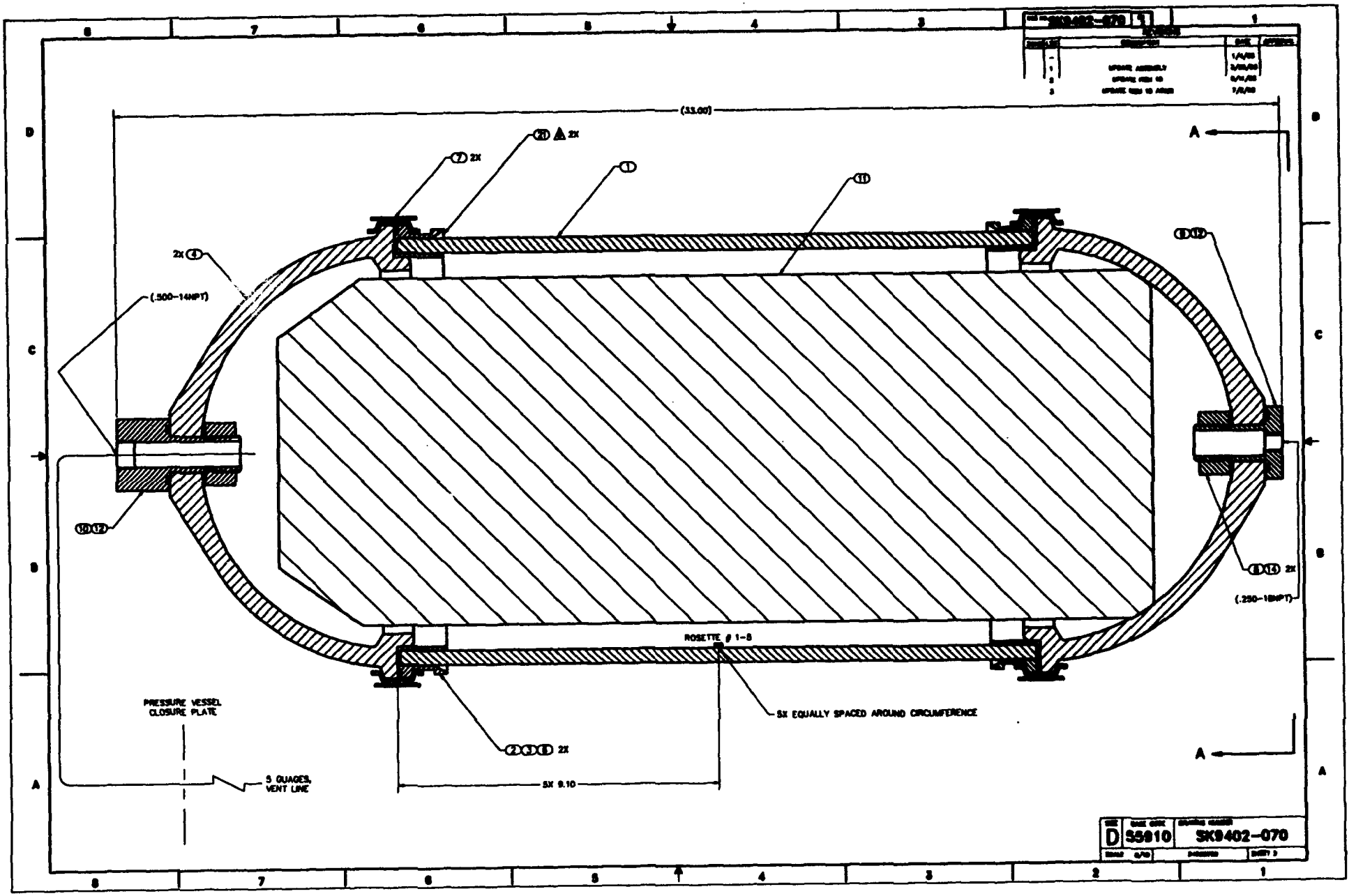

Figure 3. 12-inch cylinder test assembly I configuration, Sheet 2.

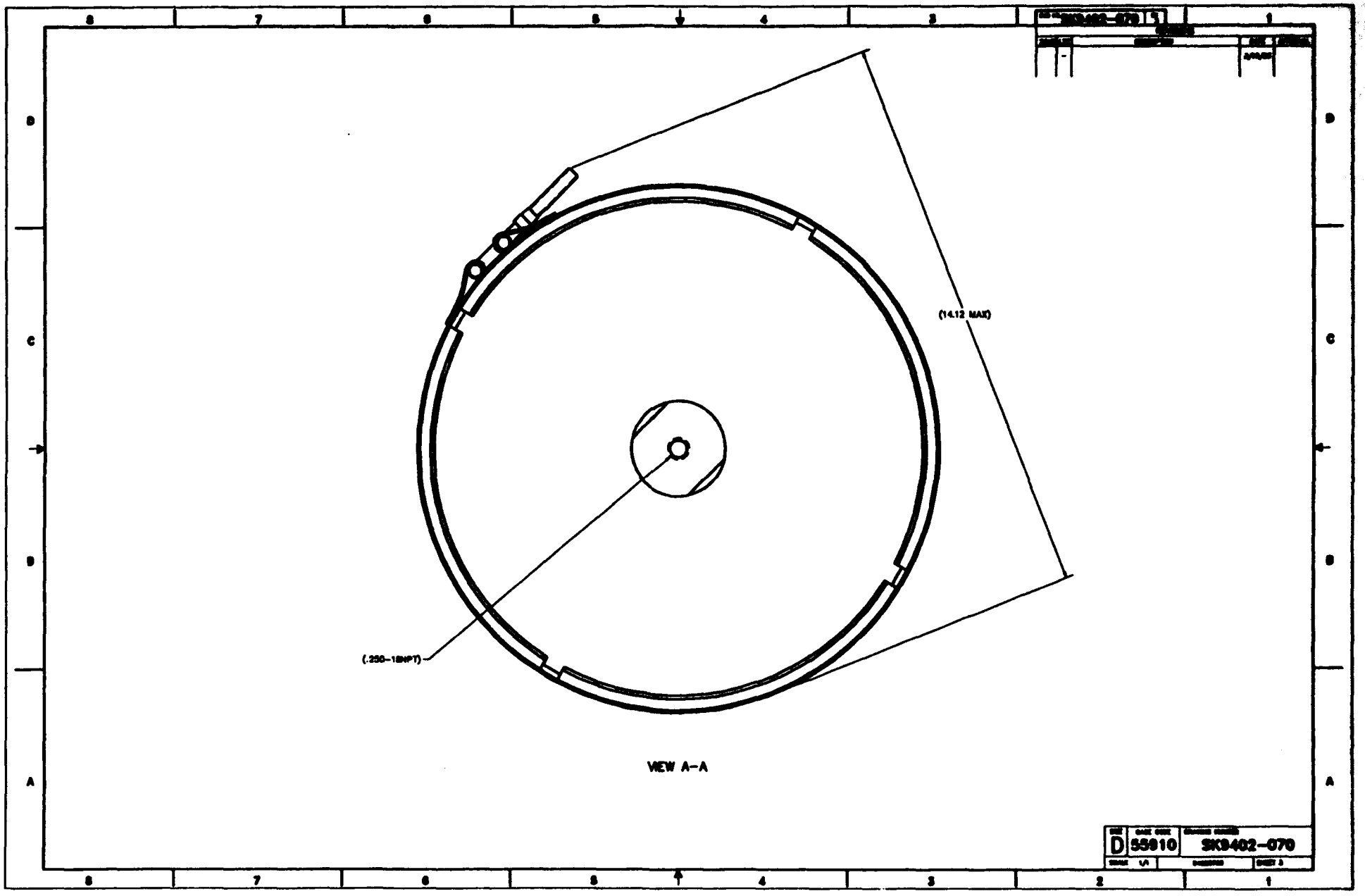

Figure 3. 12-inch cylinder test assembly I configuration, Sheet 3.

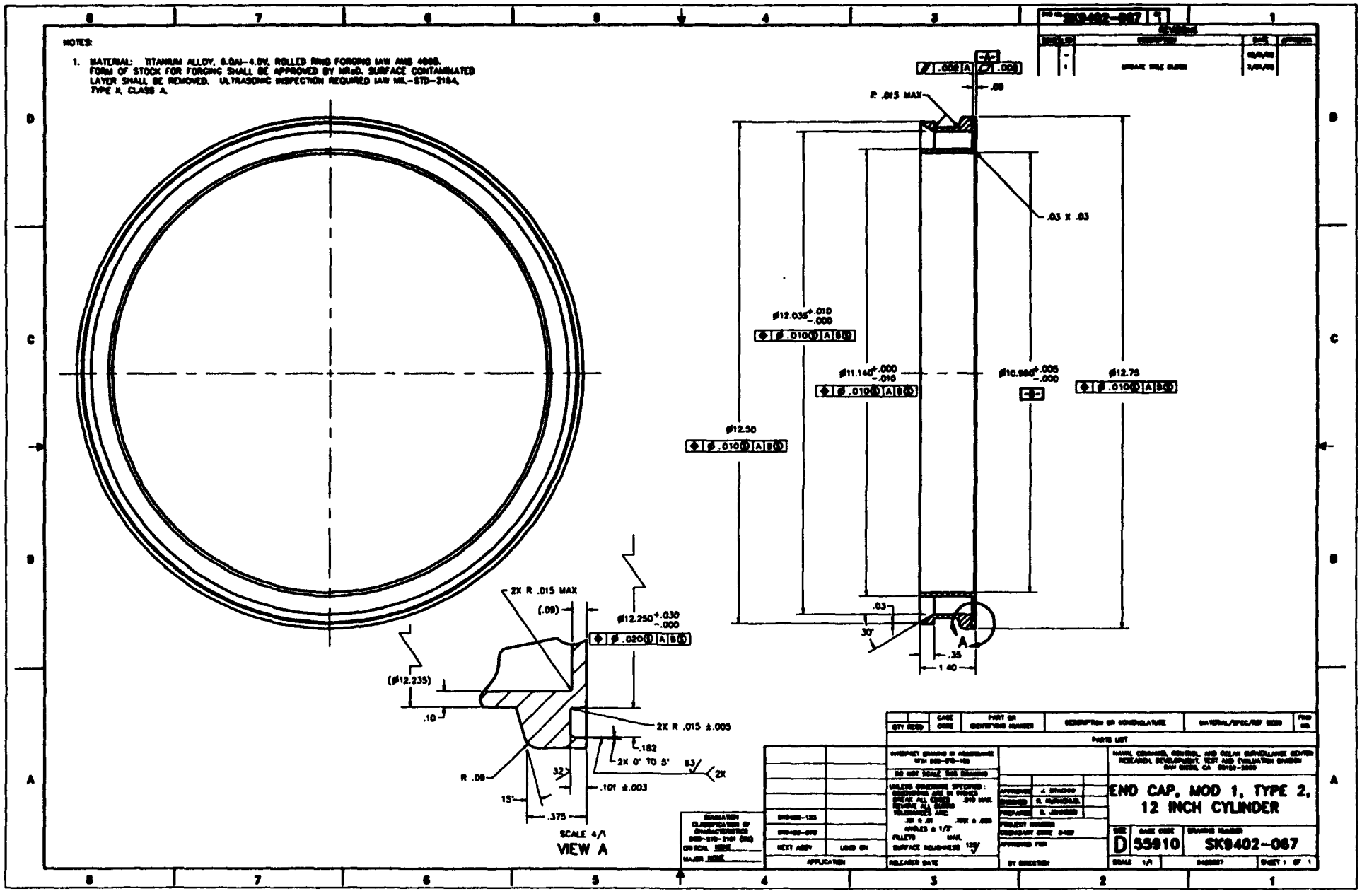

Figure 4. 12-inch cylinder Mod 1, Type 2 end-cap joint ring.

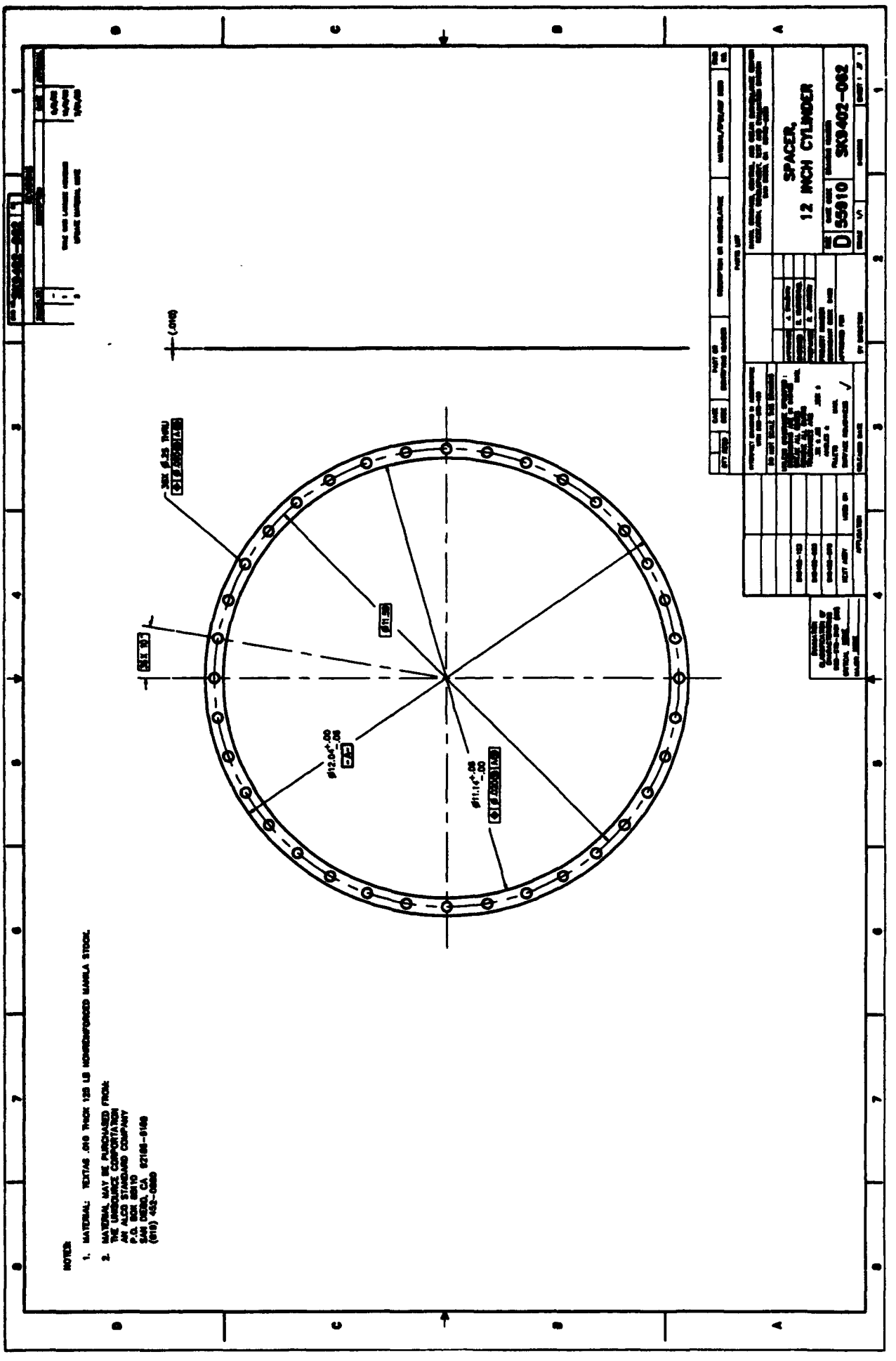

Figure 5. 12-inch cylinder spacer.

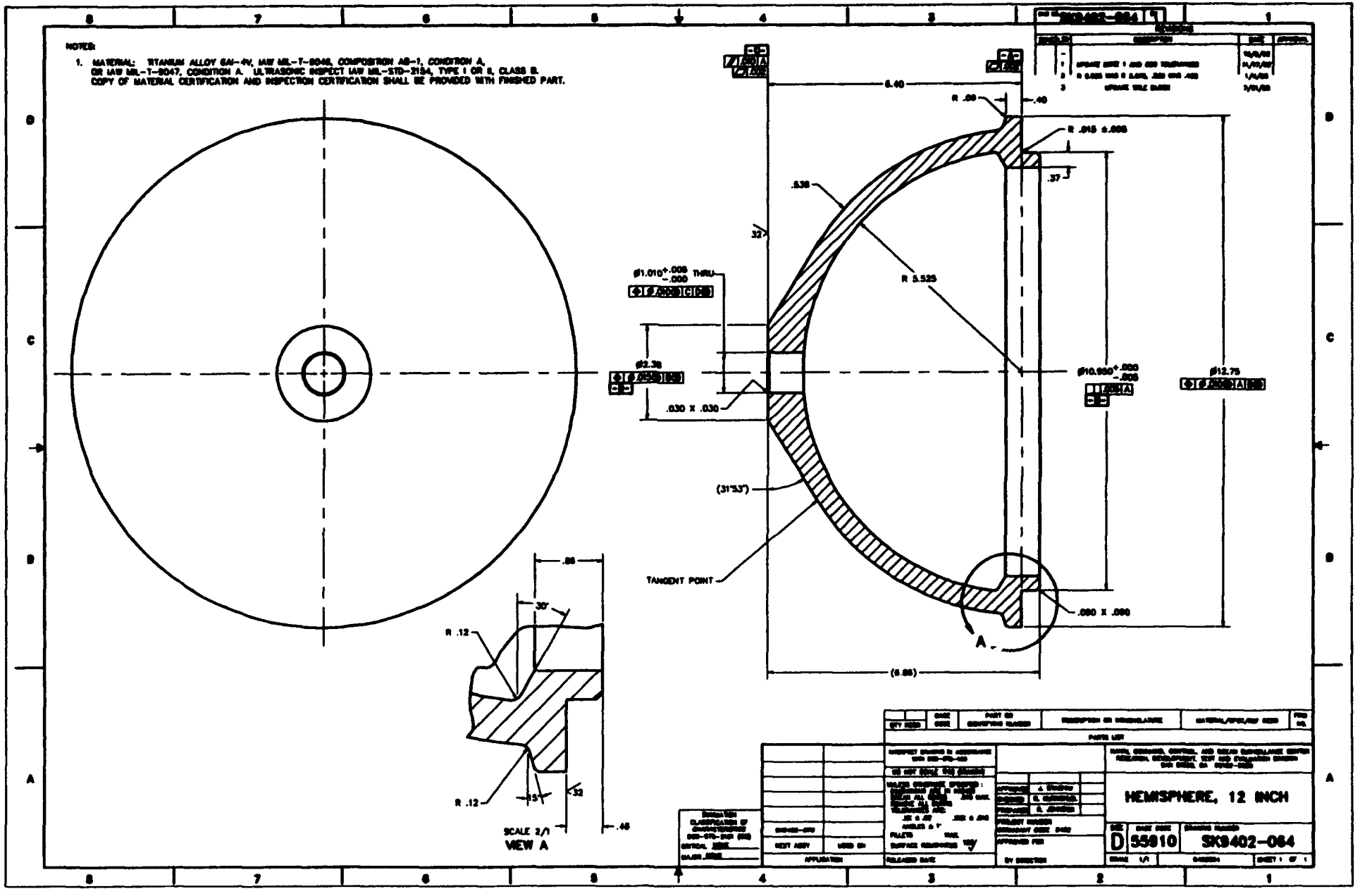

Figure 6. 12-inch hemisphere.

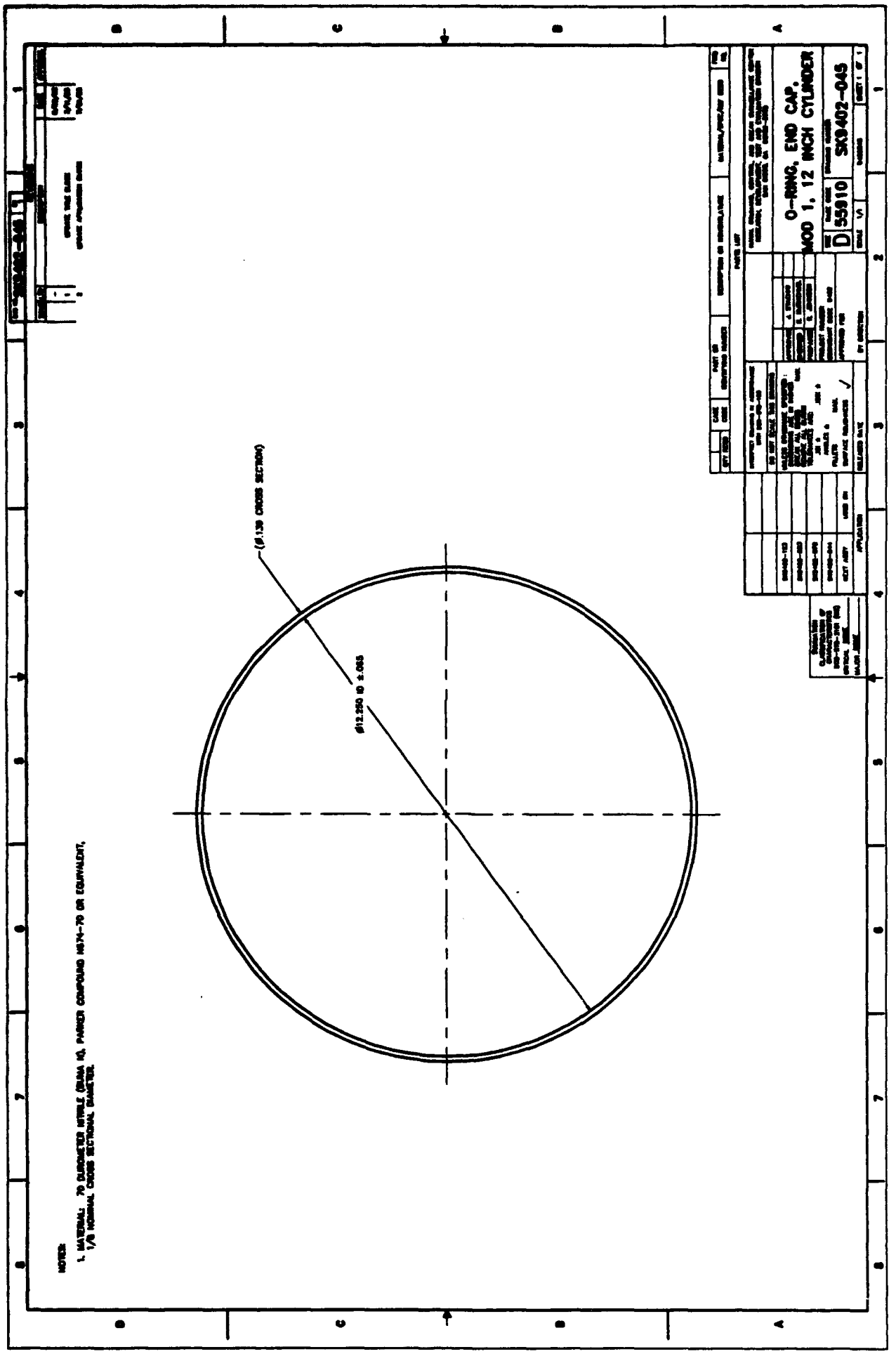

Figure 7. 12-inch cylinder Mod 1 end-cap joint ring O-ring.

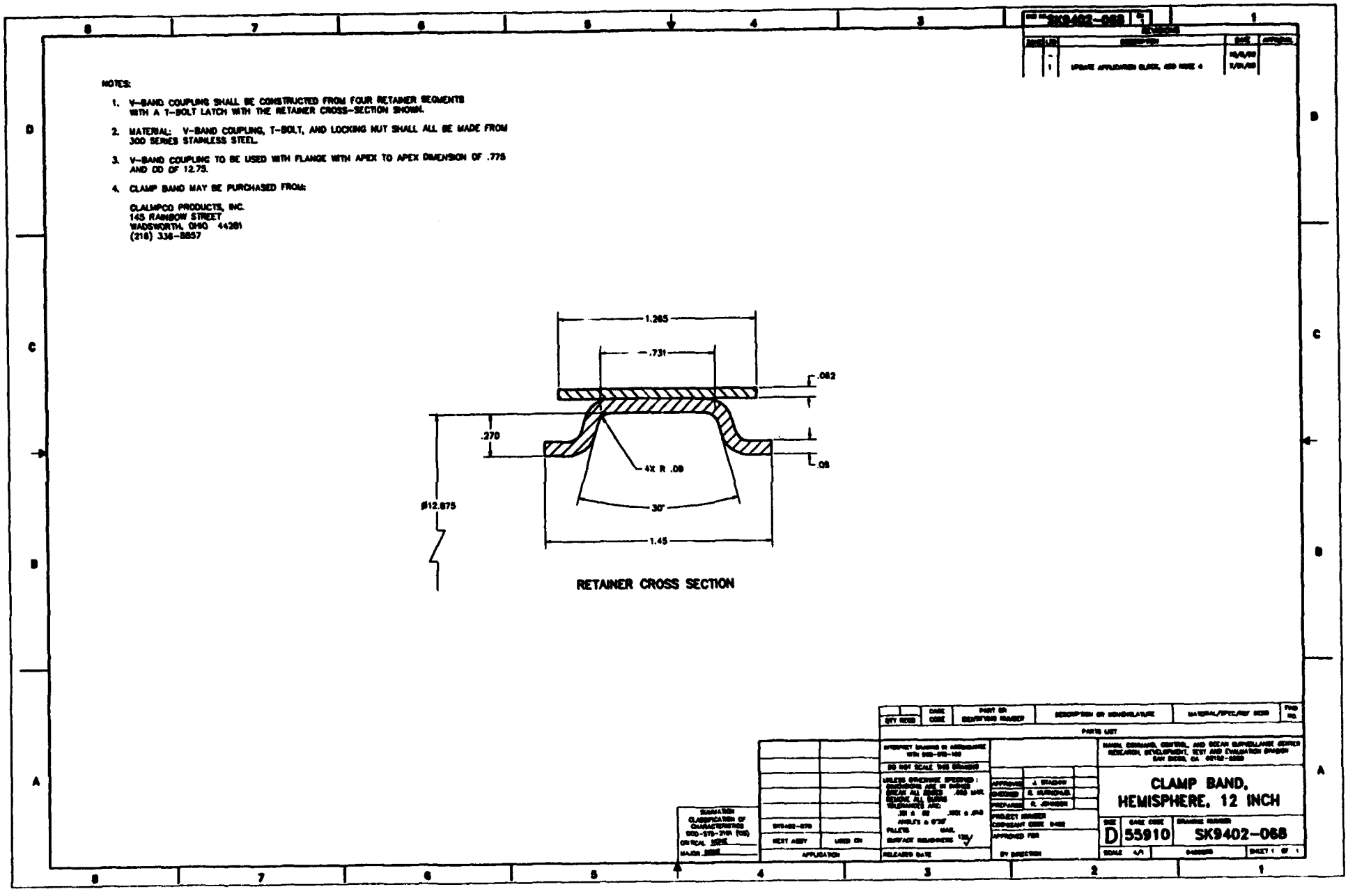

Figure 8. 12-inch hemisphere clamp band.

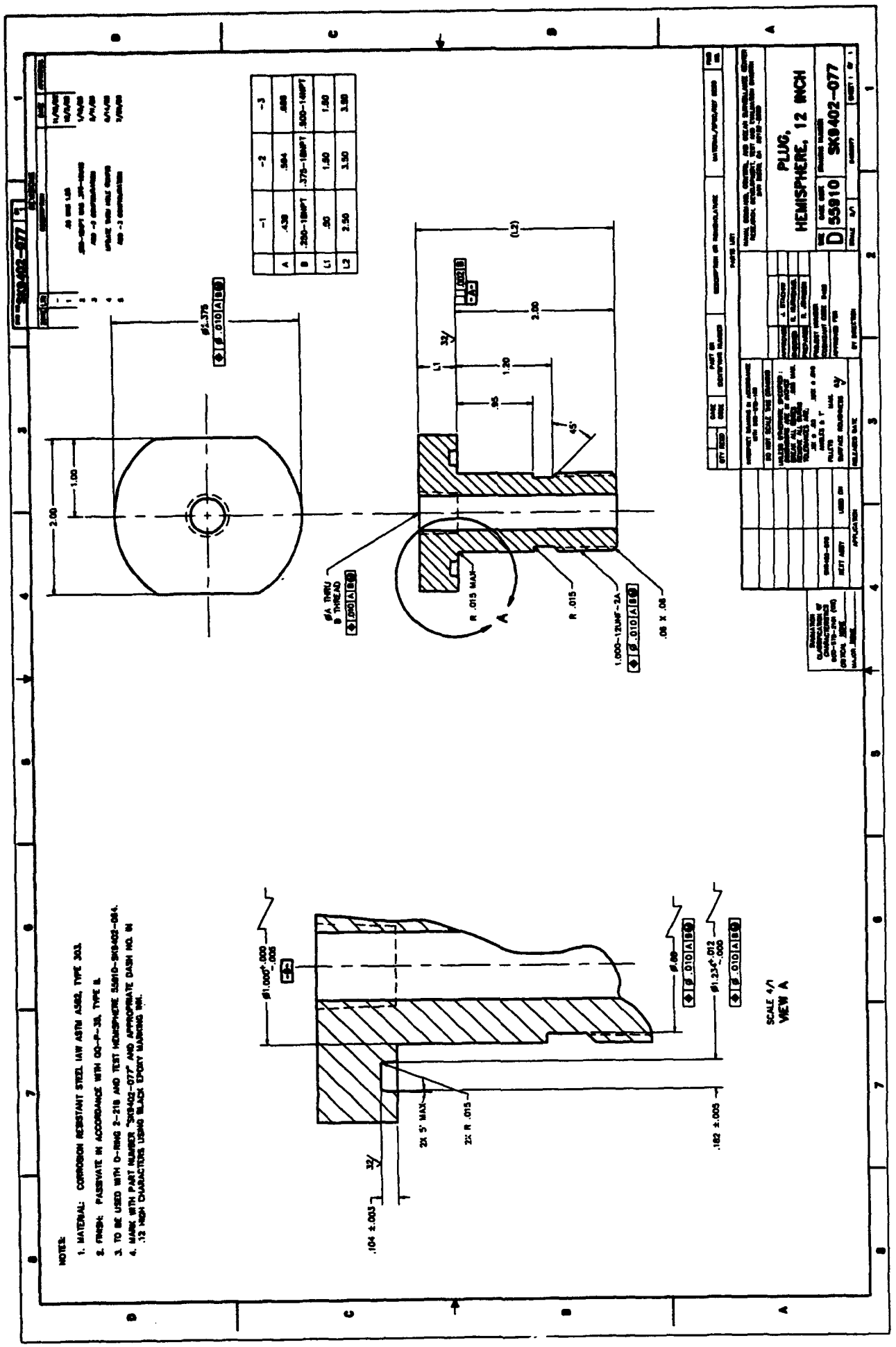

Figure 9. 12-inch hemisphere plug.

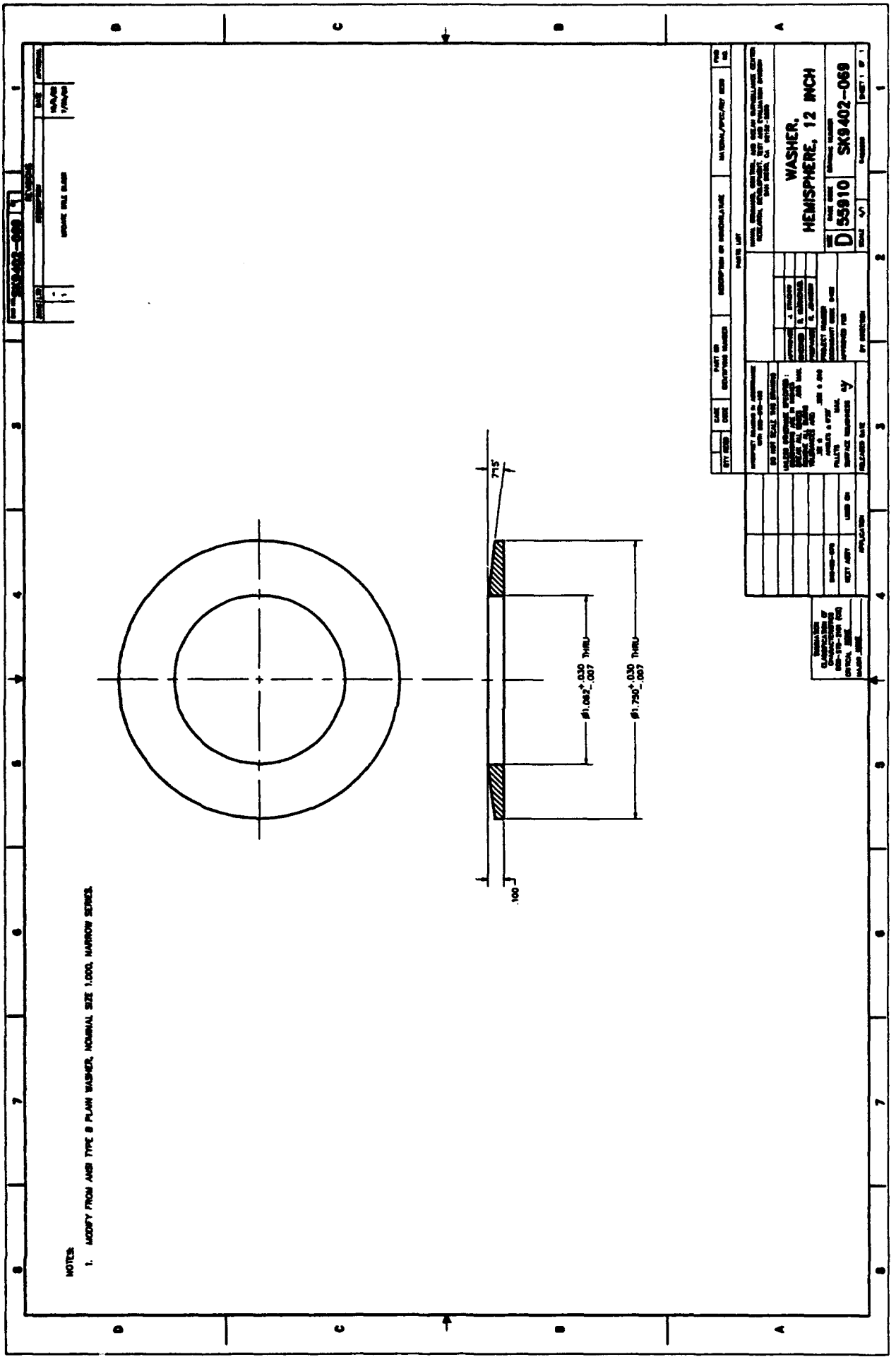

Figure 10. 12-inch hemisphere washer.

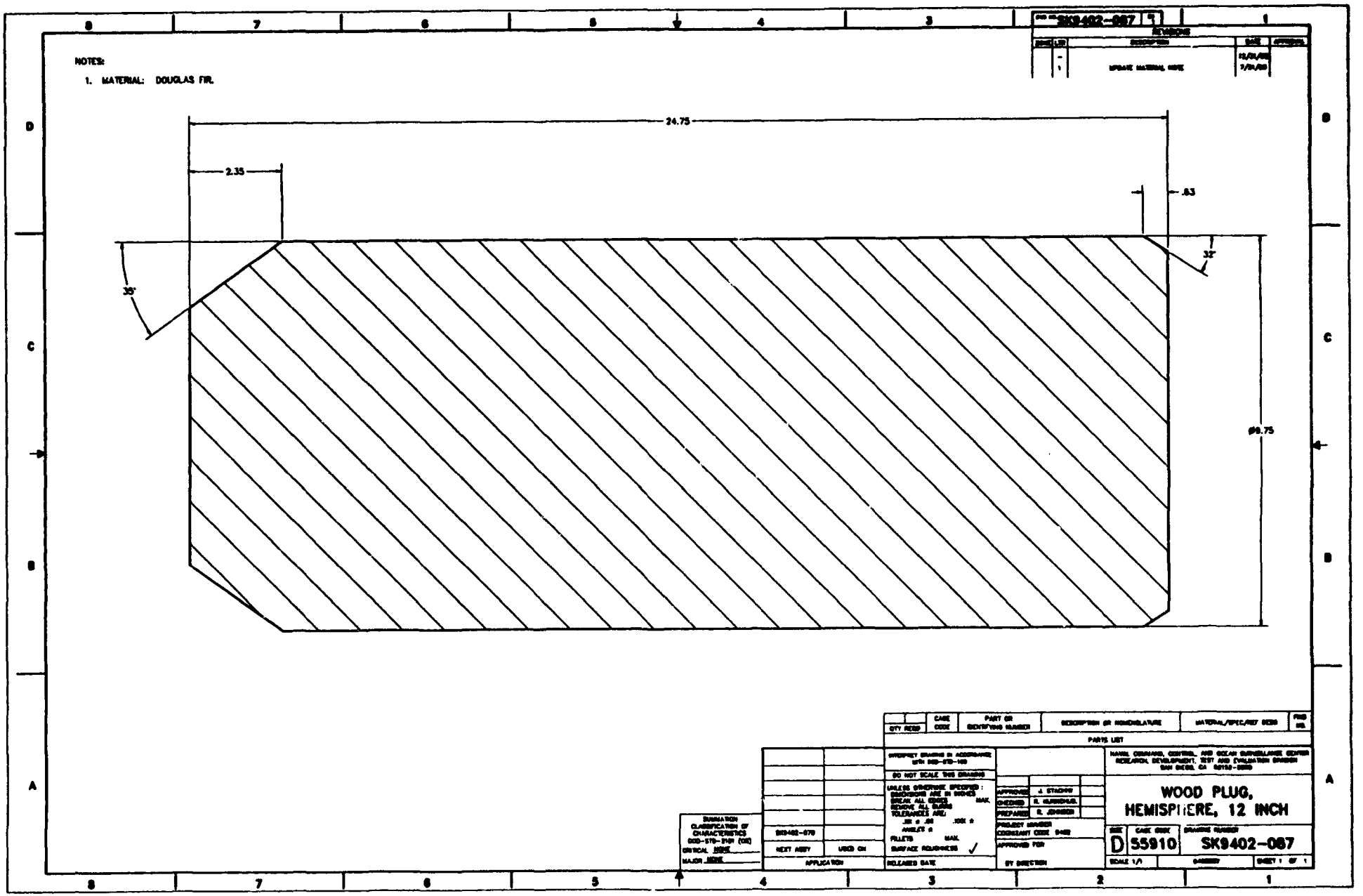

Figure 11. 12-inch hemisphere wood plug.

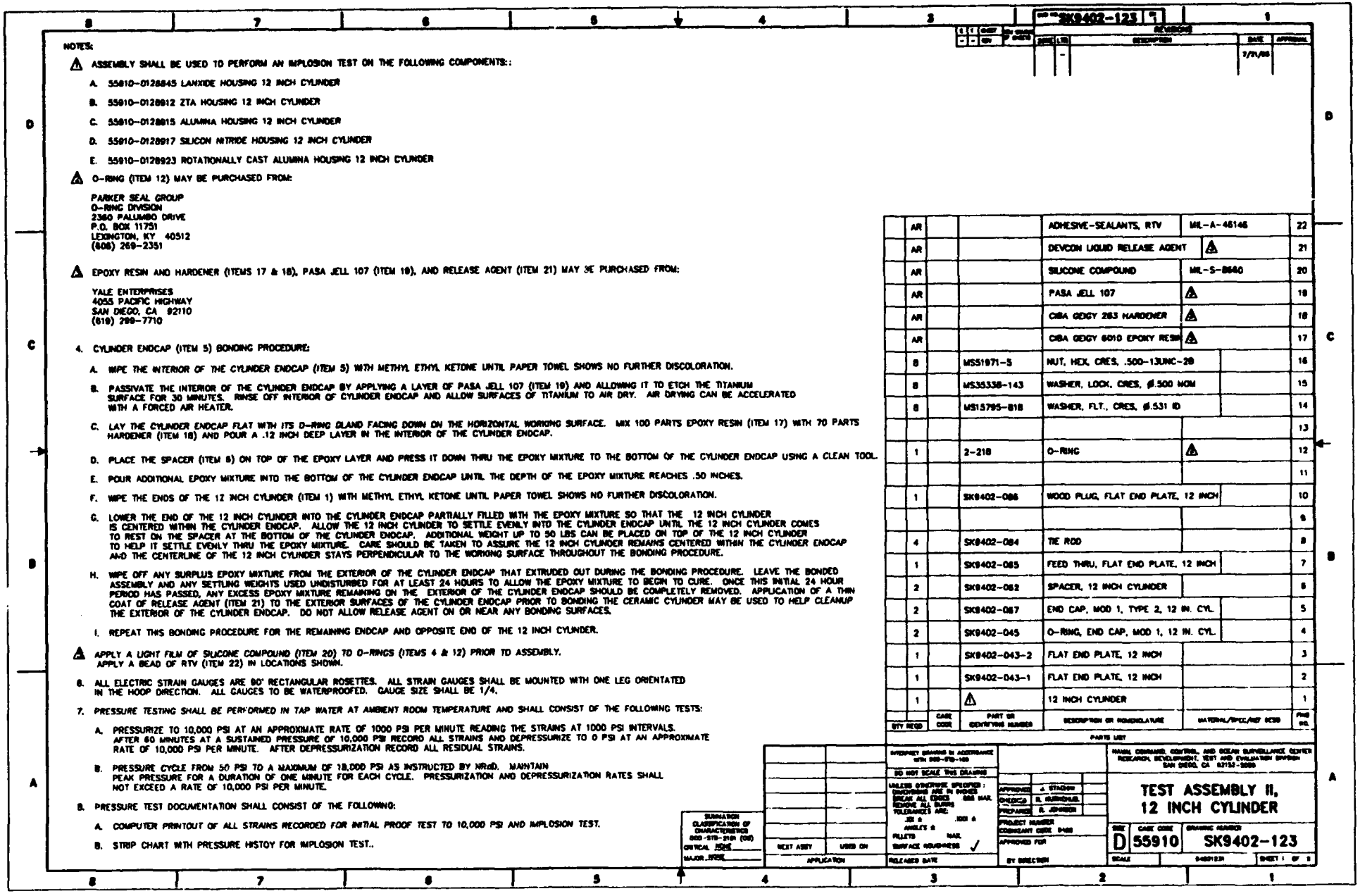

NOTES:

1. ⚠ ASSEMBLY SHALL BE USED TO PERFORM AN IMPLOSION TEST ON THE FOLLOWING COMPONENTS::
   - A. 55910-0128845 LANXIDE HOUSING 12 INCH CYLINDER
   - B. 55910-0128912 ZTA HOUSING 12 INCH CYLINDER
   - C. 55910-0128915 ALUMINA HOUSING 12 INCH CYLINDER
   - D. 55910-0128917 SILICON NITRIDE HOUSING 12 INCH CYLINDER
   - E. 55910-0128923 ROTATIONALLY CAST ALUMINA HOUSING 12 INCH CYLINDER
2. ⚠ O-RING (ITEM 12) MAY BE PURCHASED FROM:

   PARKER SEAL GROUP
   O-RING DIVISION
   2360 PALUMBO DRIVE
   P.O. BOX 11751
   LEXINGTON, KY 40512
   (606) 269-2351

3. ⚠ EPOXY RESIN AND HARDENER (ITEMS 17 & 18), PASA JELL 107 (ITEM 19), AND RELEASE AGENT (ITEM 21) MAY BE PURCHASED FROM:

   YALE ENTERPRISES
   4055 PACIFIC HIGHWAY
   SAN DIEGO, CA 92110
   (619) 299-7710

4. CYLINDER ENDCAP (ITEM 5) BONDING PROCEDURE:
   - A. WIPE THE INTERIOR OF THE CYLINDER ENDCAP (ITEM 5) WITH METHYL ETHYL KETONE UNTIL PAPER TOWEL SHOWS NO FURTHER DISCOLORATION.
   - B. PASSIVATE THE INTERIOR OF THE CYLINDER ENDCAP BY APPLYING A LAYER OF PASA JELL 107 (ITEM 19) AND ALLOWING IT TO ETCH THE TITANIUM SURFACE FOR 30 MINUTES. RINSE OFF INTERIOR OF CYLINDER ENDCAP AND ALLOW SURFACES OF TITANIUM TO AIR DRY. AIR DRYING CAN BE ACCELERATED WITH A FORCED AIR HEATER.
   - C. LAY THE CYLINDER ENDCAP FLAT WITH ITS O-RING GLAND FACING DOWN ON THE HORIZONTAL WORKING SURFACE. MIX 100 PARTS EPOXY RESIN (ITEM 17) WITH 70 PARTS HARDENER (ITEM 18) AND POUR A .12 INCH DEEP LAYER IN THE INTERIOR OF THE CYLINDER ENDCAP.
   - D. PLACE THE SPACER (ITEM 6) ON TOP OF THE EPOXY LAYER AND PRESS IT DOWN THRU THE EPOXY MIXTURE TO THE BOTTOM OF THE CYLINDER ENDCAP USING A CLEAN TOOL.
   - E. POUR ADDITIONAL EPOXY MIXTURE INTO THE BOTTOM OF THE CYLINDER ENDCAP UNTIL THE DEPTH OF THE EPOXY MIXTURE REACHES .50 INCHES.
   - F. WIPE THE ENDS OF THE 12 INCH CYLINDER (ITEM 1) WITH METHYL ETHYL KETONE UNTIL PAPER TOWEL SHOWS NO FURTHER DISCOLORATION.
   - G. LOWER THE END OF THE 12 INCH CYLINDER INTO THE CYLINDER ENDCAP PARTIALLY FILLED WITH THE EPOXY MIXTURE SO THAT THE 12 INCH CYLINDER IS CENTERED WITHIN THE CYLINDER ENDCAP. ALLOW THE 12 INCH CYLINDER TO SETTLE EVENLY INTO THE CYLINDER ENDCAP UNTIL THE 12 INCH CYLINDER COMES TO REST ON THE SPACER AT THE BOTTOM OF THE CYLINDER ENDCAP. ADDITIONAL WEIGHT UP TO 50 LBS CAN BE PLACED ON TOP OF THE 12 INCH CYLINDER TO HELP IT SETTLE EVENLY THRU THE EPOXY MIXTURE. CARE SHOULD BE TAKEN TO ASSURE THE 12 INCH CYLINDER REMAINS CENTERED WITHIN THE CYLINDER ENDCAP AND THE CENTERLINE OF THE 12 INCH CYLINDER STAYS PERPENDICULAR TO THE WORKING SURFACE THROUGHOUT THE BONDING PROCEDURE.
   - H. WIPE OFF ANY SURPLUS EPOXY MIXTURE FROM THE EXTERIOR OF THE CYLINDER ENDCAP THAT EXTRUDED OUT DURING THE BONDING PROCEDURE. LEAVE THE BONDED ASSEMBLY AND ANY SETTLING WEIGHTS USED UNDISTURBED FOR AT LEAST 24 HOURS TO ALLOW THE EPOXY MIXTURE TO BEGIN TO CURE. ONCE THIS INITIAL 24 HOUR PERIOD HAS PASSED, ANY EXCESS EPOXY MIXTURE REMAINING ON THE EXTERIOR OF THE CYLINDER ENDCAP SHOULD BE COMPLETELY REMOVED. APPLICATION OF A THIN COAT OF RELEASE AGENT (ITEM 21) TO THE EXTERIOR SURFACES OF THE CYLINDER ENDCAP PRIOR TO BONDING THE CERAMIC CYLINDER MAY BE USED TO HELP CLEANUP THE EXTERIOR OF THE CYLINDER ENDCAP. DO NOT ALLOW RELEASE AGENT ON OR NEAR ANY BONDING SURFACES.
   - I. REPEAT THIS BONDING PROCEDURE FOR THE REMAINING ENDCAP AND OPPOSITE END OF THE 12 INCH CYLINDER.
5. ⚠ APPLY A LIGHT FILM OF SILICONE COMPOUND (ITEM 20) TO O-RINGS (ITEMS 4 & 12) PRIOR TO ASSEMBLY. APPLY A BEAD OF RTV (ITEM 22) IN LOCATIONS SHOWN.
6. ALL ELECTRIC STRAIN GAUGES ARE 90° RECTANGULAR ROSETTES. ALL STRAIN GAUGES SHALL BE MOUNTED WITH ONE LEG ORIENTATED IN THE HOOP DIRECTION. ALL GAUGES TO BE WATERPROOFED. GAUGE SIZE SHALL BE 1/4.
7. PRESSURE TESTING SHALL BE PERFORMED IN TAP WATER AT AMBIENT ROOM TEMPERATURE AND SHALL CONSIST OF THE FOLLOWING TESTS:
   - A. PRESSURIZE TO 10,000 PSI AT AN APPROXIMATE RATE OF 1000 PSI PER MINUTE READING THE STRAINS AT 1000 PSI INTERVALS. AFTER 60 MINUTES AT A SUSTAINED PRESSURE OF 10,000 PSI RECORD ALL STRAINS AND DEPRESSURIZE TO 0 PSI AT AN APPROXIMATE RATE OF 10,000 PSI PER MINUTE. AFTER DEPRESSURIZATION RECORD ALL RESIDUAL STRAINS.
   - B. PRESSURE CYCLE FROM 50 PSI TO A MAXIMUM OF 18,000 PSI AS INSTRUCTED BY NRaD. MAINTAIN PEAK PRESSURE FOR A DURATION OF ONE MINUTE FOR EACH CYCLE. PRESSURIZATION AND DEPRESSURIZATION RATES SHALL NOT EXCEED A RATE OF 10,000 PSI PER MINUTE.
8. PRESSURE TEST DOCUMENTATION SHALL CONSIST OF THE FOLLOWING:
   - A. COMPUTER PRINTOUT OF ALL STRAINS RECORDED FOR INITIAL PROOF TEST TO 10,000 PSI AND IMPLOSION TEST.
   - B. STRIP CHART WITH PRESSURE HISTOY FOR IMPLOSION TEST..

QTY REQD	CAGE CODE	PART OR IDENTIFYING NUMBER	DESCRIPTION OR NOMENCLATURE	MATERIAL/SPEC/ASY DESIG	FIND NO.
AR			ADHESIVE-SEALANTS, RTV	MIL-A-46146	22
AR			DEVCON LIQUID RELEASE AGENT	⚠	21
AR			SILICONE COMPOUND	MIL-S-8660	20
AR			PASA JELL 107	⚠	19
AR			CIBA GEIGY 283 HARDENER	⚠	18
AR			CIBA GEIGY 6010 EPOXY RESIN	⚠	17
8		MS51971-5	NUT, HEX, CRES, .500-13UNC-2B		16
8		MS35338-143	WASHER, LOCK, CRES, ø.500 NOM		15
8		MS15795-818	WASHER, FLT., CRES, ø.531 ID		14
					13
1		2-218	O-RING	⚠	12
					11
1		SK9402-086	WOOD PLUG, FLAT END PLATE, 12 INCH		10
					9
4		SK9402-084	TIE ROD		8
1		SK9402-085	FEED THRU, FLAT END PLATE, 12 INCH		7
2		SK9402-082	SPACER, 12 INCH CYLINDER		6
2		SK9402-087	END CAP, MOD 1, TYPE 2, 12 IN. CYL.		5
2		SK9402-045	O-RING, END CAP, MOD 1, 12 IN. CYL.		4
1		SK9402-043-2	FLAT END PLATE, 12 INCH		3
1		SK9402-043-1	FLAT END PLATE, 12 INCH		2
1		⚠	12 INCH CYLINDER		1

PARTS LIST

REV	ZONE	DESCRIPTION	DATE	APPROVAL
	-		7/21/88	

SK9402-123

NEXT ASSY | USED ON | APPLICATION

INTERPRET DRAWING IN ACCORDANCE WITH 000-STD-100

DO NOT SCALE THIS DRAWING

UNLESS OTHERWISE SPECIFIED: DIMENSIONS ARE IN INCHES. BREAK ALL EDGES .005 MAX. REMOVE ALL BURRS. TOLERANCES ARE: .XX ± .010, .XXX ± .005, ANGLES ± 1°, FILLETS .005 MAX. SURFACE ROUGHNESS ✓

RELEASED DATE

APPROVED A. STACHOW
CHECKED R. HUMPHRIES
PREPARED R. JOHNSON

PROJECT NUMBER
CONSTRAINT CODE 0460
APPROVED FOR
BY DIRECTION

NAVAL COMMAND, CONTROL, AND OCEAN SURVEILLANCE CENTER RESEARCH, DEVELOPMENT, TEST AND EVALUATION DIVISION SAN DIEGO, CA 92152-5000

TEST ASSEMBLY II, 12 INCH CYLINDER

SIZE D | CAGE CODE 55910 | DRAWING NUMBER SK9402-123

SCALE | SHEET 1 OF 3

SUMMARIZE CLASSIFICATION OF CHARACTERISTICS 000-STD-2101 (00) CRITICAL NONE MAJOR NONE

Figure 12. 12-inch cylinder test assembly II configuration, Sheet 1.

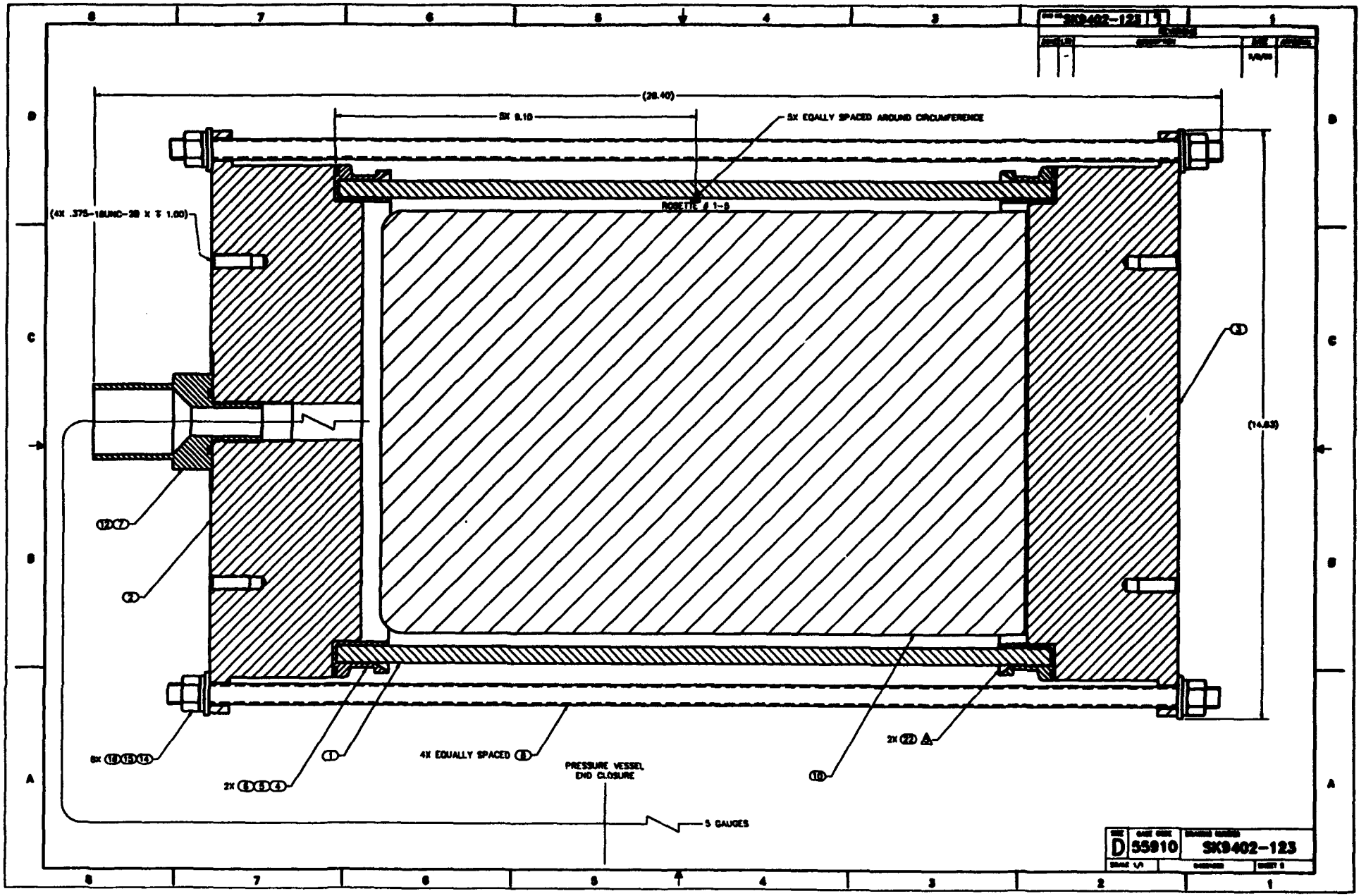

Figure 12. 12-inch cylinder test assembly II configuration, Sheet 2.

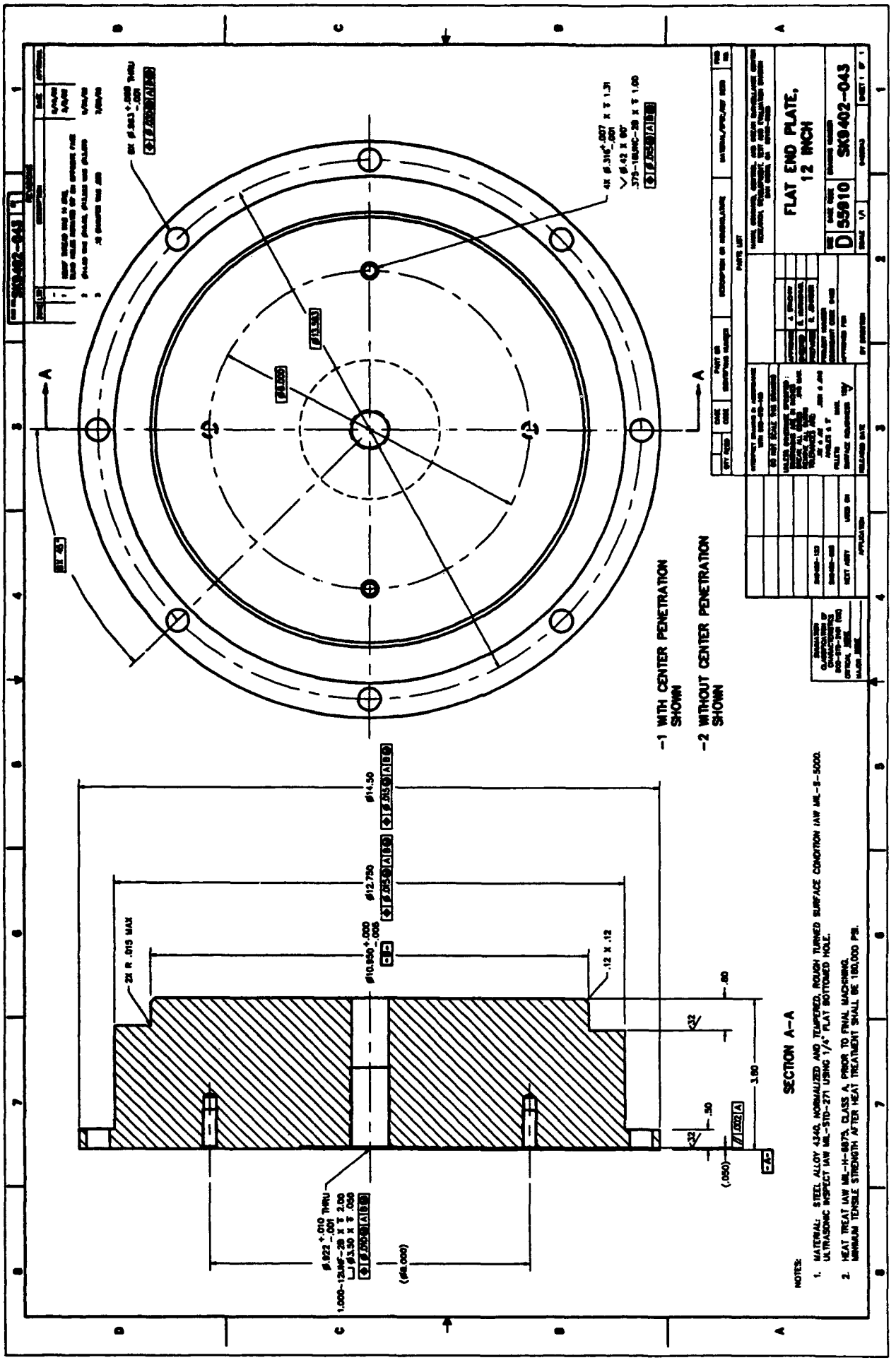

Figure 13. 12-inch flat end plate.

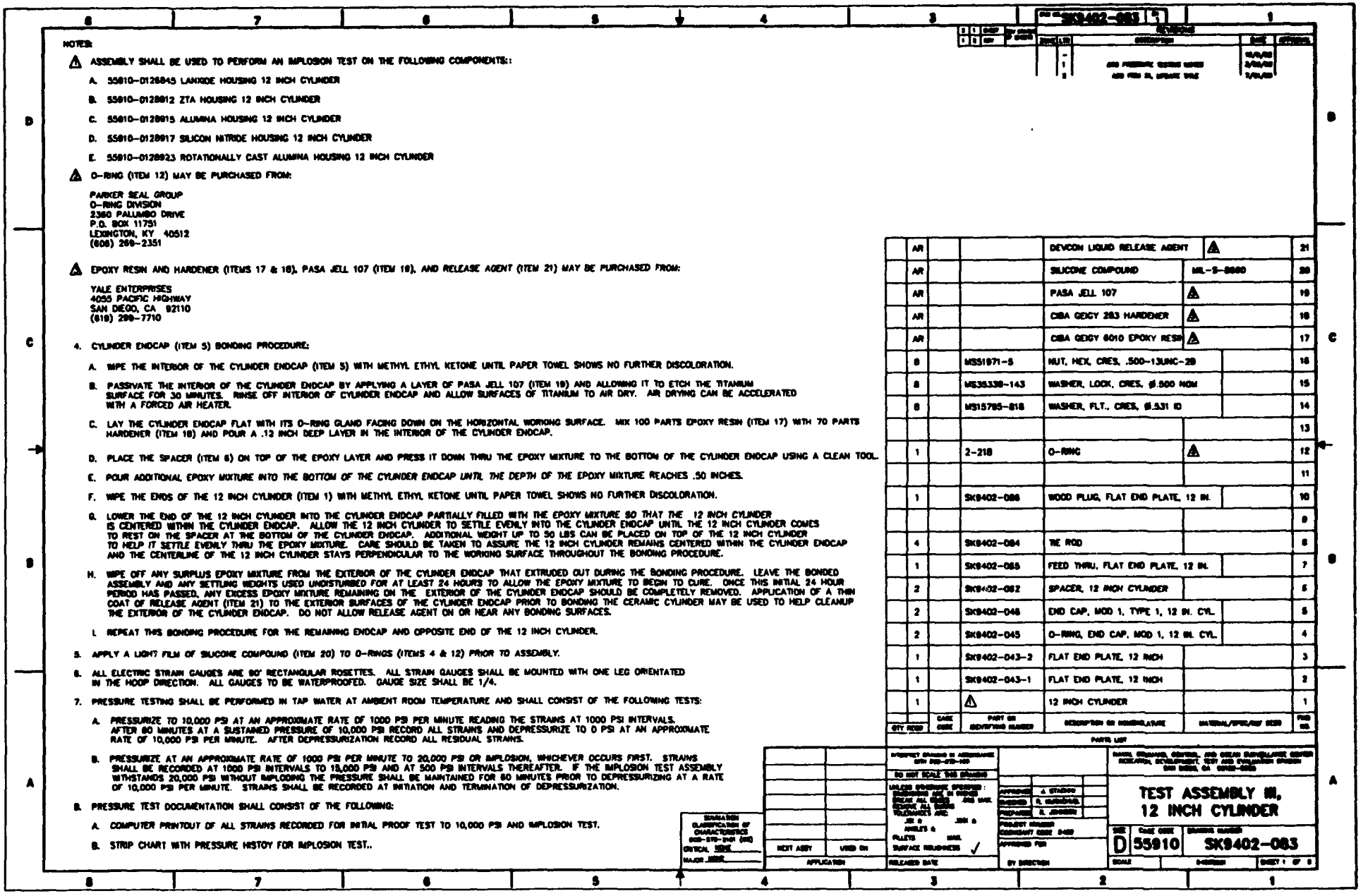

NOTES:

1. ⚠ ASSEMBLY SHALL BE USED TO PERFORM AN IMPLOSION TEST ON THE FOLLOWING COMPONENTS:
   - A. 55810-0126845 LANXIDE HOUSING 12 INCH CYLINDER
   - B. 55810-0128912 ZTA HOUSING 12 INCH CYLINDER
   - C. 55810-0128915 ALUMINA HOUSING 12 INCH CYLINDER
   - D. 55810-0128917 SILICON NITRIDE HOUSING 12 INCH CYLINDER
   - E. 55810-0128923 ROTATIONALLY CAST ALUMINA HOUSING 12 INCH CYLINDER
2. ⚠ O-RING (ITEM 12) MAY BE PURCHASED FROM:

   PARKER SEAL GROUP
   O-RING DIVISION
   2360 PALUMBO DRIVE
   P.O. BOX 11751
   LEXINGTON, KY 40512
   (606) 269-2351

3. ⚠ EPOXY RESIN AND HARDENER (ITEMS 17 & 18), PASA JELL 107 (ITEM 19), AND RELEASE AGENT (ITEM 21) MAY BE PURCHASED FROM:

   YALE ENTERPRISES
   4055 PACIFIC HIGHWAY
   SAN DIEGO, CA 92110
   (619) 299-7710

4. CYLINDER ENDCAP (ITEM 5) BONDING PROCEDURE:
   - A. WIPE THE INTERIOR OF THE CYLINDER ENDCAP (ITEM 5) WITH METHYL ETHYL KETONE UNTIL PAPER TOWEL SHOWS NO FURTHER DISCOLORATION.
   - B. PASSIVATE THE INTERIOR OF THE CYLINDER ENDCAP BY APPLYING A LAYER OF PASA JELL 107 (ITEM 19) AND ALLOWING IT TO ETCH THE TITANIUM SURFACE FOR 30 MINUTES. RINSE OFF INTERIOR OF CYLINDER ENDCAP AND ALLOW SURFACES OF TITANIUM TO AIR DRY. AIR DRYING CAN BE ACCELERATED WITH A FORCED AIR HEATER.
   - C. LAY THE CYLINDER ENDCAP FLAT WITH ITS O-RING GLAND FACING DOWN ON THE HORIZONTAL WORKING SURFACE. MIX 100 PARTS EPOXY RESIN (ITEM 17) WITH 70 PARTS HARDENER (ITEM 18) AND POUR A .12 INCH DEEP LAYER IN THE INTERIOR OF THE CYLINDER ENDCAP.
   - D. PLACE THE SPACER (ITEM 6) ON TOP OF THE EPOXY LAYER AND PRESS IT DOWN THRU THE EPOXY MIXTURE TO THE BOTTOM OF THE CYLINDER ENDCAP USING A CLEAN TOOL.
   - E. POUR ADDITIONAL EPOXY MIXTURE INTO THE BOTTOM OF THE CYLINDER ENDCAP UNTIL THE DEPTH OF THE EPOXY MIXTURE REACHES .50 INCHES.
   - F. WIPE THE ENDS OF THE 12 INCH CYLINDER (ITEM 1) WITH METHYL ETHYL KETONE UNTIL PAPER TOWEL SHOWS NO FURTHER DISCOLORATION.
   - G. LOWER THE END OF THE 12 INCH CYLINDER INTO THE CYLINDER ENDCAP PARTIALLY FILLED WITH THE EPOXY MIXTURE SO THAT THE 12 INCH CYLINDER IS CENTERED WITHIN THE CYLINDER ENDCAP. ALLOW THE 12 INCH CYLINDER TO SETTLE EVENLY INTO THE CYLINDER ENDCAP UNTIL THE 12 INCH CYLINDER COMES TO REST ON THE SPACER AT THE BOTTOM OF THE CYLINDER ENDCAP. ADDITIONAL WEIGHT UP TO 50 LBS CAN BE PLACED ON TOP OF THE 12 INCH CYLINDER TO HELP IT SETTLE EVENLY THRU THE EPOXY MIXTURE. CARE SHOULD BE TAKEN TO ASSURE THE 12 INCH CYLINDER REMAINS CENTERED WITHIN THE CYLINDER ENDCAP AND THE CENTERLINE OF THE 12 INCH CYLINDER STAYS PERPENDICULAR TO THE WORKING SURFACE THROUGHOUT THE BONDING PROCEDURE.
   - H. WIPE OFF ANY SURPLUS EPOXY MIXTURE FROM THE EXTERIOR OF THE CYLINDER ENDCAP THAT EXTRUDED OUT DURING THE BONDING PROCEDURE. LEAVE THE BONDED ASSEMBLY AND ANY SETTLING WEIGHTS USED UNDISTURBED FOR AT LEAST 24 HOURS TO ALLOW THE EPOXY MIXTURE TO BEGIN TO CURE. ONCE THIS INITIAL 24 HOUR PERIOD HAS PASSED, ANY EXCESS EPOXY MIXTURE REMAINING ON THE EXTERIOR OF THE CYLINDER ENDCAP SHOULD BE COMPLETELY REMOVED. APPLICATION OF A THIN COAT OF RELEASE AGENT (ITEM 21) TO THE EXTERIOR SURFACES OF THE CYLINDER ENDCAP PRIOR TO BONDING THE CERAMIC CYLINDER MAY BE USED TO HELP CLEANUP THE EXTERIOR OF THE CYLINDER ENDCAP. DO NOT ALLOW RELEASE AGENT ON OR NEAR ANY BONDING SURFACES.
   - I. REPEAT THIS BONDING PROCEDURE FOR THE REMAINING ENDCAP AND OPPOSITE END OF THE 12 INCH CYLINDER.
5. APPLY A LIGHT FILM OF SILICONE COMPOUND (ITEM 20) TO O-RINGS (ITEMS 4 & 12) PRIOR TO ASSEMBLY.
6. ALL ELECTRIC STRAIN GAUGES ARE 90° RECTANGULAR ROSETTES. ALL STRAIN GAUGES SHALL BE MOUNTED WITH ONE LEG ORIENTATED IN THE HOOP DIRECTION. ALL GAUGES TO BE WATERPROOFED. GAUGE SIZE SHALL BE 1/4.
7. PRESSURE TESTING SHALL BE PERFORMED IN TAP WATER AT AMBIENT ROOM TEMPERATURE AND SHALL CONSIST OF THE FOLLOWING TESTS:
   - A. PRESSURIZE TO 10,000 PSI AT AN APPROXIMATE RATE OF 1000 PSI PER MINUTE READING THE STRAINS AT 1000 PSI INTERVALS. AFTER 60 MINUTES AT A SUSTAINED PRESSURE OF 10,000 PSI RECORD ALL STRAINS AND DEPRESSURIZE TO 0 PSI AT AN APPROXIMATE RATE OF 10,000 PSI PER MINUTE. AFTER DEPRESSURIZATION RECORD ALL RESIDUAL STRAINS.
   - B. PRESSURIZE AT AN APPROXIMATE RATE OF 1000 PSI PER MINUTE TO 20,000 PSI OR IMPLOSION, WHICHEVER OCCURS FIRST. STRAINS SHALL BE RECORDED AT 1000 PSI INTERVALS TO 15,000 PSI AND AT 500 PSI INTERVALS THEREAFTER. IF THE IMPLOSION TEST ASSEMBLY WITHSTANDS 20,000 PSI WITHOUT IMPLODING THE PRESSURE SHALL BE MAINTAINED FOR 60 MINUTES PRIOR TO DEPRESSURIZING AT A RATE OF 10,000 PSI PER MINUTE. STRAINS SHALL BE RECORDED AT INITIATION AND TERMINATION OF DEPRESSURIZATION.
8. PRESSURE TEST DOCUMENTATION SHALL CONSIST OF THE FOLLOWING:
   - A. COMPUTER PRINTOUT OF ALL STRAINS RECORDED FOR INITIAL PROOF TEST TO 10,000 PSI AND IMPLOSION TEST.
   - B. STRIP CHART WITH PRESSURE HISTOY FOR IMPLOSION TEST..

QTY	ROD	CAGE CODE	PART OR IDENTIFYING NUMBER	DESCRIPTION OR NOMENCLATURE	MATERIAL/SPEC/REF DESIG	FIND NO.
	AR			DEVCON LIQUID RELEASE AGENT ⚠		21
	AR			SILICONE COMPOUND	MIL-S-8660	20
	AR			PASA JELL 107 ⚠		19
	AR			CIBA GEIGY 283 HARDENER ⚠		18
	AR			CIBA GEIGY 6010 EPOXY RESIN ⚠		17
	8		MS51971-8	NUT, HEX, CRES, .500-13UNC-2B		16
	8		MS35338-143	WASHER, LOCK, CRES, Ø.500 NOM		15
	8		MS15795-818	WASHER, FLT., CRES, Ø.531 ID		14
						13
	1		2-218	O-RING ⚠		12
						11
	1		SK9402-088	WOOD PLUG, FLAT END PLATE, 12 IN.		10
						9
	4		SK9402-084	TIE ROD		8
	1		SK9402-089	FEED THRU, FLAT END PLATE, 12 IN.		7
	2		SK9402-082	SPACER, 12 INCH CYLINDER		6
	2		SK9402-046	END CAP, MOD 1, TYPE 1, 12 IN. CYL.		5
	2		SK9402-045	O-RING, END CAP, MOD 1, 12 IN. CYL.		4
	1		SK9402-043-2	FLAT END PLATE, 12 INCH		3
	1		SK9402-043-1	FLAT END PLATE, 12 INCH		2
	1		⚠	12 INCH CYLINDER		1

PARTS LIST

NEXT ASSY	USED ON
APPLICATION	

DO NOT SCALE THIS DRAWING

UNLESS OTHERWISE SPECIFIED: DIMENSIONS ARE IN INCHES. BREAK ALL EDGES .010 MAX. REMOVE ALL BURRS AND SHARP CORNERS. TOLERANCES ARE: .XX ± .030, .XXX ± .010, ANGLES ± 1°, FILLETS .010 MAX. SURFACE ROUGHNESS ✓

APPROVED: A. STADSON
DESIGNED: R. SORENSEN
PREPARED: R. JOHNSON
PROJECT ENGINEER
CONTRACT CODE 9-469
APPROVED FOR RELEASE BY DIRECTION

SANDIA NATIONAL LABORATORIES, ENERGY DIRECTORATE, RESEARCH, DEVELOPMENT, TEST AND EVALUATION DIVISION, ALBUQUERQUE, NEW MEXICO 87185

TEST ASSEMBLY III, 12 INCH CYLINDER

SIZE	CAGE CODE	DRAWING NUMBER
D	55910	SK9402-083
SCALE		SHEET 1 OF 8

Figure 14. 12-inch cylinder test assembly III configuration, Sheet 1.

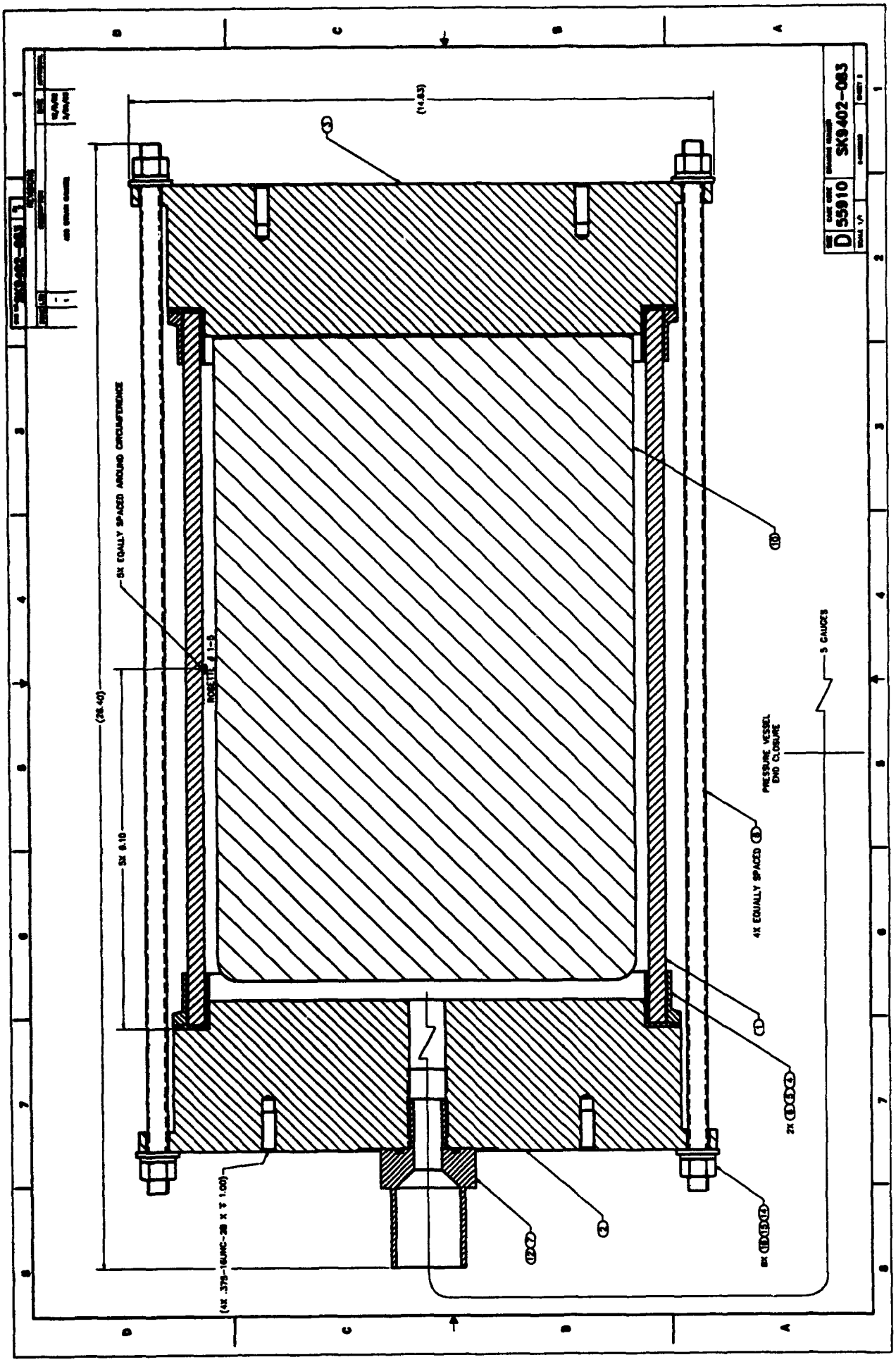

Figure 14. 12-inch cylinder test assembly III configuration, Sheet 2.

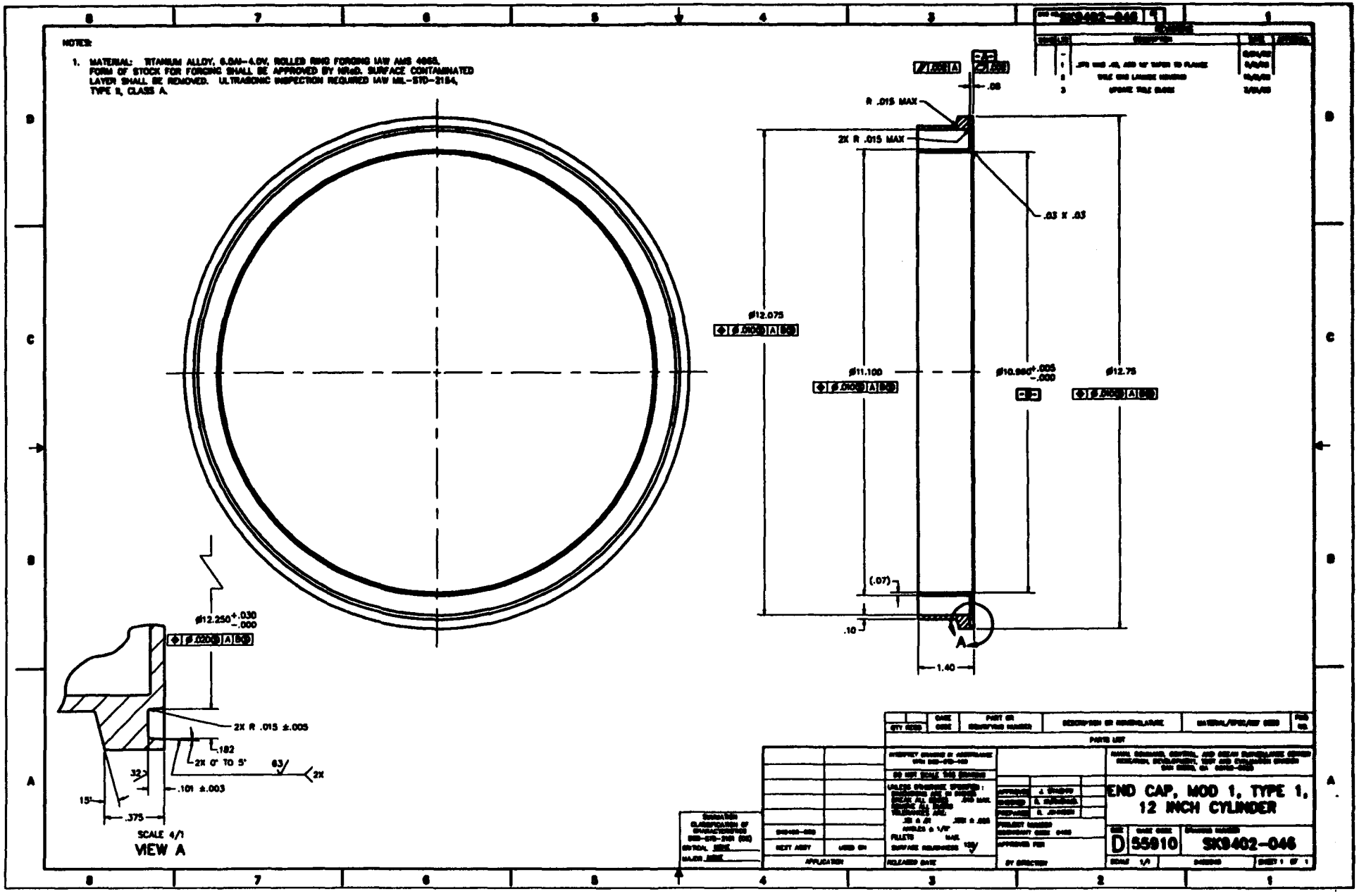

Figure 15. 12-inch cylinder Mod 1, Type 1 end-cap joint ring.

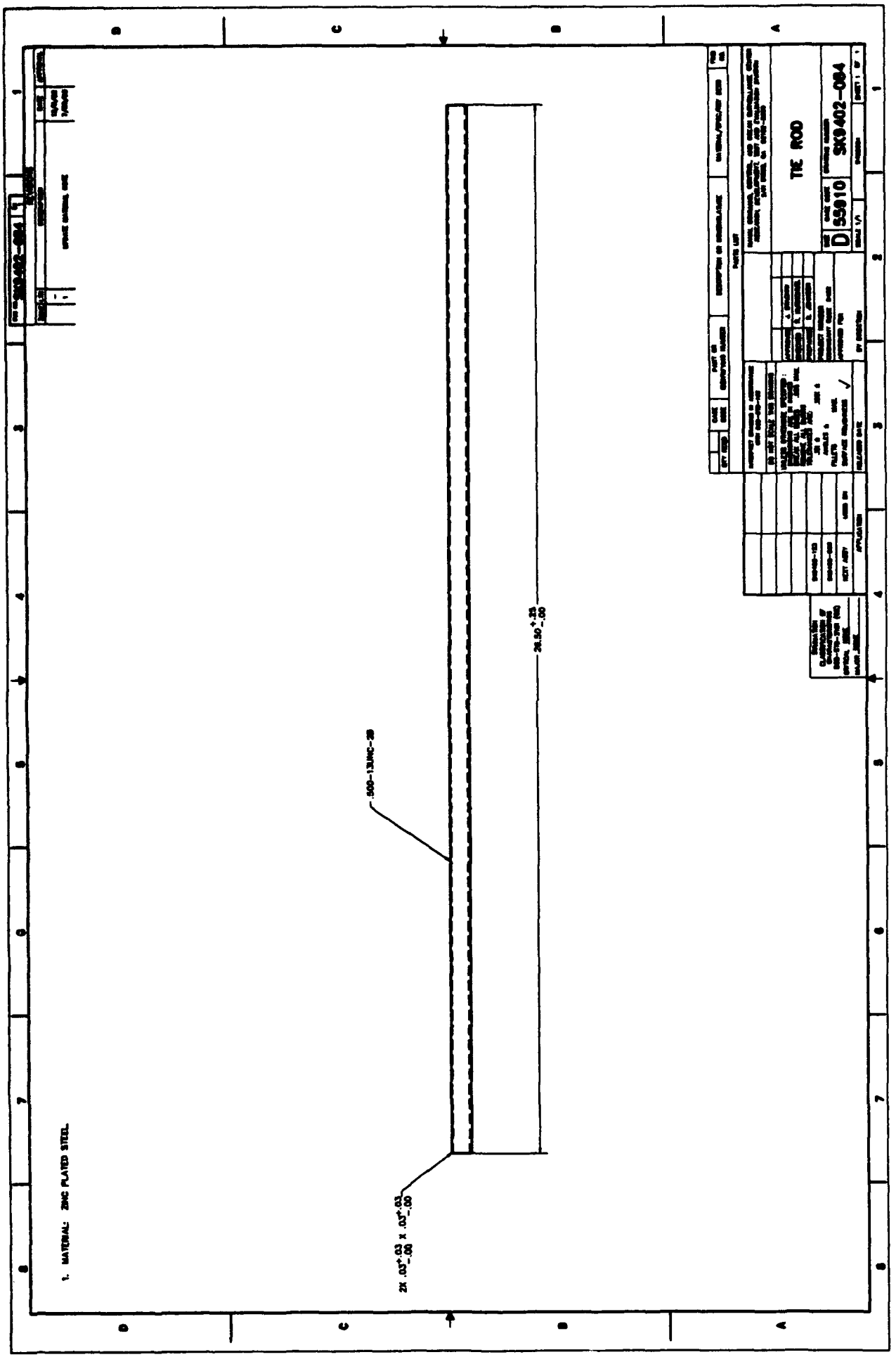

Figure 16. 12-inch flat end-plate tie rod.

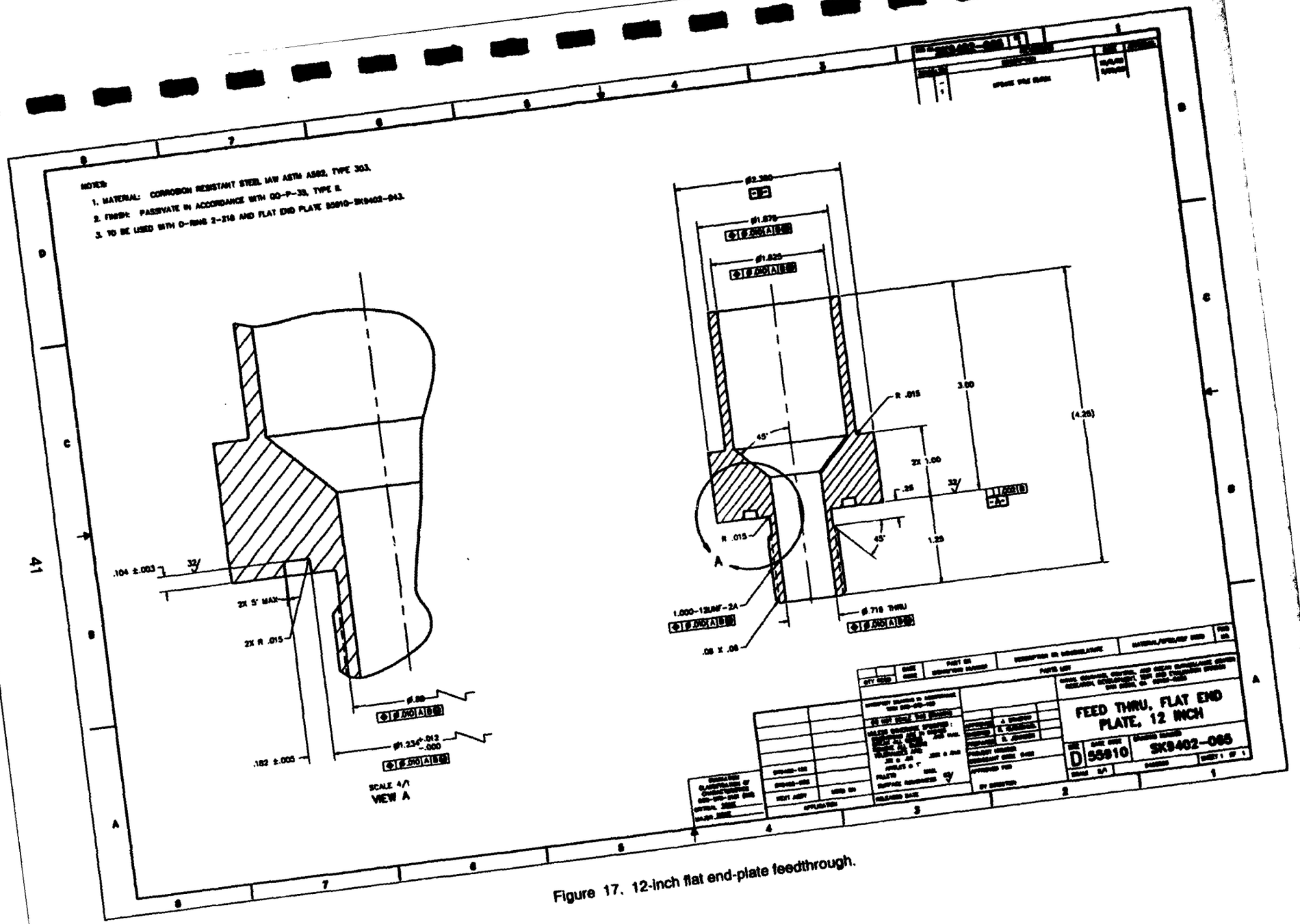

Figure 17. 12-inch flat end-plate feedthrough.

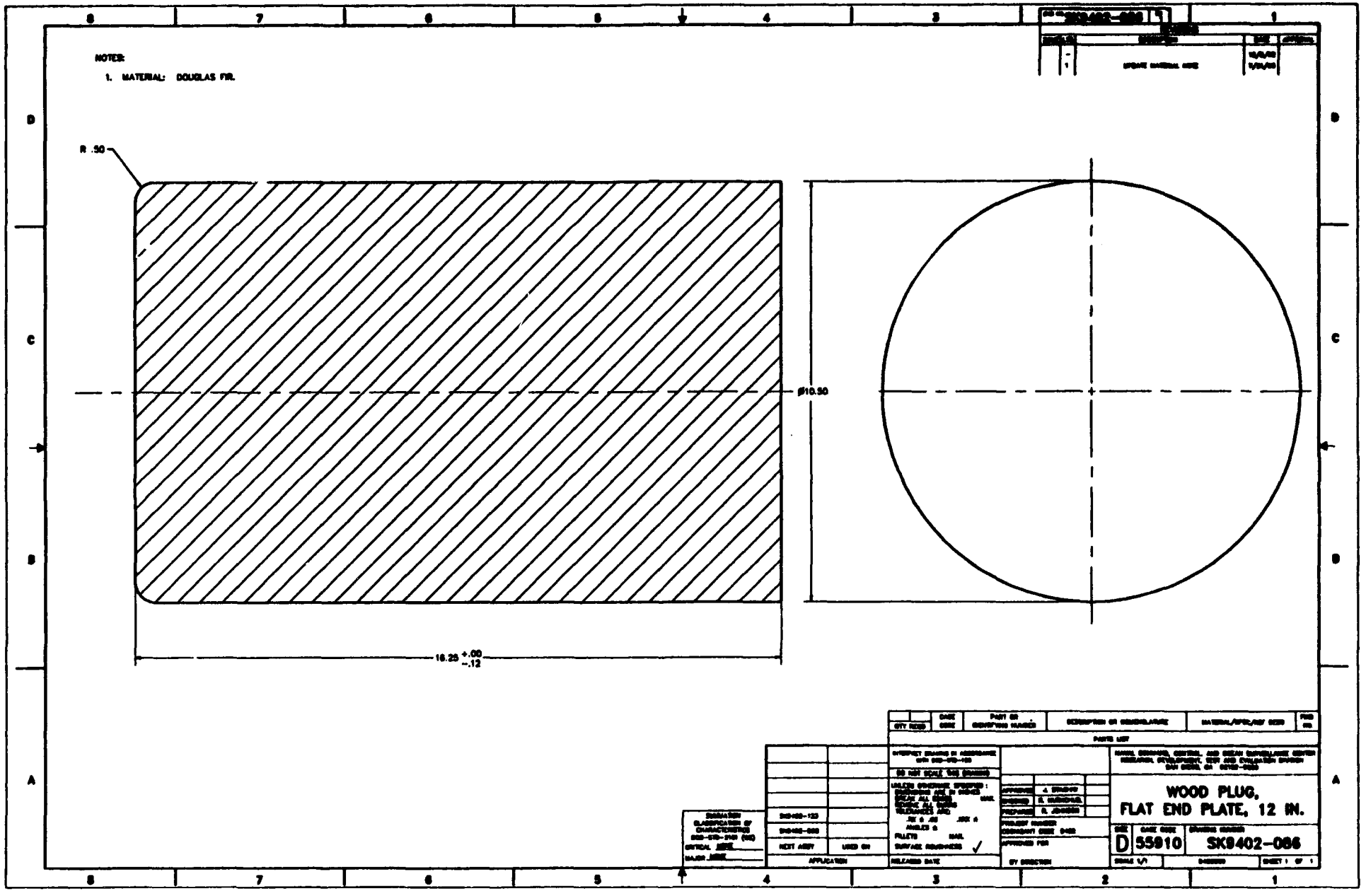

Figure 18. 12-inch flat end-plate wood plug.

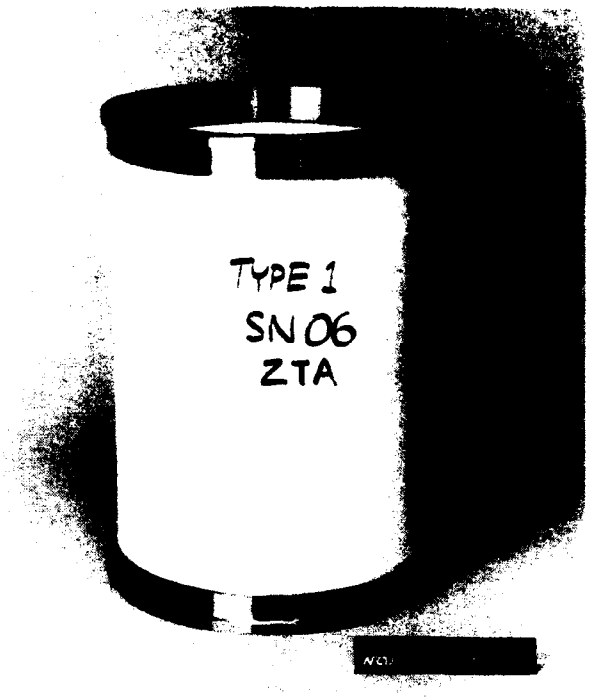

Figure 19. ZTA cylinder with Mod 1, Type 1 titanium end-cap joint rings, side view.

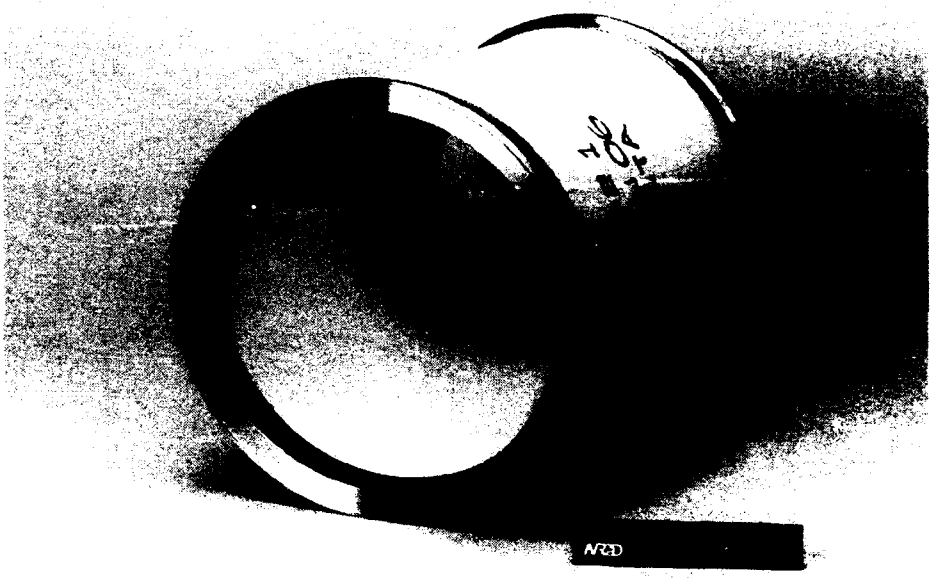

Figure 20. ZTA cylinder with Mod 1, Type 1 titanium end-cap joint rings, end view.

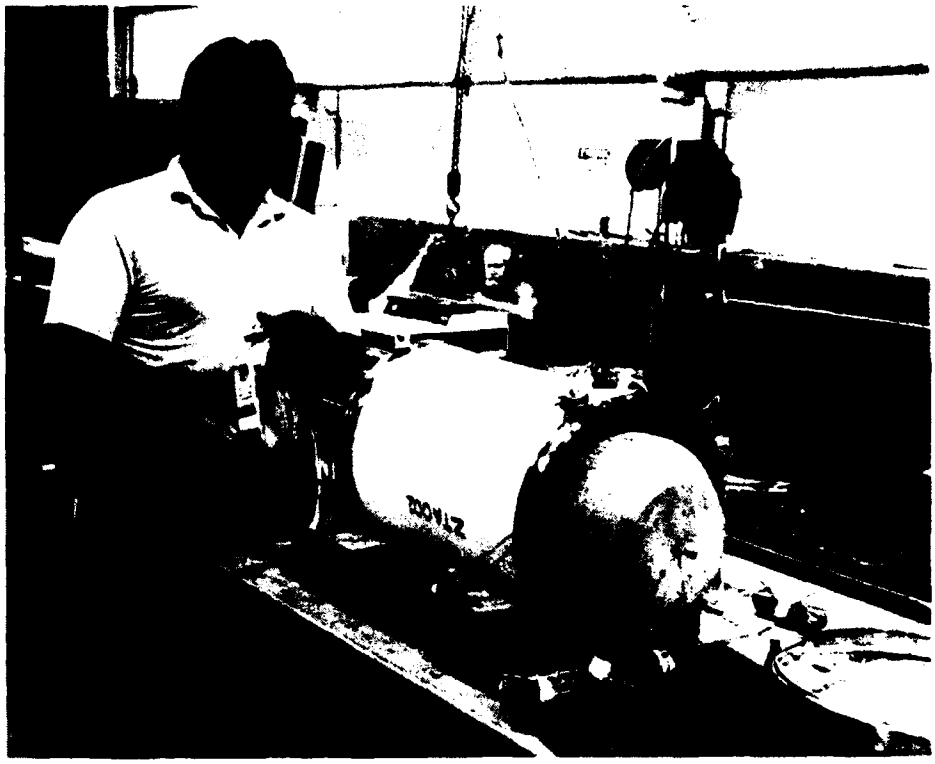

Figure 21. ZTA cylinder being prepared for cyclic pressure testing.

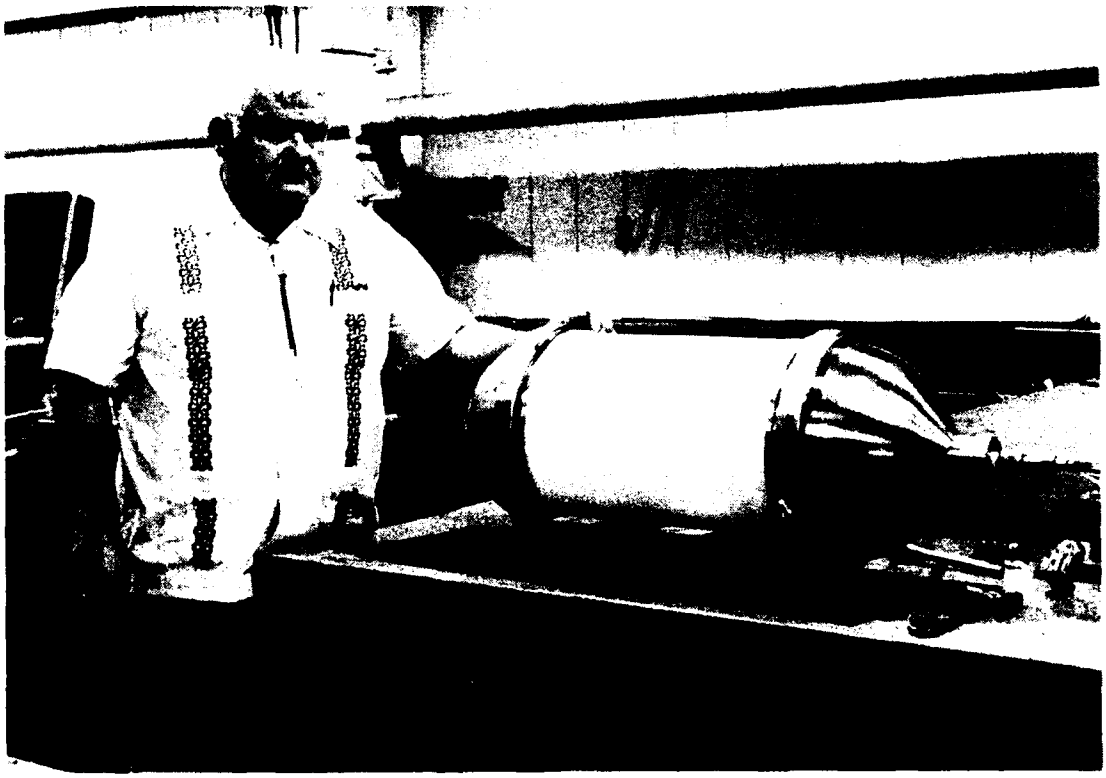

Figure 22.Test assembly I configuration for cyclic pressure testing.

Figure 23. Test assembly II configuration for cyclic pressure testing.

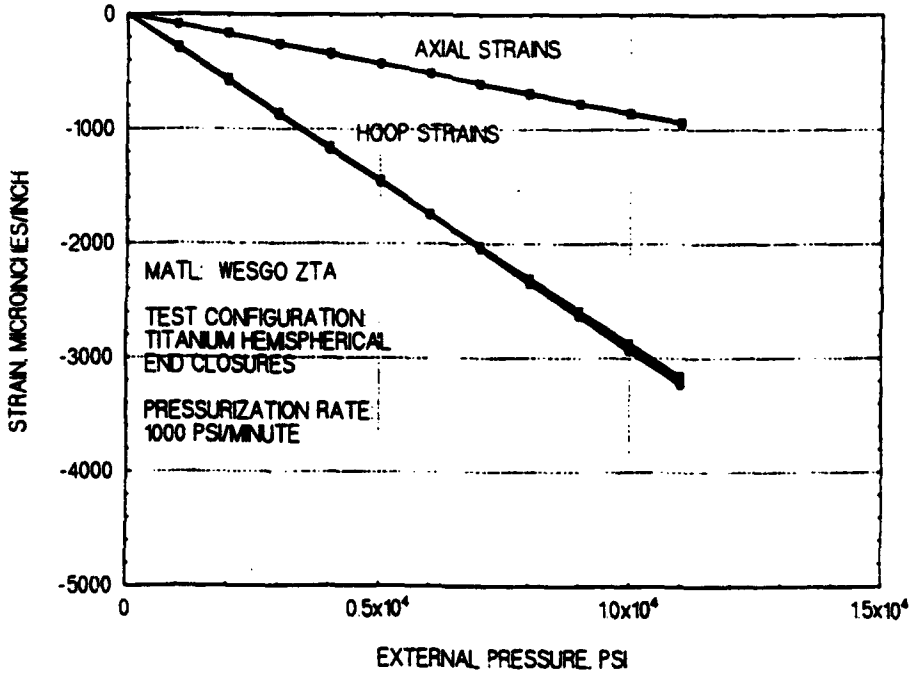

Figure 24. Plot of strains recorded during first pressurization of test 01 cylinder to 11,000 psi.

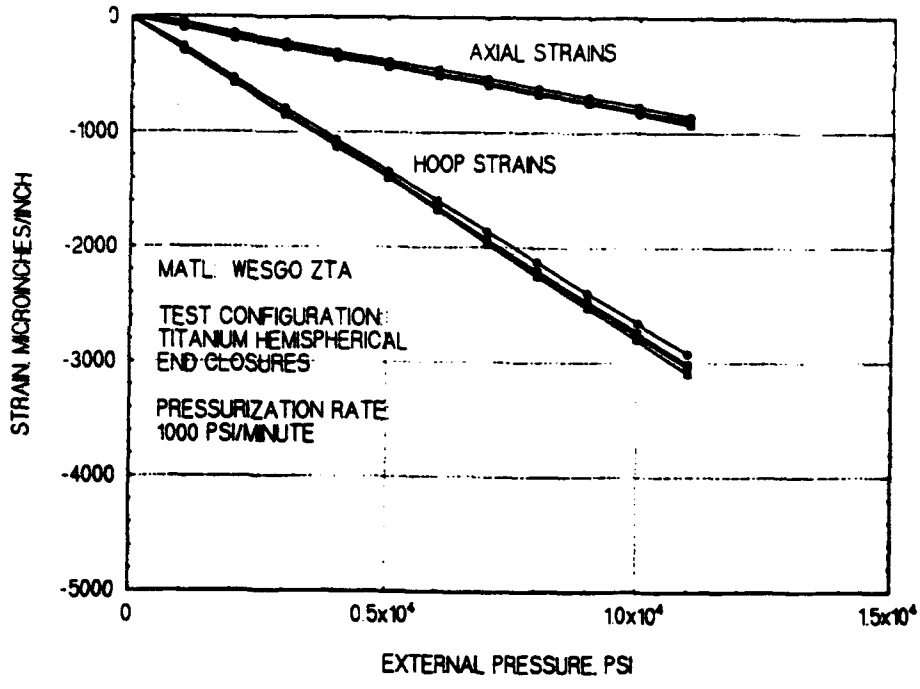

Figure 25. Plot of strains recorded during first pressurization of test 02 cylinder to 11,000 psi.

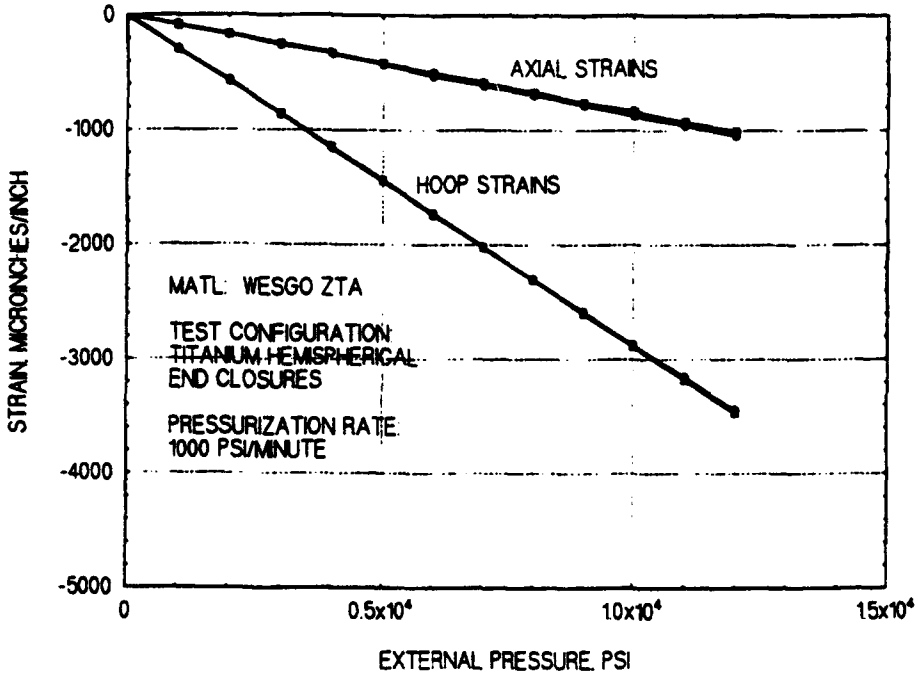

Figure 26. Plot of strains recorded during first pressurization of test 03 cylinder to 12,000 psi.

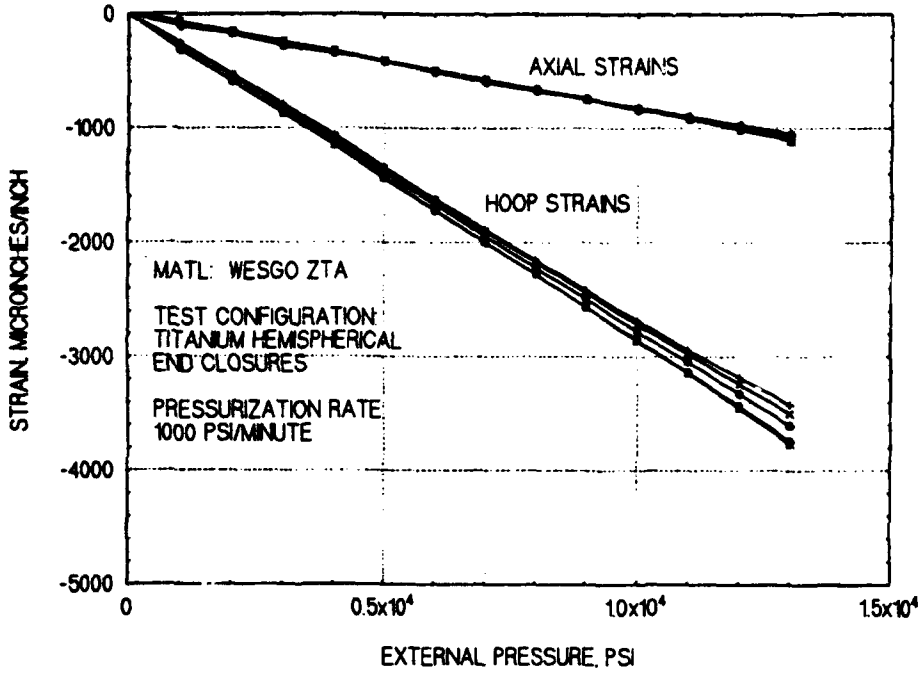

Figure 27. Plot of strains recorded during first pressurization of test 04 cylinder to 13,000 psi.

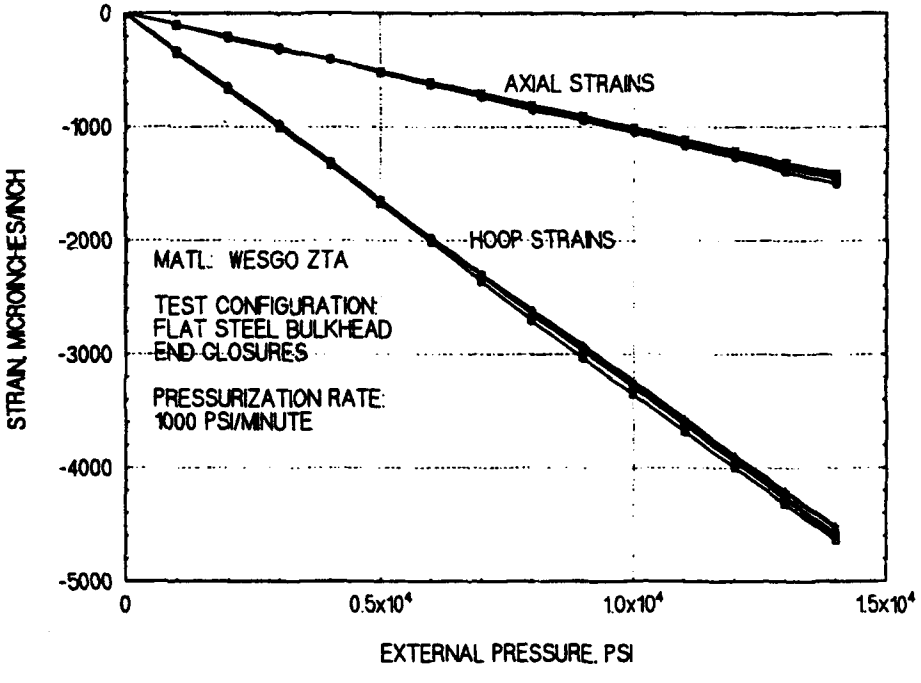

Figure 28. Plot of strains recorded during first pressurization of test 05 cylinder to 14,000 psi.

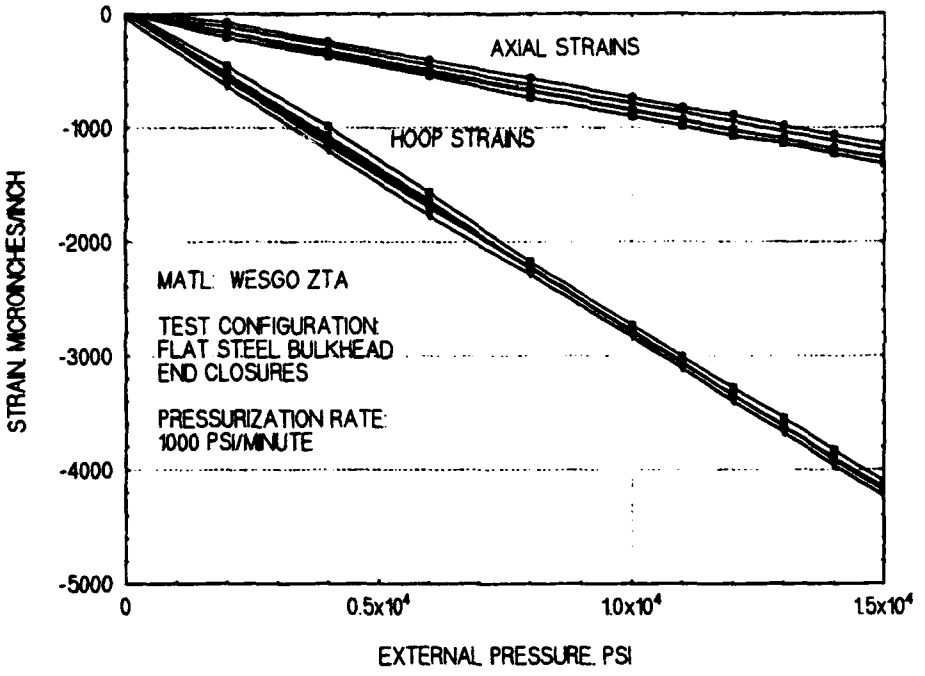

Figure 29. Plot of strains recorded during first pressurization of test 06 cylinder to 15,000 psi.

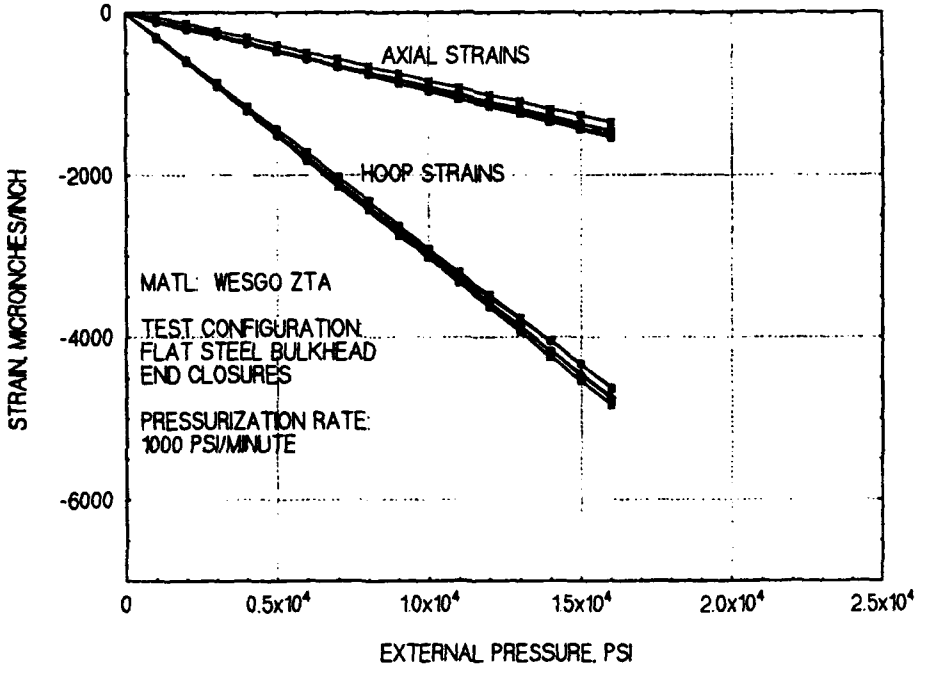

Figure 30. Plot of strains recorded during first pressurization of test 07 cylinder to 16,000 psi.

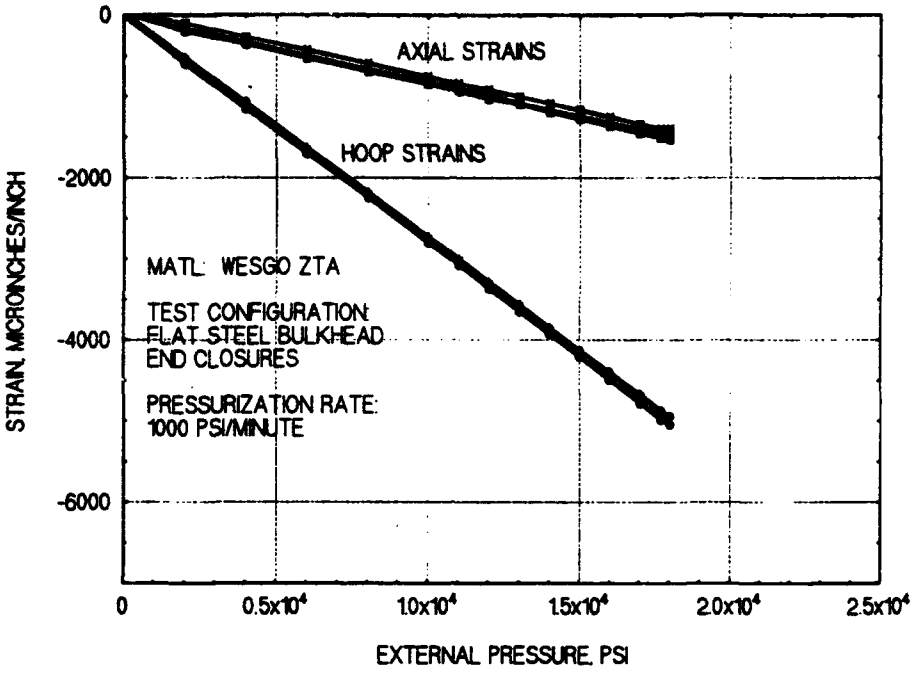

Figure 31. Plot of strains recorded during first pressurization of test 08 cylinder to 18,000 psi.

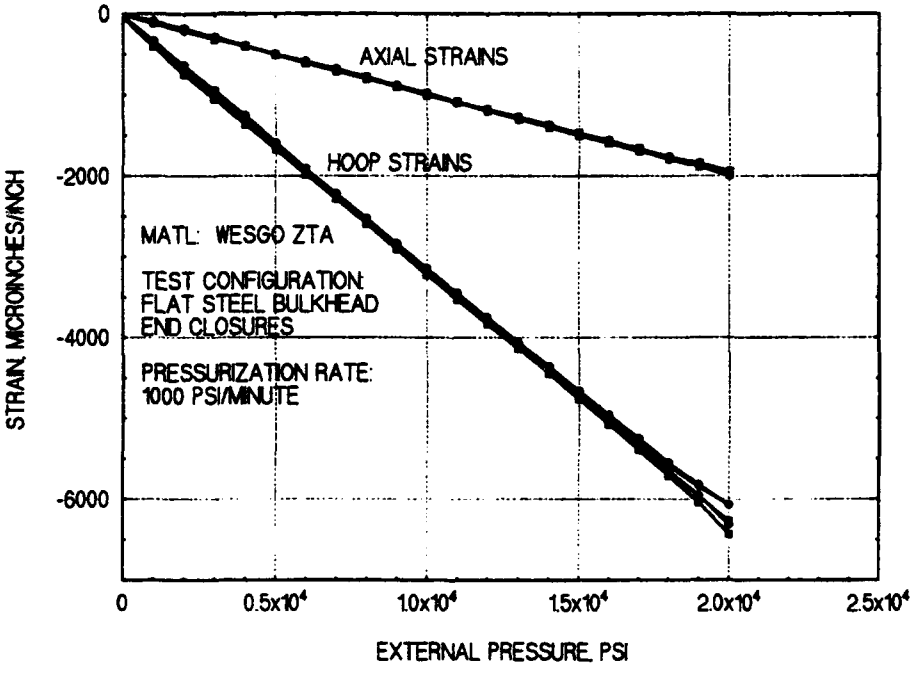

Figure 32. Plot of strains recorded during first pressurization of test 09 cylinder to 20,000 psi.

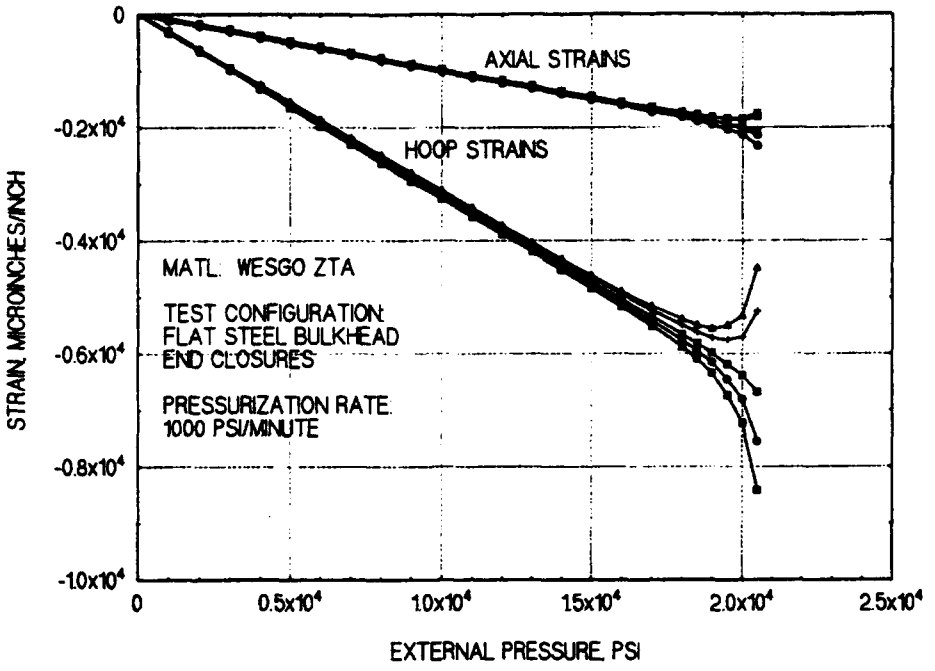

Figure 33. Plot of strains recorded during pressurization of test 10 cylinder to failure at 20,600 psi.

Figure 35. Circumferential cracks on the bearing surface of test 02 cylinder after 4,059 cycles to 11,000 psi.

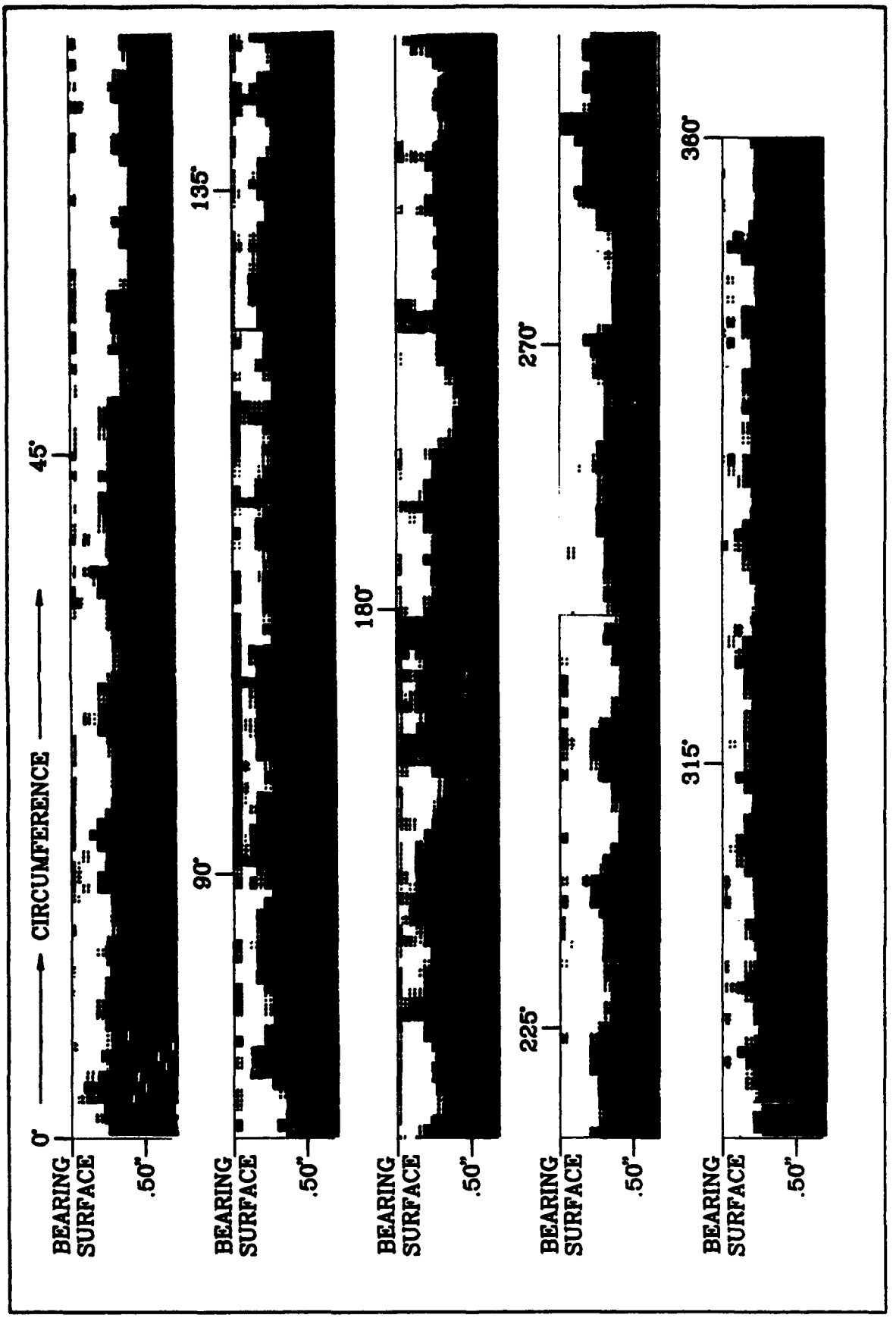

Figure 34. Pulse-echo C-scan of subcritical crack growth in test 01 cylinder after 1,039 cycles to 11,000 psi.

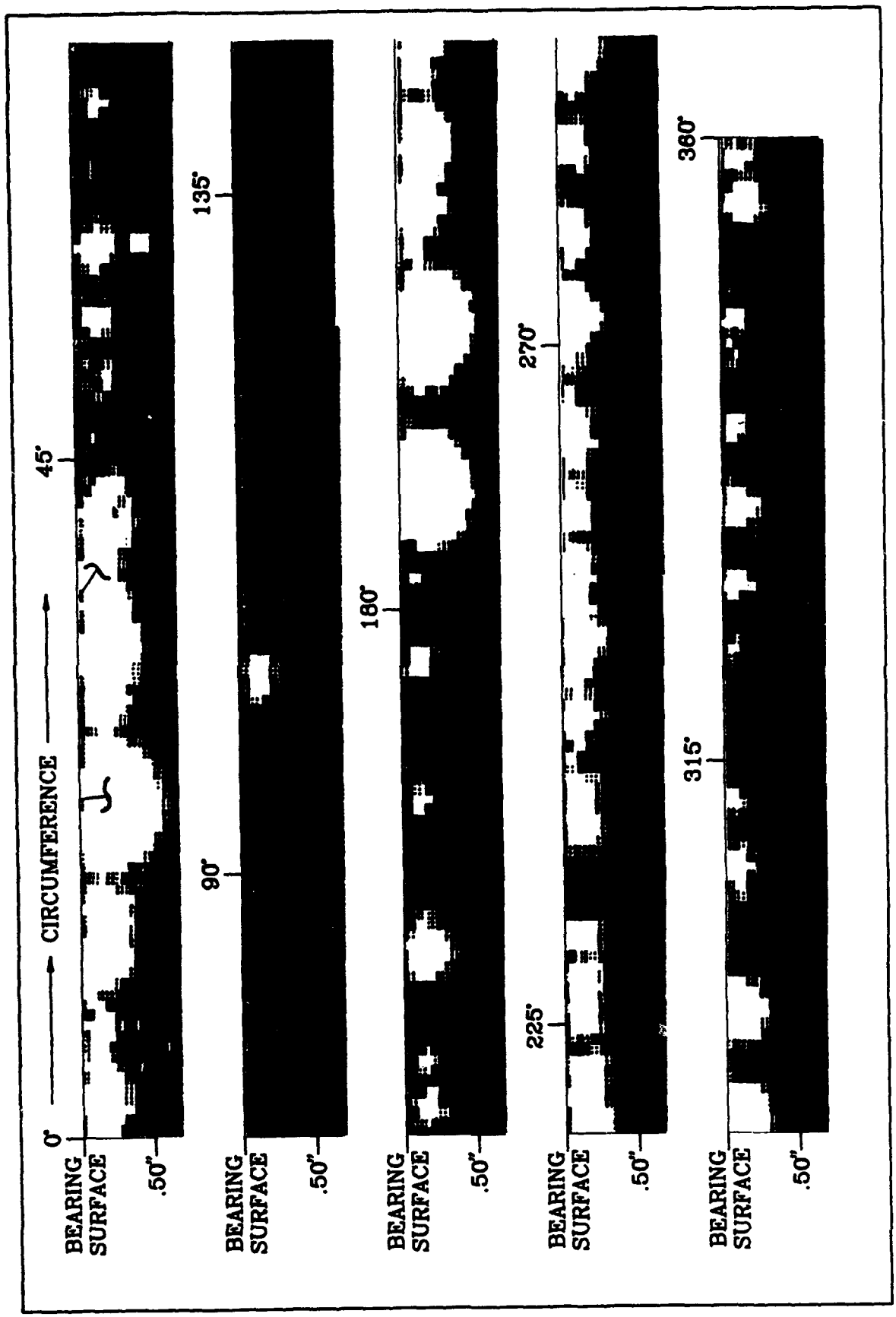

Figure 36. Pulse-echo C-scan of subcritical crack growth in test 02 cylinder after 4,059 cycles to 11,000 psi.

Figure 39. Remains of end-cap joint ring after implosion of test 04 cylinder after 1,854 cycles to 13,000 psi.

Figure 40. Spalling on ID of test 06 cylinder after 361 cycles to 15,000 psi.

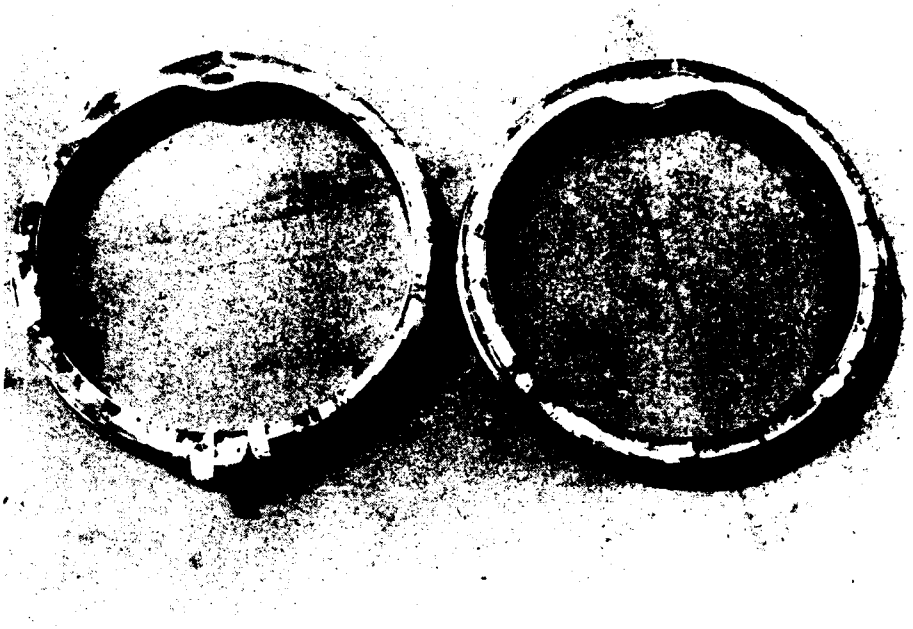

Figure 43. Remains of end-cap joint rings after failure from test 08 after 88 cycles to 18,000 psi, gland view.

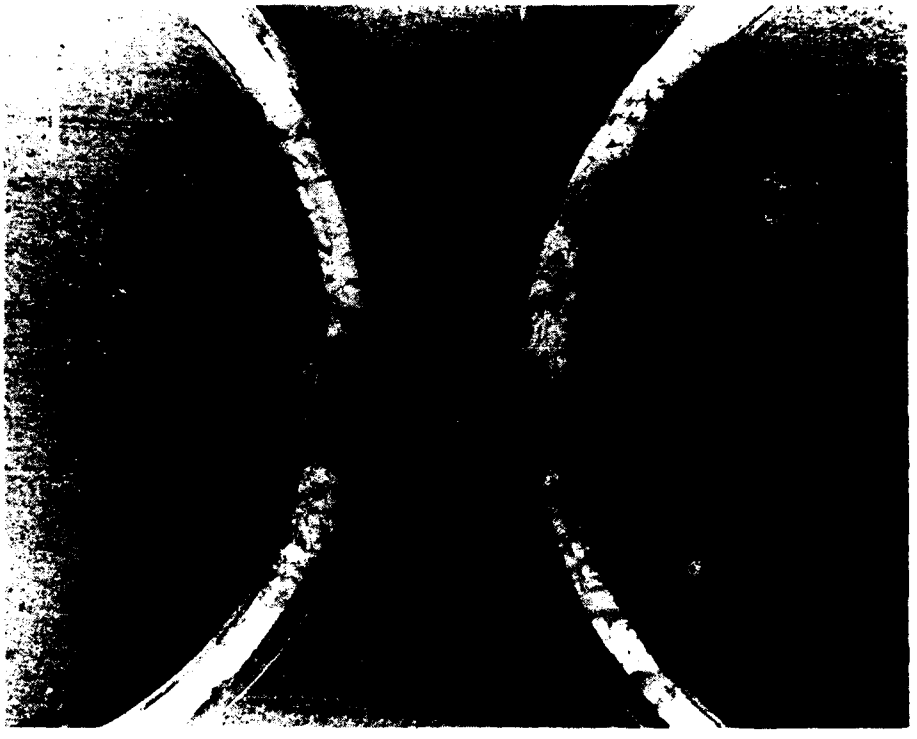

Figure 43. Remains of end-cap joint rings after failure from test 08 after 88 cycles to 18,000 psi, gland view enlargement.

Figure 44. Remains of end-cap joint rings after failure from test 08 after 88 cycles to 18,000 psi, bearing surface view.

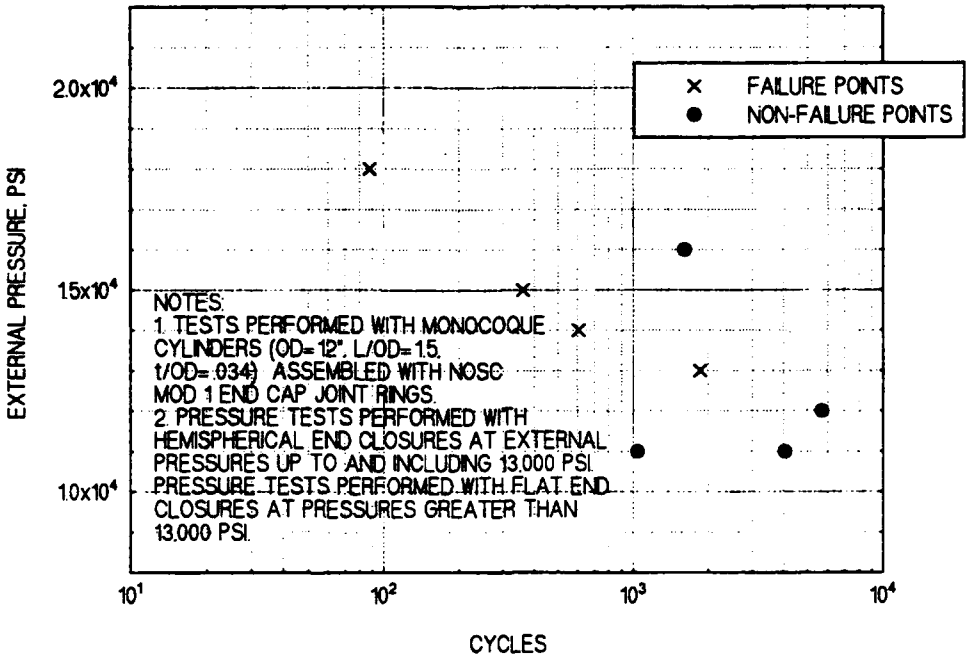

Figure 45. Cyclic external pressure loading test data for ZTA test 01 through 08 cylinders.

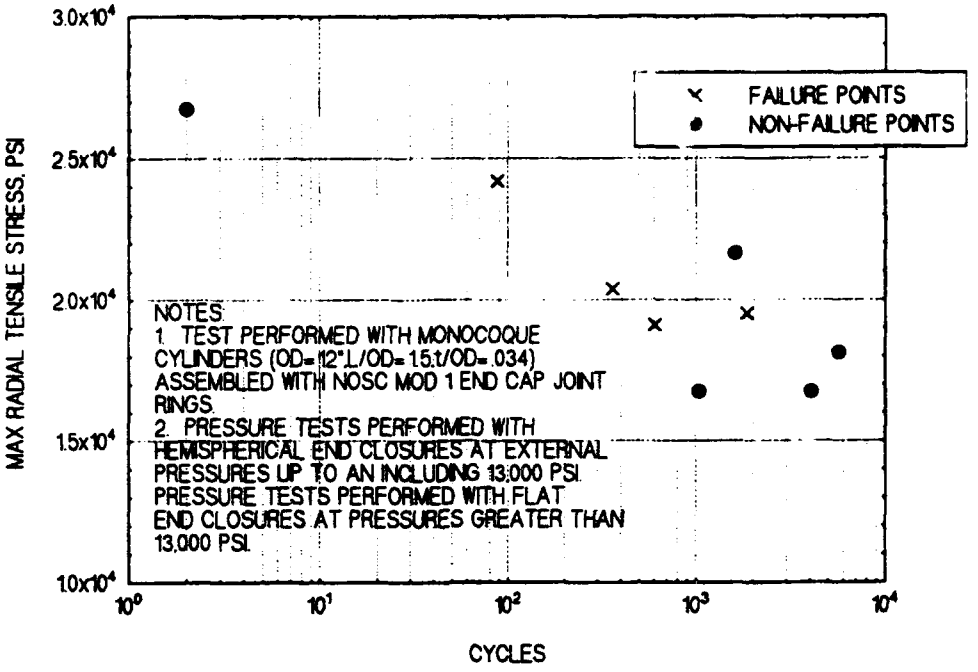

Figure 46. ZTA cylinder cyclic fatigue life, versus maximum calculated tensile bearing-surface stress.

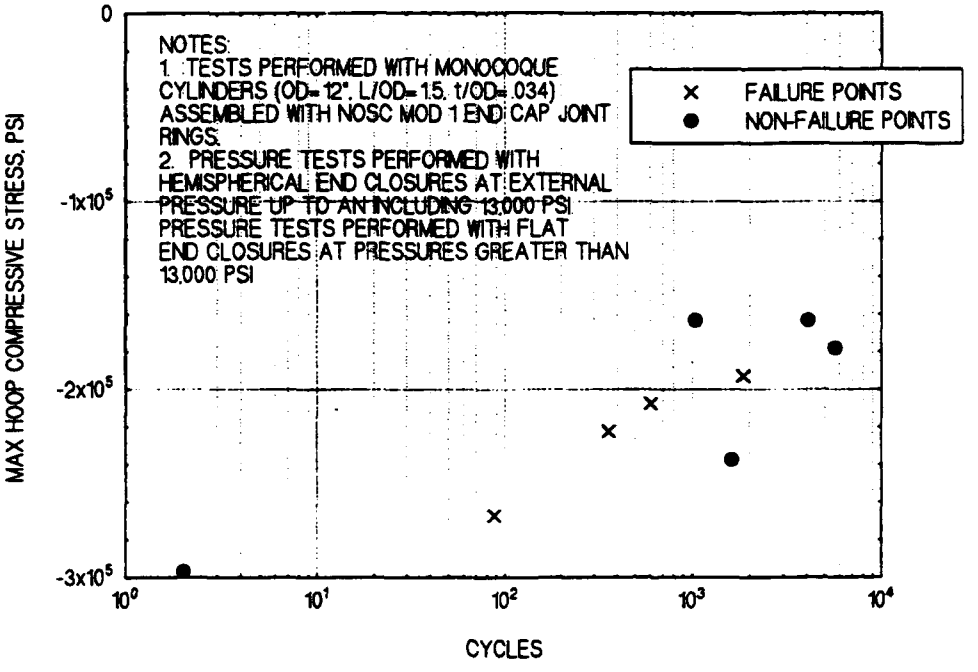

Figure 47. ZTA cylinder cyclic fatigue life, versus maximum calculated compressive hoop stress.

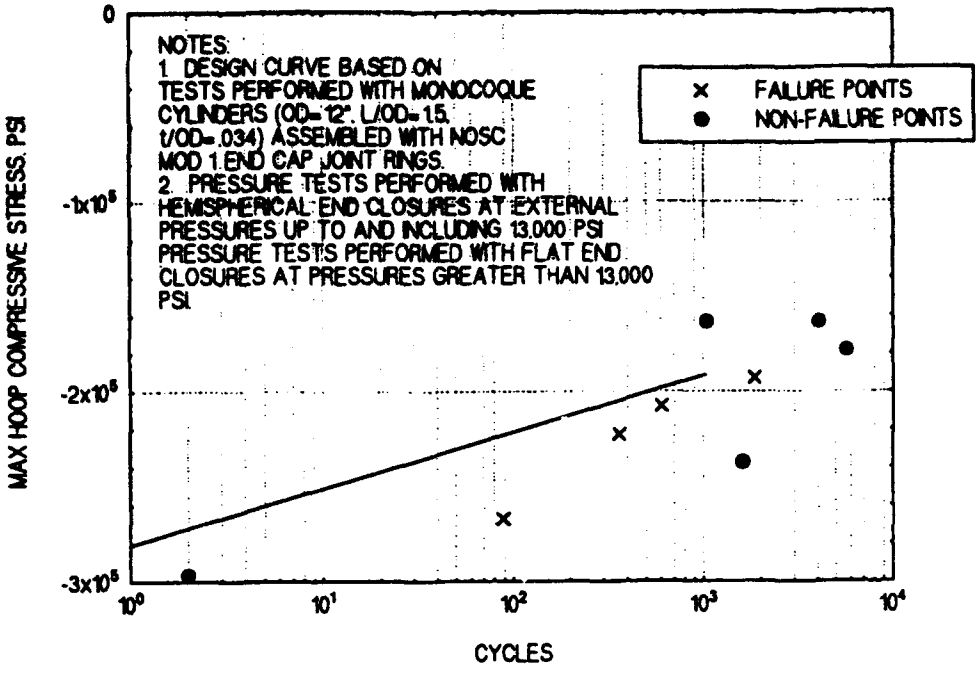

Figure 48. Cyclic fatigue design curve for external pressure loading of ZTA ceramic cylinders.

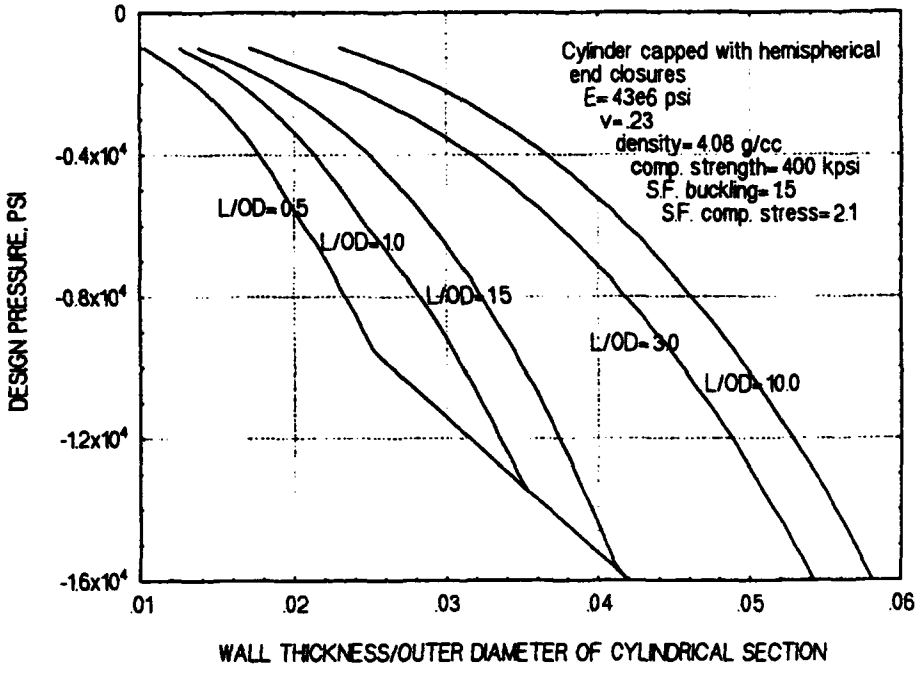

Figure 49. Calculated t/OD ratios of monocoque ZTA ceramic cylinders for 1,000 cycles to design depth.

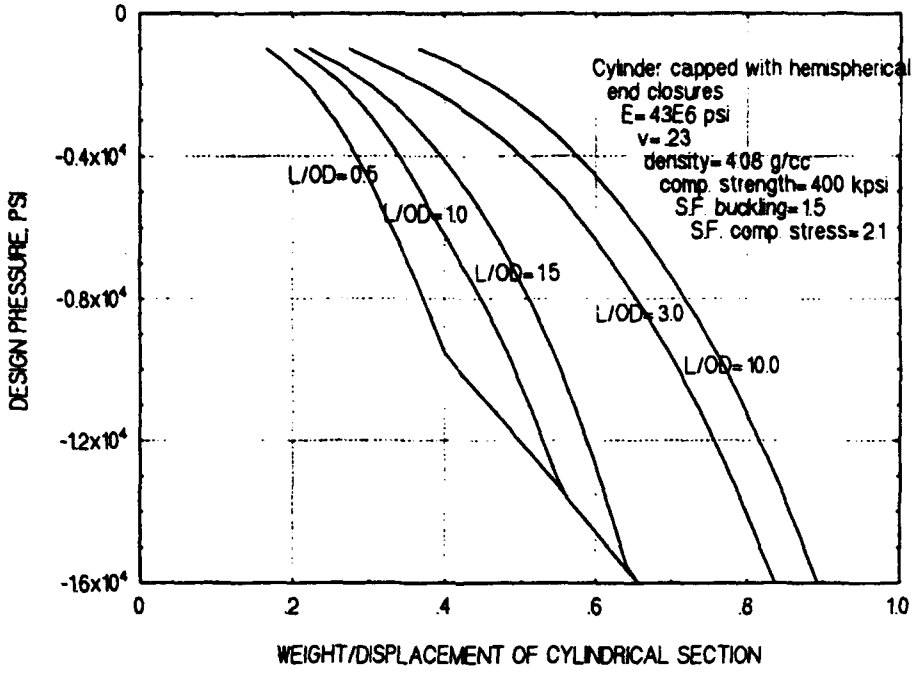

Figure 50. Calculated W/D ratios of monocoque ZTA ceramic cylinders for 1,000 cycles to design depth.

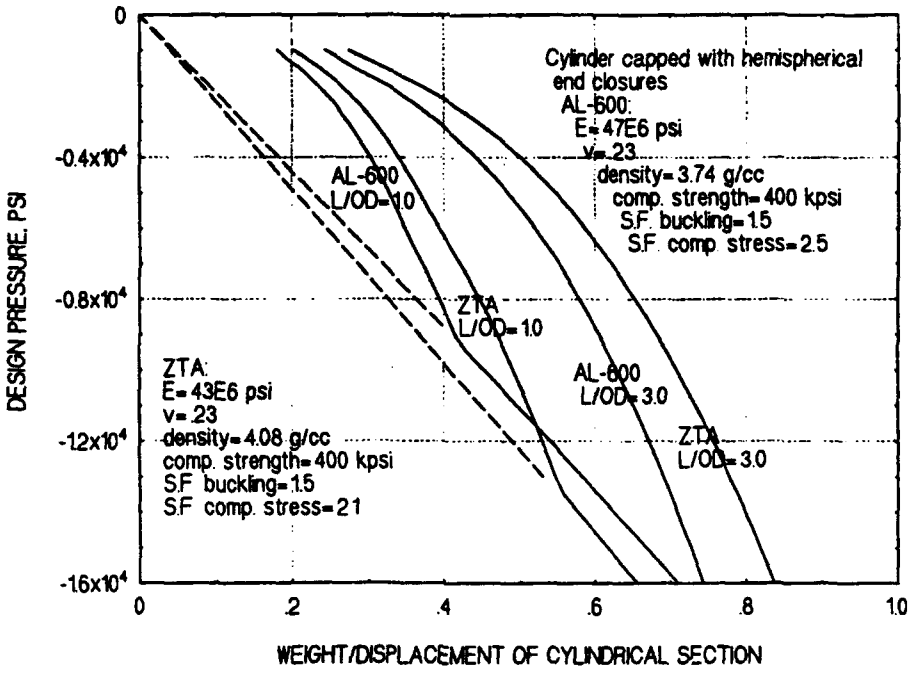

Figure 51. Comparison of calculated W/D ratios of AL-600 and ZTA ceramic cylinders for 1,000 cycles to design depth.

Table 1. Internal defects in ZTA cylinders detected using pulse-echo ultrasonic NDE techniques.

INTERNAL DEFECTS DETECTED IN ZIRCONIA TOUGHENED ALUMINA CYLINDERS 55910-0128912 USING ULTRASONIC NDE TECHNIQUES		
CYLINDER PART #	# OF DEFECTS	SIZE* AND DEPTH** OF DEFECTS
001	2	22% @ .206, 35% @ .206
002	3	50% @ .206, 49% @ .206, 22% @ .336
003	3	50% @ ID, 22% @ .206, 74% @ .206
004	8	25% @ ID, 32% @.206, 28% @ .309, 41% @ .206 52% @ ID, 22% @ OD, 36% @ .206, 20 % @ OD
005	2	6.5 INCH LENGTH INTERNAL CRACK, 66% @ .274
006	8	53% @ .206, 34% @ ID, 16% @ .274, 49% @ .274 39% @ .137, 58% @ .274, 69% @ .137, 61% @ .206
008	0	NA
009	0	NA (THICKNESS VARIATIONS)
010	1	4dB > .030 PORE @ .125
011	1	41% @ .206
012	2	38% @ .309, 34% @ .125

*SIZE INDICATED BY A % OF THE AVERAGE AMPLITUDE OF REFLECTION FROM A .030 INCH VOID IN CALIBRATION STANDARD SK9402-093-C2
**DEPTH OF EACH DEFECT IS MEASURED IN INCHES FROM THE OD OF THE CYLINDER

Table 2. External pressure test plan for ZTA cylinders.

TEST PLAN FOR ZIRCONIA TOUGHENED ALUMINA CYLINDERS 55910-0128912				
CYLINDER PART #	TEST #	TEST CONFIGURATION	TEST PRESSURE (psi)	TEST PLAN
012	01	TEST ASSEMBLY I	11,000	1000 CYCLES
006	02	TEST ASSEMBLY I	11,000	4000 CYCLES OR UNTIL FAILURE
011	03	TEST ASSEMBLY I	12,000	6000 CYCLES OR UNTIL FAILURE
002	04	TEST ASSEMBLY I	13,000	2000 CYCLES OR UNTIL FAILURE
008	05	TEST ASSEMBLY II	14,000	2000 CYCLES OR UNTIL FAILURE
004	06	TEST ASSEMBLY II	15,000	2000 CYCLES OR UNTIL FAILURE
009	07	TEST ASSEMBLY II	16,000	1600 CYCLES OR UNTIL FAILURE
003	08	TEST ASSEMBLY II	18,000	1000 CYCLES OR UNTIL FAILURE
001	09	TEST ASSEMBLY III	20,000	PROOF TEST
010	10	TEST ASSEMBLY III	TBD	PRESSURIZE TO FAILURE

TEST ASSEMBLY I: TITANIUM HEMISPHERE END CLOSURES, MOD 1, TYPE 2, END CAP JOINT RINGS
TEST ASSEMBLY II: FLAT STEEL PLATE END CLOSURES, MOD 1, TYPE 2, END CAP JOINT RINGS
TEST ASSEMBLY III: FLAT STEEL PLATE END CLOSURES, MOD 1, TYPE 1, END CAP JOINT RINGS

Table 3. Calculated stresses (psi) in ZTA cylinders for test assembly I configuration.

CALCULATED STRESSES (psi) IN ZTA CYLINDER 55910-0128912 FOR TEST ASSEMBLY I, SK9402-070					
EXTERNAL PRESSURE	9000 psi	10,000 psi	11,000 psi	12,000 psi	13,000 psi
RADIAL STRESS					
LOCAL MAX	+13,990	+15,370	+16,750	+18,120	+19,500
AXIAL STRESS					
LOCAL MIN	-28,160	-31,260	-34,350	-37,450	-40,540
LOCAL MAX	-90,540	-100,430	-110,310	-120,200	-130,080
MAX NOMINAL MEMBRANE	-66,620	-74,020	-81,420	-88,830	-96,230
HOOP STRESS					
LOCAL MIN	-108,380	-120,420	-132,460	-144,500	-156,540
MAX NOMINAL MEMBRANE	-133,530	-148,370	-163,210	-178,040	-192,880

Table 4. Calculated stresses (psi) in ZTA cylinders for test assembly II and III configurations.

CALCULATED STRESSES (psi) IN ZTA CYLINDER SK9402-0128912 FOR TEST ASSEMBLY II, SK9402-123, AND TEST ASSEMBLY III, SK9402-083					
	TEST ASSEMBLY II				TEST ASSEMBLY III
EXTERNAL PRESSURE	14,000 psi	15,000 psi	16,000 psi	18,000 psi	20,000 psi
RADIAL STRESS					
LOCAL MAX	+19,110	+20,380	+21,650	+24,200	+26,750
AXIAL STRESS					
LOCAL MIN	-43,500	-46,620	-49,740	-55,970	-62,200
LOCAL MAX	-152,910	-163,320	-173,730	-194,540	-215,350
MAX NOMINAL MEMBRANE	-103,680	-111,080	-118,470	-133,290	-148,040
HOOP STRESS					
LOCAL MIN	-168,130	-180,210	-192,290	-216,460	-240,620
MAX NOMINAL MEMBRANE	-207,720	-222,550	-237,380	-267,050	-296,720

Table 5. External pressure test results for ZTA cylinders.

TEST RESULTS FOR ZIRCONIA TOUGHENED ALUMINA CYLINDERS 55910-0128912			
TEST #	TEST CONFIGURATION	TEST PRESSURE (psi)	TEST RESULT
01	TEST ASSEMBLY I	11,000	WITHSTOOD 1039 CYCLES W/O FAILURE
02	TEST ASSEMBLY I	11,000	WITHSTOOD 4059 CYCLES W/O FAILURE
03	TEST ASSEMBLY I	12,000	WITHSTOOD 5689 CYCLES W/O FAILURE
04	TEST ASSEMBLY I	13,000	FAILED ON CYCLE 1854
05	TEST ASSEMBLY II	14,000	FAILED ON CYCLE 605
06	TEST ASSEMBLY II	15,000	FAILED ON CYCLE 361*
07	TEST ASSEMBLY II	16,000	WITHSTOOD 1608 CYCLES W/O FAILURE
08	TEST ASSEMBLY II	18,000	FAILED ON CYCLE 88
09	TEST ASSEMBLY III	20,000	WITHSTOOD PROOF TEST
10	TEST ASSEMBLY III	20,600	FAILED AT 20,600 psi

TEST ASSEMBLY I: TITANIUM HEMISPHERE END CLOSURES, MOD 1, TYPE 2, END CAP JOINT RINGS
TEST ASSEMBLY II: FLAT STEEL PLATE END CLOSURES, MOD 1, TYPE 2, END CAP JOINT RINGS
TEST ASSEMBLY III: FLAT STEEL PLATE END CLOSURES, MOD 1, TYPE 1, END CAP JOINT RINGS
*CYLINDER LEAKED DUE TO SPALLING, BUT DID NOT FAIL CATASTROPHICALLY

APPENDIX A: QUALITY CONTROL DATA

FIGURES

SHEET ____ OF ____

DIMENSIONAL RANGE DATA FORM

WESGO
Technical Ceramics and Brazing Alloys

PURCHASE ORDER NO.	PART NAME	S.O.
N66001-93 C-0045	HOUSING CYLINDER 12" ZTA -	126595
DRAWING NUMBER (GRAPHIC)	ISSUE	LOT# ZTA1 I0308
55910-0128912	B	

	DRAWING DIMENSION OR NOTE		RANGE MIN.	RANGE MAX.	SAMPLE SIZE
1.	18.00 ± .01		18.007	18.018	
2.	Ø 12.000 ± .005		11.997	11.9985	
3.	⊥ .010 A		Ø	<.001	
4.	▱ .002 -A-		Ø	<.001	
5.	.410 / .415 WALL		.4105	.4125	
6.	4 X R .03 ± .010		.020	.027	
7.					
8.	// .010 A		Ø	<.001	
9.	▱ .002		Ø	<.001	
10.					
11.	16✓				
12.			12	16	
13.	SERIAL # 126912-001				
14.					
15.	VISUAL CLASS A	W/1 Spec			
16.					
17.	CANDLING	No Visual Defects			
18.	POROSITY	Observed			
19.					
20.					

REMARKS: STATEMENT OF WORK NRAD CODE 9402 REV. 3 DATED 11/18/92.

C. Russell
INSPECTOR

QUALITY ASSURANCE

4/29/93
DATE COMPLETED

(6-78)

Figure A-1. Dimensional data form of cylinder part 001.

SHEET ____ OF ____

DIMENSIONAL RANGE DATA FORM

WESGO
Technical Ceramics and Brazing Alloys

PURCHASE ORDER NO.	PART NAME	S.O.
N66001-93 C-0045	HOUSING CYLINDER 12" ZIA -	126595
DRAWING NUMBER (GRAPHIC)	ISSUE	LOT# ZIA1
55910-0128912	B	I0315

	DRAWING DIMENSION OR NOTE		RANGE MIN.	RANGE MAX.	SAMPLE SIZE
1.	18.00 ± .01		18.0055	18.006	
2.	Ø 12.000 ± .005		11.9985	12.003	
3.	⊥ .010 A		.001	.002	
4.	▱ .002 -A-		∅	≤.001	
5.	.410 / .415 WALL		.4125	.414	
6.	4 X R .03 ± .010		.020	.030	
7.					
8.	// .010 A		∅	≤.001	
9.	▱ .002		∅	≤.001	
10.					
11.	16✓		4	10	
12.					
13.	SERIAL # 12912-010				
14.					
15.	VISUAL CLASS A	w/1 Spec			
16.					
17.	CANDLING	No Visual Defects Observed			
18.	POROSITY				
19.					
20.					

REMARKS: STATEMENT OF WORK NRAD CODE 9402 REV. 3 DATED 11/18/92.

C. Rusell
INSPECTOR

Rick Davis
QUALITY ASSURANCE

5/20/93
DATE COMPLETED

16-761

Figure A-2. Dimensional data form of cylinder part 010.

THE AUTHORS

RICHARD P. JOHNSON is an Engineer for the Ocean Engineering Division. He has held this position since 1987. Before that, he was a Laboratory Technician for the Ocean Engineering Laboratory, University of California at Santa Barbara from 1985–1986, and Design Engineer in the Energy Projects Division of SAIC from 1986–1987. His education includes a B.S. in Mechanical Engineering from the University of California at Santa Barbara in 1986, and an M.S. in Structural Engineering from the University of California, San Diego, in 1991. He is a member of the Marine Technology Society and has published "Stress Analysis Considerations for Deep Submergence Ceramic Pressure Housings," *Intervention '92*, and "Structural Design Criteria for Alumina-Ceramic Deep Submergence Pressure Housings," *MTS '93 Proceedings.*

RAMON R. KURKCHUBASCHE is a Research Engineer for the Ocean Engineering Division and has worked since November 1990 in the field of deep submergence pressure housings fabricated from ceramic materials. His education includes a B.S. in Structural Engineering from the University of California at San Diego, 1989; and an M.S. in Aeronautical/Astronautical Engineering from Stanford University in 1990. His experience includes conceptual design, procurement, assembly, testing, and documentation of ceramic housings. Other experience includes buoyancy concepts utilizing ceramic, nondestructive evaluation of ceramic components. He is a member of the Marine Technology Society, and has published "Elastic Stability Considerations for Deep Submergence Ceramic Pressure Housings," *Intervention '92*, and "Nondestructive Evaluation Techniques for Deep Submergence Housing Components Fabricated from Alumina Ceramic," *MTS '93 Proceedings.*

DR. JERRY STACHIW is Staff Scientist for Marine Materials in the Ocean Engineering Division. He received his undergraduate engineering degree from Oklahoma State University in 1955 and graduate degree from Pennsylvania State University in 1961.

Since that time he has devoted his efforts at various U.S. Navy Laboratories to the solution of challenges posed by exploration, exploitation, and surveillance of hydrospace. The primary focus of his work has been the design and fabrication of pressure resistant structural components of diving systems for the whole range of ocean depths. Because of his numerous achievements in the field of ocean engineering, he is considered to be the leading expert in the structural application of plastics and brittle materials to external pressure housings.

Dr. Stachiw is the author of over 100 technical reports, articles, and papers on design and fabrication of pressure resistant viewports of acrylic plastic, glass, germanium, and zinc sulphide, as well as pressure housings made of wood, concrete, glass, acrylic plastic, and ceramics. His book on "Acrylic Plastic Viewports" is the standard reference on that subject.

For the contributions to the Navy's ocean engineering programs, the Navy honored him with the Military Oceanographer Award and the NCCOSC's RDT&E Division honored him with the Lauritsen-Bennett Award. The American Society of Mechanical Engineers recognized his contributions to the engineering profession by election to the grade of Life-Fellow, as well as the presentation of Centennial Medal, Dedicated Service Award and Pressure Technology Codes Outstanding Performance Certificate.

Dr. Stachiw is past-chairman of ASME Ocean Engineering Division and ASME Committee on Safety Standards for Pressure Vessels for Human Occupancy. He is a member of the Marine Technology Society, New York Academy of Science, Sigma Xi and Phi Kappa Honorary Society.

REPORT DOCUMENTATION PAGE

Form Approved
OMB No. 0704-0188

1. AGENCY USE ONLY *(Leave blank)*	2. REPORT DATE	3. REPORT TYPE AND DATES COVERED
	December 1993	Final

4. TITLE AND SUBTITLE

STRUCTURAL PERFORMANCE OF CYLINDRICAL PRESSURE HOUSINGS OF DIFFERENT CERAMIC COMPOSITIONS UNDER EXTERNAL PRESSURE LOADING
Part II, Zirconia Toughened Alumina Ceramic

5. FUNDING NUMBERS

PE: 0603713N
PROJ: S0397
ACC: DN302232

6. AUTHOR(S)

R. P. Johnson, R. R. Kurkchubasche, J. D. Stachiw, and P. C. Smith

7. PERFORMING ORGANIZATION NAME(S) AND ADDRESS(ES)

Naval Command, Control and Ocean Surveillance Center (NCCOSC)
RDT&E Division
San Diego, CA 92152–5000

8. PERFORMING ORGANIZATION REPORT NUMBER

TR 1593

9. SPONSORING/MONITORING AGENCY NAME(S) AND ADDRESS(ES)

Naval Sea Systems Command
Washington, DC 20362

10. SPONSORING/MONITORING AGENCY REPORT NUMBER

11. SUPPLEMENTARY NOTES

12a. DISTRIBUTION/AVAILABILITY STATEMENT

Approved for public release; distribution is unlimited.

12b. DISTRIBUTION CODE

13. ABSTRACT *(Maximum 200 words)*

Ten 12-inch-outside diameter (OD) by 18-inch-long by 0.412-inch-thick monocoque cylinders fabricated by WESGO, Inc. from zirconia-toughened alumina (ZTA) ceramic were assembled into external pressure housings and experimentally evaluated under short-term, and cyclic-pressure loadings. This study was undertaken as part of a program to promote the application of ceramics to large external pressure housings for underwater vehicles. Pressure testing was performed to generate structural performance data that could be used to establish design criteria for external pressure housings constructed using ZTA ceramic as the primary hull material. Design curves for ZTA ceramic housings are presented that relate the maximum number of operational dive cycles to the maximum allowable stresses in the ceramic housing during each dive cycle. ZTA ceramic was found to be a reliable structural material for fabrication of cylindrical external pressure housings with a minimum fatigue life of 1,000 cycles at nominal design stresses of −190,000 psi in the hoop direction. ZTA was also evaluated by comparing its structural performance to that of alumina ceramic for use as the primary structural material for deep submergence external pressure housings.

14. SUBJECT TERMS

ceramics
external pressure housing
ocean engineering

15. NUMBER OF PAGES

82

16. PRICE CODE

17. SECURITY CLASSIFICATION OF REPORT	18. SECURITY CLASSIFICATION OF THIS PAGE	19. SECURITY CLASSIFICATION OF ABSTRACT	20. LIMITATION OF ABSTRACT
UNCLASSIFIED	UNCLASSIFIED	UNCLASSIFIED	SAME AS REPORT

21a. NAME OF RESPONSIBLE INDIVIDUAL	21b. TELEPHONE (Include Area Code)	21c. OFFICE SYMBOL
R. P Johnson	(619) 553–1935	Code 564